MULTI SOURCE HEAT PUMP FOR GEOEXCHANGE SYSTEMS (GXS)

By

Aaron Rendina

Emily Robinson

Eric Jacobsohn

A report presented to the

British Columbia Institute of Technology

in partial fulfilment of the requirement for the degree of

Bachelor of Engineering (Mechanical)

Faculty Advisors:	Dr. Joseph Cheung, P. Eng.
	Dr. Vahid Askari, P. Eng.
	Dr. Johan Fourie, P. Eng.
Program Head:	Dr. Mehrzad Tabatabaian, P. Eng.

Burnaby, British Columbia, Canada, 2018

© Aaron Rendina, Emily Robinson, Eric Jacobsohn, 2018

Author’s Declaration

We hereby declare that we are the sole authors of this report.

X Aaron R	X	X Eric
Aaron Rendina	Emily Robinson	Eric Jacobsohn

We further authorize the British Columbia Institute of Technology to distribute digitally, or printed paper, copies of this report, in total or in part,
at the request of other institutions or individuals for the purpose of scholarly activity.

X Aaron R	X	X Eric
Aaron Rendina	Emily Robinson	Eric Jacobsohn

Abstract

With the use and effectiveness of conventional heat pumps decreasing drastically in colder climate regions, geo-exchange systems have become the solution to allow heat pumps to still be operable in these colder regions. However, with the high costs of installation required for deep-well heat exchangers and horizontal-trench heat exchangers, and the high cost of land in high-density urban/suburban areas, their adoption is still small. For this reason, this project aims to increase the energy density of geo-exchange systems so that high installation costs are not required, and large land requirements become non-existent.

The increased energy density was theorized to be achieved by installing the outdoor heat exchanger in a fluid filled tank that would itself passively transfer heat with the surrounding soil in which it was buried; by burying the tank below the frost line, a stable temperature could be achieved, providing an optimal location for year-round heat transfer.

The project focused on the outdoor heat exchanger, specifically tank thermodynamics and heat transfer, and aimed to improve upon a project from the previous year that began this feasibility study.

In order to gain further insight into the optimal designs and expected operations, the project team used a computational fluid dynamics (CFD), and computation heat transfer (CHT) software, COMSOL Multiphysics, to create a virtual model that could first be compared against a real-life prototype to ensure verification of the design. The virtual model only focused on the outdoor heat exchanger submerged in water, with simplifications of water being used instead of refrigerant through the piping due to the

complexity of two-phase flow and uploading a new material, which includes determining the thermophysical and fluid-mechanic properties for the refrigerant being used in the current system. Therefore, to compare the real-life and virtual model, an energy method will be used where heat transfer across both heat exchangers is compared.

Using a first-principles approach, and observations from the operation of the incumbent design, the main issue with the existing system was found to be a lack of heat transfer through the outdoor coil. Therefore, looking at all the ways to increase heat transfer, surface area was seen as the most viable, and the design of the flat-plate heat exchangers were made and connected to two separate loops with serpentine piping setups.

Results were gathered first through data collection of the incumbent design with still tank water, still tank water and anti-freeze to increase total available energy before freezing, and with agitated water. Next data collection took place with the team's flat plate design for still water and agitated water. Comparing results from the incumbent and new design found increases in run times even when tank water temperatures were significantly lower for some of the new design tests: 30 minutes versus ten hours for still water; 15 hours with a starting water temperature above 20°C versus 12 hours with a starting water temperature around 2°C for agitated tank water. With these results, there was an obvious improvement in system performance—especially with respect to the system continuing to run for many hours after ice formed on the piping and plates. This was because there was still sufficient surface area on the flat plate farther away from the piping that still had a much lower thermal resistance compared to heat transfer across the forming ice.

Focusing more on system specifications and comparisons between the virtual and physical model, it was found that the system had an experimental COP of approximately 3.7, and a heat transfer across the outdoor coil of approximately 3.88kW. When compared to the virtual model, an error of 16% resulted, which is still high, but errors from simplifications in the virtual model, as well as a lack of in-depth data collection and analysis, and manufacturing tolerances play a role in this difference between the two.

Improvements and iterations to this system are still required and include things such as further increasing heat transfer in the outdoor heat exchanger, increasing the amount of instrumentation, and its sensitivity, improving the manufacturing methods, and physically burying the tank and system in the ground to get more realistic data.

Acknowledgements

The design team received a lot of help from many faculty members of BCIT's mechanical engineering department as well as outside sales reps and trades that assisted with the design and manufacturing of this project.

Firstly, we would like to thank the project sponsors and members of the department:

Dr. Joseph Cheung, who came up with the original idea for increasing the energy density of geo-exchange systems and made this project possible. Thank you very much for all your assistance, organizing of trades, material expediting, and guidance throughout the project.

Dr. Vahid Askari, who organized and supervised the direction of the theoretical development for this second iteration of the project while also helping and offering guidance with the virtual model and manufacturing of the prototype. Thank you very much for all your insight, involvement, and mentoring throughout the project.

Dr. Henry Chang, who assisted in ensuring calculations, and theory were acceptable. Thank you very much for all your help.

Dr. Johan Fourie, who oversaw the entire capstone project and made sure all project management activities were met, ordered and picked up materials, as well as taught and guided us through the entire engineering approach of the design of products in the mechanical discipline. Thank you very much for everything.

We would also like to thank Dave Lewis, and Brian Ennis for all their assistance with shop-related activities and excellent feedback to different design ideas, their viability for manufacturing, and how to go about fabricating them.

Next, we would like to thank Ian Winning from Control Temp Ltd. for his help with the install of the new heat exchanger, and all refrigeration-related work that was required to implement this new design.

Lastly, the team would like to thank Tyler Sander from Refrigerative Supply Limited for assisting in material and product procurement.

Chapter 1. Table of Contents

Author's Declaration iii

Abstract v

Acknowledgements ix

List of Tables xvii

List of Figures xix

Chapter 1. Introduction 1

1.1 Introduction 1

1.1.1 Project Objective 1

1.1.2 Project Scope 1

1.2 Background 2

1.2.1 History 2

1.2.2 Previous Work 5

1.3 Project Quantification 6

1.3.1 Coefficient of Performance 6

1.3.2 Cycle Time 6

1.3.3 Validation of COMSOL model 6

1.3.4 Boundary Conditions 11

Chapter 2. Detailed Description of the Current Status 13

2.1 Problem Statement 13

2.2 Project Hypothesis 13

Chapter 3. Theoretical Background 15

3.1 Patent Search 15

3.1.1 Latent Heat Thermal Battery 15

3.1.2 Thermoelectric Generator with Latent Heat Storage 15

3.2 Theoretical Fundamentals 17
3.2.1 Thermodynamics 17
3.2.2 Latent Heat 18
3.2.3 General Heat Pump Operation 19
3.2.4 Heat Pump Performance 19
3.2.5 Geo-Exchange Heat Pumps 22
3.2.6 Boiling and Condensation 22
3.2.7 Balance point 27
3.2.8 Heat Transfer through COMSOL Multiphysics 28
Chapter 4. Detailed Project Activities and Equipment 31
4.1 Design Calculations 31
4.1.1 Building Heat Loss 31
4.1.2 Heat Transfer through Outdoor Coil (Horizontal) 31
4.1.3 Energy & Power Capacity in Tank 31
4.1.4 Pipe Losses through Outdoor Coil 32
4.1.5 Changing Heat Capacity and Freezing Point of Fluid 32
4.1.6 Refrigerant Volume 33
4.2 Design Approach 34
4.2.1 Incumbent Design 34
4.2.2 Calculations 35
4.3 Design Selection 35
4.3.1 Helical Design 35
4.3.2 Fin Design 36
4.3.3 Flat Plate Design 37
4.4 Final Design 38

4.5 COMSOL ... 40
  4.5.1 COMSOL Practice ... 40
  4.5.2 COMSOL Models ... 40
  4.5.3 Future Prototype Testing ... 42
4.6 Physical Prototype Manufacturing ... 43
  4.6.1 Incumbent design ... 43
  4.6.2 Modifications ... 44
Chapter 5. Discussion of results ... 55
5.1 COMSOL Results ... 55
  5.1.1 300 Second Time Interval Test using Water ... 55
  5.1.2 7200 Second Time Interval Test Using Water ... 60
5.2 Verification of COMSOL Model ... 64
  5.2.1 COMSOL Simulation ... 64
  5.2.2 Physical Prototype ... 65
  5.2.3 Discussion of Results ... 67
5.3 Physical Results ... 68
  5.3.1 Incumbent Design ... 68
  5.3.2 Vertical Plate Design ... 72
5.4 Comparison of Incumbent with Plate Design ... 74
  5.4.1 Results without Agitator ... 74
  5.4.2 Results with Agitator ... 75
Chapter 6. Conclusion ... 77
Chapter 7. Lessons Learned ... 79
Chapter 8. Bibliography ... 81
Chapter 9. Index ... 83

Appendix A – Request for Proposal 85
A.1 Introduction & Background 86
A.2 Submission Guidelines & Requirements 86
A.3 Project Description 87
A.4 Project Scope 87
A.5 RFP Timelines 87
A.7 Budget 87
A.8 Evaluation Factors 87
Appendix B - Design Review 89
B.1 Design Review Purpose and Objective 90
B.2 Project Objective 90
B.3 Deliverables 90
B.4 Constraints 90
B.5 Calculations 90
B.5.1 Building Heat Loss 90
B.5.2 Heat Transfer through Outdoor Coil (Horizontal) 91
B.5.3 Energy & Power Capacity in Tank 91
B.5.4 Pipe Losses through Outdoor Coil 92
B.6 Incumbent Design 93
B.7 Current Concepts 93
B.7.1 Helical Design 93
B.7.2 Fin Design – Coil and Fin 94
B.7.3 Fin Design – Serpentine Coil and Fin 94
B.7.4 Horizontal Flat Plate Design 95
B.8 Final Design - Vertical Flat Plate Design 95

        - B.8.1 Support Designs 96
    - B.9 Schedule Status 98
    - B.10 Areas of Concern 99
        - B.10.1 COMSOL 99
        - B.10.2 Manufacturing before Simulation 99
- Appendix C – Mathematical Derivations 101
    - C.1 Building Heat Loss 101
    - C.2 Heat Transfer through Outdoor Coil 104
    - C.3 Energy & Power Capacity in Tank 108
    - C.4 Pipe Losses Through Outdoor Coil 111
    - C.5 Changing Heat Capacity and Freezing Point of Fluid 115
    - C.6 Heat Transfer Rate across a Straight Pipe 117
- Appendix D – Programming 121
    - D.1 Pipe Losses Through Outdoor Coil 121
    - D.2 Heat Transfer through Horizontal Outdoor Coil 123
    - D.3 Heat Transfer through Vertical Outdoor Coil 124
- Appendix E – Product Specifications 127

List of Tables

Table 1.1 - Pressure Drop Validation Parameters 7
Table 1.2 - Heat Trasfer Validation Parameters 9
Table 1.3 - Heat Pump Parameters of Interest 11
Table 5.1 - Parameters for Horizontal Plate Design over 300 seconds 56
Table 5.2 - COMSOL Parameters for Energy Calculation 64
Table 5.3 - Recorded Values for Indoor Heat Exchanger 66

List of Figures

Figure 1.1- Water-Based Exchange System 3
Figure 1.2 - Direct Exchange Heat Pump Operation 5
Figure 1.3 - Incumbent Design Vertical Tee 5
Figure 3.1 - T-v Diagram for a Fluid at Constant Pressure 18
Figure 3.2 - T-v Diagram for a Pure Substance 18
Figure 3.3 - Vapour-Compression Refrigeration Cycle 19
Figure 3.4 - Ideal Vapour Compression Cycle 21
Figure 3.5 - Actual Vapour Compression Cycle 21
Figure 3.6 - Isenthalpic Throttling Temperature-Pressure Relationship 22
Figure 3.7 - Pool Boiling Regimes 25
Figure 3.8 - Pool Boiling Regimes versus Heat Transfer 25
Figure 3.9 - External Flow Boiling 25
Figure 3.10 - Two-Phase Flow 26
Figure 3.11 - Forms of Condensation 27
Figure 4.1 - Incumbent Pipe Configuration 34
Figure 4.2 - Helical Design for Pipe Configuration Selection 36
Figure 4.3 - Helical Fin Design for Pipe Configuration Selection [12] 37
Figure 4.4 - Serpentine Fin Design for Pipe Configuration Selection [12] 37
Figure 4.5 - Horizontal Plate Design for Pipe Configuration Selection 38
Figure 4.6- Vertical Plate and Piping Configuration 39
Figure 4.7 - Vertical Plate with Tubular Fins and Piping Configuration 39
Figure 4.8 - Vertical Plate Bend Design 44
Figure 4.9 - Wood Milling to create Test Bend Block 45
Figure 4.10 - Test Bend Block and Bend Mold Clearance 46
Figure 4.11 - Hydraulic Press used for Test Bends 46
Figure 4.12 - Clearance around Pipe using Bend Mold and Light Gauge Stainless Steel 47
Figure 4.13 - Practice Bends using the Wood Press 47
Figure 4.14 - Crooked Bends from the First Wood Mold Design 48
Figure 4.15 - New Wood Mold with Locator 48

Figure 4.16 - Screws for First Bend 49
Figure 4.17 - Bending of the Aluminum Sheet Metal 49
Figure 4.18 - Two Plates after Bending 50
Figure 4.19 - Brazed Pipe set in a Single Plate 51
Figure 4.20 - Brazed Pipe between Two Plates 51
Figure 4.21 - Installed Plate Design Prototype 52
Figure 4.22 - Plate Support Connection 53
Figure 5.1- Outlet Temperature for Horizontal Plate Design over 300 seconds 55
Figure 5.2 - Final Pipe Temperature for Horizontal Plate Design over 300 seconds 56
Figure 5.3 - Final Plate Temperature for Horizontal Plate Design over 300 seconds 57
Figure 5.4 - Outlet Temperature for Horizontal Plate Design with Tubular Fins over 300 seconds 58
Figure 5.5 - Final Pipe Temperature for Horizontal Plate Design with Tubular Fins over 300 seconds 58
Figure 5.6 - Final Plate Temperature for Horizontal Plate Design with Tubular Fins over 300 seconds 59
Figure 5.7 - Outlet Temperature for Horizontal Plate Design over 7200 seconds 60
Figure 5.8 - Final Pipe Temperature for Horizontal Plate Design over 7200 seconds 61
Figure 5.9 - Final Plate Temperature for Horizontal Plate Design over 7200 seconds 61
Figure 5.10 - Outlet Temperature for Horizontal Plate Design with Tubular Fins over 7200 seconds 62
Figure 5.11 - Final Pipe Temperature for Horizontal Plate Design with Tubular Fins over 7200 seconds 63
Figure 5.12 - Final Plate Temperature for Horizontal Plate Design with Tubular Fins over 7200 seconds 63
Figure 5.13 - Heat Transfer from COMSOL Simulation 65
Figure 5.14 - High and Low Temperature Sides for Incumbent Design without Agitator 69
Figure 5.15 - High and Low Temperature Sides for Incumbent Design without Agitator and with Plumbing Antifreeze 70
Figure 5.16 - High and Low Temperature Sides for Incumbent Design with Agitator 71
Figure 5.17 - High and Low Temperature Sides for Vertical Plate Design without Agitator 72

Figure 5.18- Vertical Plate Design with the Agitator.. 73

Chapter 1. Introduction

1.1 Introduction

Heating accounts for 78% of average household energy usage in Canada [1]. Most methods of heating a home involve creating that heat on site by combustion of fossil fuels or electric resistance heating. Heat pumps offer an alternative approach by moving heat from the environment to, or from a home. Because heat pumps don't have to create heat, but rather move it, the energy used is far less. A common form of heat pump configuration is to have one heat exchanger in a dwelling and one in a local body of water or buried in the earth. This configuration is called a geo-exchange system.

Geo-exchange systems have the potential to heat and cool homes at a low cost. The method works well in ideal conditions but failures in subterranean exchange coils can leave a system completely inoperable. In addition, the depth or footprint of the outdoor heat exchanger loops pose costly installation challenges.

The purpose of this project is to investigate a geo exchange system that requires a small footprint with no requirement for deep drilling. The system to be investigated has an approximate two cubic meter dimension. By utilizing both the sensible and latent heat of water, the system is potentially able to transfer as much heat as that of long subterranean loops with no use of latent heat.

To further investigate the operational parameters of the system, computer simulations are also to be developed. The chosen software is to be COMSOL as it is a proven industry leader and is the best suited for Multiphysics applications

1.1.1 Project Objective

This project will serve to provide an in-depth investigation into the viability of a multisource geo-exchange system.

1.1.2 Project Scope

The multi-source heat pump that will be designed will utilize both the latent and sensible heat of water and the ground to provide heating.

This project will solely look at the initial start-up conditions focusing only on the heating mode of the system and the outdoor coil. This is discussed further in Section 3.3.2. The system will need to run for ten consecutive hours to accurately simulate the start-up and initial heating of a dwelling.

Because this project is a continuation from work done on a previous project completed in the recent past, the team will be modifying an existing multi-source heat pump. The components purchased for this previous project will be used but the outdoor coil heat exchanger will be redesigned. The new design will then be simulated on COMSOL Multiphysics, and those simulated results will be compared with collected data from a prototype. The prototype will be in a lab setting rather than being installed underground. Therefore, the external conditions that will be simulated will have to consider this and set to room temperature instead of ground temperature. This should also be taken into account during analysis of the design because the system will be able to run longer because the initial temperature will be approximately 20 degrees higher. The comparisons between the simulated data and the collected data will be limited to outlet temperatures and pressures.

1.2 Background

The following section covers the overall background of this report. It will cover the history of geothermal systems, the current designs used in industry, as well as the previous work on this project.

1.2.1 History

Humans have been interested in heating and cooling since the first campfires were lit. The pediment driver towards the development of the heat pump was refrigeration systems. In the mid-18th century chemists discovered that by changing the pressure of a closed vessel containing a substance with a low boiling temperature, they could lower its temperature below freezing. [2]. In the early 1900's an engineer named Willis Carrier tasked with reducing the humidity in a printing plant did so by reducing the humidity using a bank of cooling coils. This was the world's first air conditioning unit [3]. It wasn't until a few decades later that the first geo exchange heat pump system was built; the earliest one was probably Robert C. Webber's home-made 2.2 kW direct-exchange system [4].

There are two commonly used heat pump systems, water-based exchange and direct exchange. There are also two commonly used loop configurations, vertical and horizontal.

1.2.1.1 Water-Based Exchange System

The water-based exchange system uses two separate loops to transfer heat from the ground into the conditioned space. This required an intermediate fluid usually a glycol water mixture. This system requires three different heat exchangers, these being the condensing coil between the refrigerant and the conditioned space, the evaporating coil that uses a tube-in-tube configuration between the intermediate fluid and the refrigerant, and, finally, the ground coil between the intermediate fluid and the ground. The heat pump operation is shown in Figure 1.1.

This system requires less refrigerant than the direct exchange method discussed below and therefore, this system is cheaper and more environmentally friendly. The main issues with this system is with the more complex implementation and losses occurred between the multiple heat exchangers.

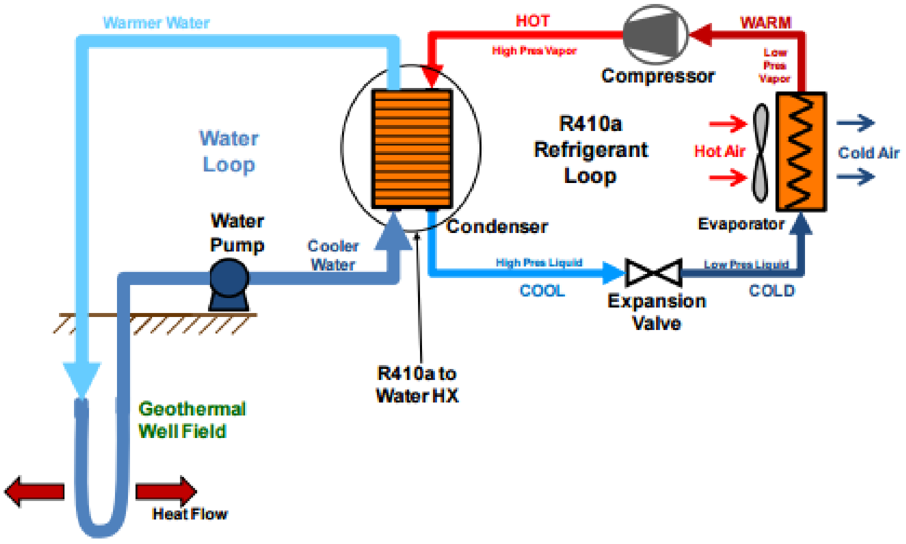
Warmer Water
HOT
High Pres Vapor
Compressor
WARM
Low Pres Vapor
Water Loop
R410a Refrigerant Loop
Hot Air
Cold Air
Water Pump
Cooler Water
Condenser
Evaporator
High Pres Liquid
Low Pres Liquid
COOL
Expansion Valve
COLD
R410a to Water HX
Geothermal Well Field
Heat Flow

Figure 1.1- Water-Based Exchange System
As Illustrated in [5]

1.2.1.1.1 Vertical Loop Configuration

The vertical loop configuration uses sealed piping loops that are inserted into small holes. The depth of these holes can range anywhere from 150 to 400 feet deep. This configuration requires less yard space as the horizontal loops discussed below, but the required drilling and the installation of these piping loops are very expensive. The other main area of concern is that there is little to no way to maintain these pipes and check for failures, therefore the system might not even work after installation.

1.2.1.1.2 Horizontal Loop Configuration

The horizontal loop configuration has the sealed piping loops placed in trenches instead of inserted into holes. These trenches are anywhere from three to six feet deep. The closer the pipes are installed to the surface, the more the sun will increase the heat absorbed but also the faster they will cool in the winter. This configuration requires a large amount of yard space but is easier to maintain if necessary and make sure installation is completed properly.

1.2.1.2 Direct Exchange System

The direct exchange system, also known as direct-expansion ground source heat pump, has a single primary refrigerant loop. This is also the system design that the team's ice bank design uses. The refrigerant runs through the full system which provides higher efficiency than the water-based systems. This is because there is only heat transfer between the ground and the refrigerant and the refrigerant and the conditioned space. The heat pump operation is shown in Figure 1.2.

This system also requires less power and is easer to implement. The main area of concern for these systems is that when pumping refrigerant throughout the whole system, there is an increased cost due to the amount of refrigerant needed and the possibility of leakage into the ground.

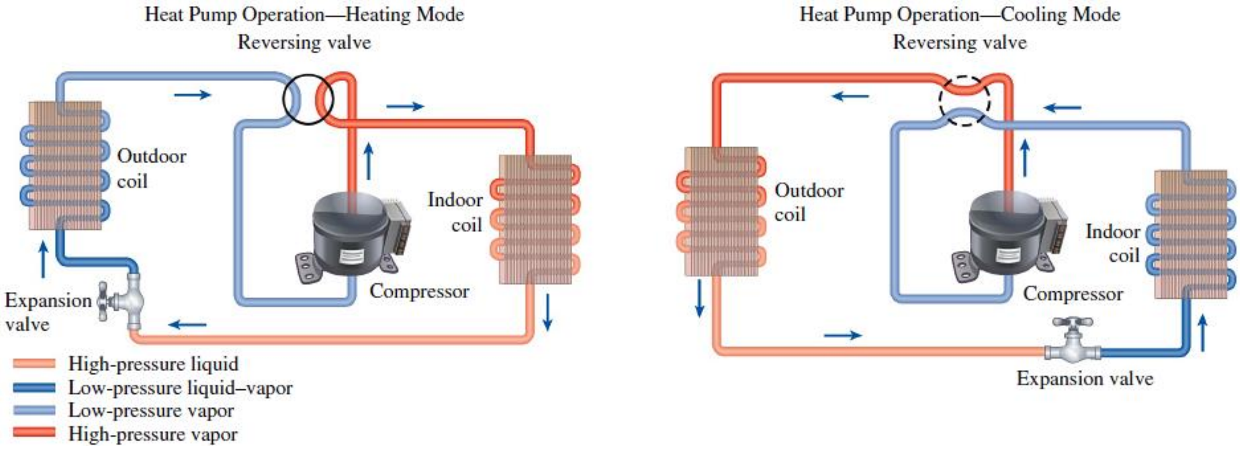
Heat Pump Operation—Heating Mode
Reversing valve
Outdoor coil
Indoor coil
Compressor
Expansion valve
High-pressure liquid
Low-pressure liquid–vapor
Low-pressure vapor
High-pressure vapor
Heat Pump Operation—Cooling Mode
Reversing valve
Outdoor coil
Indoor coil
Compressor
Expansion valve

Figure 1.2 - Direct Exchange Heat Pump Operation
As Illustrated in [6], *Fig. 11-11*

1.2.2 Previous Work

This project is the second iteration of a multi-source geo-exchange system. The previous system was developed to investigate the feasibility of a multisource heat exchanger as this project is investigating; however, the previous project didn't use COMSOL simulations. Also, the previous project final design was able to improve the COP of the unmodified supplied system, but it was unable to run for more than a few hours for a couple of reasons: Firstly, as the heat exchanger coil had insufficient surface area for heat transfer, when ice began to form around the refrigerant tubing, a reduction in heat transfer took place resulting in the inability to evaporate the refrigerant before returning to the compressor causing the unit to lock out. Secondly, the use of a vertical tee that fed the twin outdoor coil loops instead of a horizontal tee on its back led to an imbalance of refrigerant to the coils, with the lower loop containing the majority of the liquid refrigerant and being responsible for the majority of the heat transfer while the upper loop's effectiveness dropped drastically. Throughout this report this original design is referred to as the incumbent design.

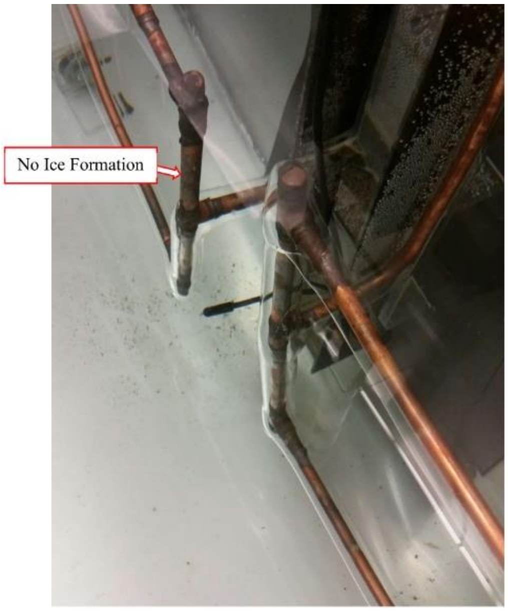
No Ice Formation

Figure 1.3 - Incumbent Design Vertical

1.3 Project Quantification

The following section covers the factors that will be considered for the quantification of the project's performance. The largest limiting factor will be the ice buildup on the heat exchanger design. If this buildup is not controlled and quickly becomes an insulator, the proposed technology will not be able to outperform the conventional geo-exchange systems.

1.3.1 Coefficient of Performance

The coefficient of performance of a heat pump is analogous to the efficiency of other devices. A heat pump is unique in that it moves energy, rather than just consuming. The coefficient of performance is defined by

$$COP = \frac{Q}{W}$$

Where Q being the energy supplied or removed from a system and W is the work required to move that energy. The COP is commonly above unity for heat pumps, as they are designed to move more energy than they use, and it is not uncommon to reach values ranging around five for water-source systems. More information on heat pump performance is provided in section 3.2.4.

1.3.2 Cycle Time

In heating systems, cycle time is the amount of time the system is active per hour. During normal operations, it is typical for heating systems to oscillate around the set point. The amount of temperature differential allowed before cycling is set by the system designer. Too small a differential will lead to over cycling and premature wear out of contacts. Too large of a differential will lead to discomfort of occupants of the space. During start up, the demand is much larger as the dwelling space needs to be heated up to the set point for the first time. As the start-up time has the highest demand, this is what the project will be simulating, by attempting to run the system for at least ten consecutive hours.

1.3.3 Validation of COMSOL model

To be able to proceed with more complex virtual models, it is important to ensure that the program is returning numerical results that are in accordance with analytical solutions. For this reason, simple fluid mechanics and heat transfer problems will be simulated in COMSOL and compared to their analytical counterparts. The scenarios of interest will involve:

- pressure drop across a straight pipe of known length and material, and
- heat transfer across a straight pipe with known parameters for pipe length and material, inlet fluid temperature, velocity, and thermodynamic properties, and surrounding fluid temperature.

With these two scenarios, the error involved will be calculated and ensured that it is below acceptable standards.

1.3.3.1 Pressure Drop across a Straight Pipe

Setting up dummy parameters as shown in Table 1.1, the analytical and numerical solutions for steady state fluid flow through a pipe can be set up and found.

Table 1.1 - Pressure Drop Validation Parameters

Parameter	**Value**
Pipe Length, $L\ [m]$	1.0
Inner Pipe Diameter, $d\ [in], [m]$	0.5, 0.0127
Outer Pipe Diameter, $D\ [in], [m]$	0.625, 0.015875
Thermal Conductivity of Copper, $k\ [W/m \cdot K]$	400
Inlet Temperature, $T_{in}\ [K]$	273.15
Inlet Velocity, $u\ [m/s]$	0.125
Inlet Pressure, $p\ [psi], [kPa]$	50, 344.738

1.3.3.1.1 Analytical Solution

Using the Darcy-Weisbach equation and substituting either the laminar equation for the friction factor or Petukhov's equation for finding the friction factor, the pressure drop in a straight pipe, can be found to be:

$$\Delta p = f\frac{\rho u_m^2}{2d}L = f\frac{u_m^2}{2dv}L, where\ f = \frac{64}{Re_d}\ or\ f = (0.790\ln(Re_d - 1.64))^{-2}$$

$$\Delta p = \frac{64}{Re_d} \cdot \frac{u_m^2}{2dv} \cdot L = \frac{32u_m^2 L}{dRe_d v}, \ \ Re_d < 3000$$

$$\Delta p = \frac{L}{2dv}\left[\frac{u_m}{0.790\ln(Re_d - 1.64)}\right]^2, \ \ 3000 < Re_d < 5 \cdot 10^6$$

With the equation now known, the resulting analytical solution is solved.

$$Re_d = \frac{4\dot{m}}{\pi d\mu} = \frac{\rho u_m d}{\mu} = \frac{(1000\ \ kg/m^3)(0.125\ \ m/s)(0.0127m)}{0.00175\ \ N \cdot s/m^2} \cong 907.143$$

$$\Rightarrow \Delta p = \frac{32(0.125\ \ m/s)^2(1.0)}{(0.0127m)(907.143)(0.001\ \ m^3/kg)} \cong 43.400\ Pa$$

1.3.3.1.2 Numerical Solution

Setting up a simple case in COMSOL Multiphysics with the same parameters from Table 1.1., the simulation results in a Reynolds number of:

$$Re_d = \frac{\rho u_m d}{\mu} \cong 885.76$$

and a pressure drop of:

$$\Delta p = \frac{32\rho u_m^2 L}{dRe_d} = 44.235\ Pa$$

1.3.3.1.3 Percent Error

The percent error in the pressure drop between the numerical and analytical solutions is:

$$\%Error = \frac{|43.400 - 44.235|}{43.400} \cong 0.0192 = \ 1.92\%$$

With a percent error below two, this simple case with a known analytical solution seems acceptable to validate basic numerical simulations with COMSOL of flow within a circular pipe.

1.3.3.2 Heat Transfer Rate across a Straight Pipe

Setting up dummy parameters as shown in Table 1.2, the analytical and numerical solutions for steady state hydro-dynamically and thermally developed fluid flow through a pipe can be set up and found.

Table 1.2 - Heat Trasfer Validation Parameters

Parameter	**Value**
Pipe Length, $L\ [m]$	10.0
Inner Pipe Diameter, $d\ [in], [m]$	0.5, 0.0127
Outer Pipe Diameter, $D\ [in], [m]$	0.625, 0.015875
Thermal Conductivity of Copper, $k\ [W/m \cdot K]$	400
Inlet Temperature, $T_{in}\ [K]$	273.15
Surrounding Temperature, $T_s\ [K]$	1000
Inlet Velocity, $u\ [m/s]$	0.0625

1.3.3.2.1 Analytical Solution

Using the calculations shown in Appendix C.6 and iteratively finding a mean outlet temperature, it was found that the outlet temperature was $T_{m_o} \cong 484.52K$. The assumption involved a value of $473.15K$ resulting in an average mean temperature for the entire span of the pipe of $\overline{T}_m = 373.15K$. With the average temperature known, the thermophysical properties of saturated water at that temperature could then be found and resulted in flow that was very near laminar conditions, slightly above the cut-off value of 2300, with a value of $Re_D = 2725.1 \therefore Laminar/Turbulent$.

The final condition of interest is to make sure that the flow is hydrodynamically and thermally fully developed early on in the pipe length to ensure fairly accurate results, with the two calculations shown below:

$$x_{fd,h_{lam}} \cong 0.05Re_D D = (0.05)(2725.1)(0.0127m) \cong 1.73m$$

$$x_{fd,t_{lam}} \cong 0.05Re_D Pr D = x_{fd,h_{lam}} Pr = (1.73m)(1.76) = 3.0448$$

With a hydrodynamically fully developed flow within the first twenty percent of the pipe length, results shouldn't be too erroneous and can be compared to those of the virtual model.

1.3.3.2.2 Numerical Solution

Setting up a simple case in COMSOL Multiphysics with the same parameters from Table 1.2. The simulation used different equations to calculate the Nusselt number, and, therefore, the heat transfer coefficient values were also different than those used in the analytical solution. The analytical system used equations previously used in the team's education, while COMSOL uses more advanced methods. The team decided to use external forced convection for the External Film Resistance section of the COMSOL simulation based on similarities in the results.

When this simulation was run, the results did not match the team's understanding of real life application or the analytical results. When the velocity of the fluid was increased to 5 m/s and the length increased to 100m, a temperature change was seen. Before this, the simulation returned zero temperature change. The results of the simulation with 5 m/s velocity with an outlet temperature of only $273.69K$, with the inlet temperature being equal $273.15K$ which is equal to the value in Table 1.2.

These results are hypothesized to come from the team's lack of COMSOL experience and the lack of time available to spend on this validation. If the team was able to spend more time on this validation without sacrificing efforts on the COMSOL model for the proposed design, then it is believed that the validation would be able to achieve accurate results.

Because of the success of the previous validation, time constraints of the project, and the large acceptance of this software in the industry, the team decided to exclude this validation and move forward with the project.

1.3.4 Boundary Conditions

The following values in Table 1.3 give product specifications that will be used for calculations later in this report.

Table 1.3 - Heat Pump Parameters of Interest

Parameter	**Value**
Potential Voltage Difference, E $[V]$	240
Unit Current Draw, I_u $[A]^*$	6.00
Agitator Motor Current Draw, I_a $[A]$	0.04
Total Current Draw, I $[A]$	6.04
COP_H**	4.3
Low Side Pressure, P_L $[psig]^{**}$	95.2
High Side Pressure, P_H $[psig]^{**}$	324.7
Total Refrigerant Mass, m $[lb, kg]^{**}$	1.875, 0.85
* Unit current draw does not state whether real or reactive power is given on the rating plate ** Experimentally calculated	

Chapter 2. Detailed Description of the Current Status

The current air-source geo-exchange systems have challenges related to a drop in efficiency when temperatures begin hovering around and “below freezing”, where defrost cycles and supplementary heat are required, resulting in reduced COPs [7]. To combat this, ground and water-source heat pumps (geo-exchange systems) aim to remove heat from quasi-constant temperature heat sources via the ground or large bodies of water. However, the high cost related to installation, and possibly land area cost in high-density urban environments for horizontal loop ground-source systems is a problem that still requires a solution.

The team will also focus on issues related to the previous design. The previous year’s project and investigation into combined-source geo-exchange systems has issues related to insufficient heat extraction from the outdoor coil, and a lack of in-depth investigation into heat transfer mechanics and sensitivity analysis for the design for different scenarios.

2.1 Problem Statement

The conventional geo-exchange systems that are on the market include conventional heat exchangers such as the vertical and horizontal outdoor loop designs which require large installation costs and can still catastrophically fail due to the inability to maintain. Additionally, the previous attempt at designing a multi-source system resulted in excessive ice build up which caused heat pump lock out before the desired runtime. This lock out occurred due to insulation caused by the ice layer resulting in insufficient heat transfer. For this reason, this project aims to provide a working prototype that does not lock out before the desired runtime and has a comparable COP to current standard systems while simultaneously removing the need for expensive external heat exchanger loops.

2.2 Project Hypothesis

It is expected that through a first-principles design methodology coupled with numerical simulations, the revised alpha prototype should be able to run continuously for the desired runtime of at least ten hours while still operating with a coefficient of performance near the manufacturer’s specification of $COP_H = 4.3$.

Chapter 3. Theoretical Background

3.1 Patent Search

The following section covers the patents that were researched during the beginning of the design phase of the project.

3.1.1 Latent Heat Thermal Battery

US patent No. 6105659 describes a rechargeable thermal battery for latent energy storage and heat transfer. This device is intended to work in conventional HVAC building system design. It's a thermal reservoir capable of delivering or absorbing large amounts of heat quickly. It does so without refrigerant or the standard compression expansion cycle of standard heat exchanger. It instead uses other material properties of gels, solids and aqueous solutions in conjunction with Peltier devices to keep a large amount of thermal energy ready to be utilized. A Peltier device is a solid-state heat pump that uses the Peltier effect to move head from one side of a surface to another. These devices are limited to a low level of heat transfer rate, but, used in conjunction with a substance with a large heat capacity, can provide large amounts of heating or cooling on demand.

3.1.2 Thermoelectric Generator with Latent Heat Storage

US patent No. 4251291 details a method for storing solar electricity. Rather than storing energy in batteries this design utilizes the latent heat of a material to provide a constant temperature to a thermopile. Using a latent heat medium and an absorber plate for the solar collector provides a temperature gradient to cause the thermopiles to generate electricity. The concept of this invention is that the sun would melt the latent heat medium, likely water, in the day and in the evening or cloudy periods; the thermopiles would then draw energy out of the medium to provide electricity. Further investigation would be needed to fully understand this patent, since it seems to be fundamentally flawed, but the team's understanding of the thermodynamics that are taking place here could be much more complicated than first meets the eye.

3.2 Theoretical Fundamentals

The following section will cover the theoretical fundamentals that provides a basis for the project. Sections will be built up from each other and their theory will be used in a first-principles approach throughout the design of the prototype, and for explanations of virtual and real-world results.

3.2.1 Thermodynamics

Looking at Figure 3.1, the temperature-specific volume relationship can be seen for a fluid that is held at a constant pressure. Initially, starting at point one, the fluid is called a compressed liquid or subcooled liquid: The fluid is in the liquid form at a temperature that is below its saturation temperature, or the temperature at which it will boil for a given pressure. If the substance is heated to point two, its saturation temperature, the substance is called a saturated liquid. Next, heating beyond point two and all the way to point four, the substance is a liquid-vapour mixture, and any heat added to the fluid in between these points results in increasing the ratio of vapour-to-liquid (or the quality of the fluid) but does not result in a temperature increase; it is this increase in quality without a change in temperature which results in the latent heat of vaporization, with a similar phenomenon occurring for a phase change between solid and liquid, called the latent heat of fusion. Once reaching point four, the fluid has a quality of one (or in other words, is 100 percent vapour), and is called a saturated vapour. Any subsequent added heat to the fluid will result in a temperature increase, and what is called a superheated vapour. Gathering data for temperature-specific volume relationships for various pressures, and plotting it, results in Figure 3.2 with the signature dome shaped region called the saturated liquid-vapour region. It should also be noted that for pressures at or above the critical pressure of the substance that will pass through the critical point as shown in Figure 3.2 or higher, there is no noticeable phase change between liquid and vapour, but rather the substance always appears to be in one phase, liquid or vapour with it gradually appearing as one or the other sufficiently far from the critical point.

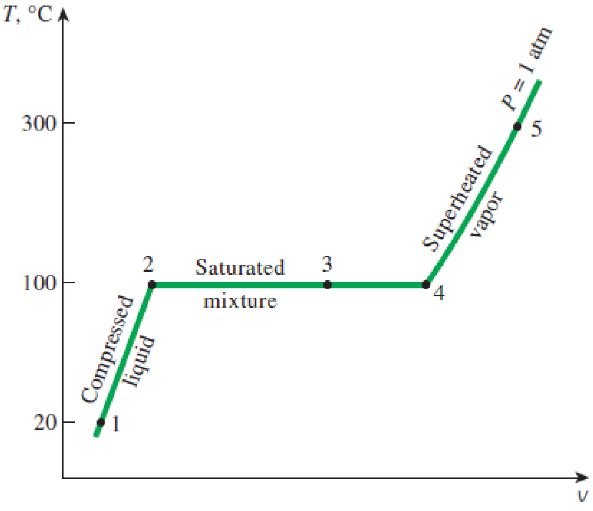

Figure 3.1 - T-v Diagram for a Fluid at Constant Pressure
As illustrated in [6], *Fig. 3-10*

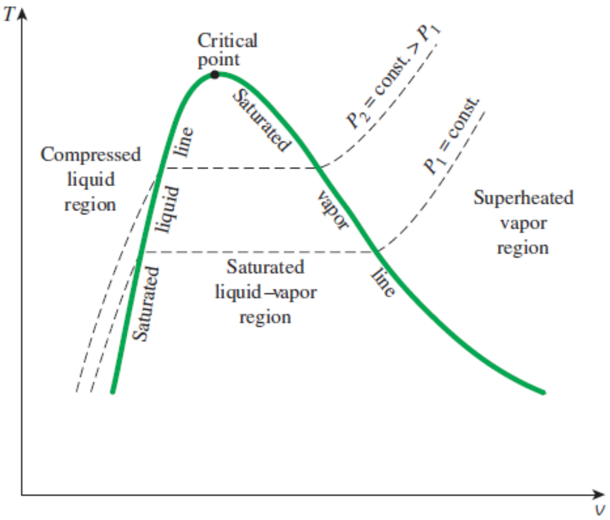
T
v
Critical point
Saturated liquid line
Saturated vapor line
Compressed liquid region
Saturated liquid–vapor region
Superheated vapor region
P₂ = const. > P₁
P₁ = const.

Figure 3.2 - T-v Diagram for a Pure Substance
As illustrated in [6], *Fig. 3-17*

3.2.2 Latent Heat

Latent heat is the energy required for a material to change phases, such as from liquid to gas or vice-versa compared to sensible heat which is just the heat required for temperature change without phase change. This heat will be extracted though the heat exchanger process when the water in the tank is frozen. Also, more energy can be extracted through the phase change process than through temperature change. A calorie is a unit of energy that is defined as the energy required to raise the temperature of one cubic centimeter liquid water by one degree. To decrease the temperature of the same amount of water from 0°C liquid to 0°C solid requires the removal of approximately 80 calories to achieve. Therefore, there is an 80-fold increase in the amount of energy that is available during liquid-solid phase change and the team's geo-exchange system design will attempt to also use this principle to further heat a home.

3.2.3 General Heat Pump Operation

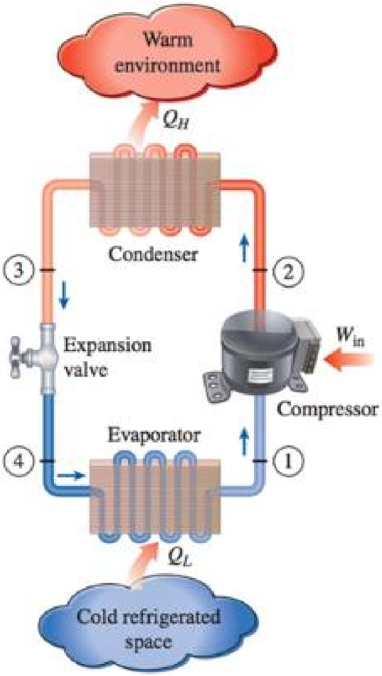

Figure 3.3 - Vapour-Compression Refrigeration Cycle

As illustrated in [6], *Fig. 11-3*

Heat pumps use the concept of refrigeration cycles to heat or cool a home. The specific type of refrigeration cycle that is used for heat pumps is the vapour-compression refrigeration system (VCRS). In a VCRS, the refrigerant undergoes a phase change just as it will with the geo-exchange heat exchanger. This includes four main components: an evaporator, a condenser, a compressor, and an expansion valve. The cycle is graphically displayed in Figure 3.3.

First, the heat is extracted from the sink (the outdoor environment either being the air, ground, or body of water), and for the current design, the heat will be extracted from the ground via the tank and water contained within it. The refrigerant flows through the heat exchanger that is placed in the ground and evaporates as it does so. Next, the evaporated refrigerant enters the compressor which is responsible for moving the refrigerant, and consequently compresses it due to the system restriction of flow, thereby increasing the pressure—in turn increasing the temperature. After leaving the compressor, the refrigerant flows through the condenser where its temperature is much higher than the surroundings, and, therefore, rejects the heat into the desired space and lowers its temperature to the point that it condenses and sub-cools (temperature drops below the saturated liquid temperature). Lastly, the returning liquid refrigerant, still above the outdoor surrounding temperature, is throttled "through an expansion valve or capillary tube," where its temperature drops below that of the surroundings, and the refrigerant ends up as a low-quality liquid-vapour mixture before re-entering the outdoor coil [6].

3.2.4 Heat Pump Performance

"The performance of refrigerators and heat pumps" is not actually expressed in efficiency like other machines, but in what is called the coefficient of performance (COP) [6]. Essentially, the COP states a ratio of how many units of heat,Q, is moved into or out of the conditioned space for every unit of energy, in the form of work, W, that is required to be put into the system. In other words, the COPs of refrigerators and heat pumps are equal to the following:

$$COP_R = \frac{Q_L}{W_{net,in}}, COP_H = \frac{Q_H}{W_{net,in}}$$

And since the work-energy put into the system is rejected into the conditioned space for heat pumps, there is a relationship between the two in that

$$COP_H = COP_R + 1.$$

To build up from this and the previous section, schematics for ideal and actual cycles, and their equivalent temperature versus entropy plots, with numbered locations where thermodynamic state variables of interest will be found are shown in Figure 3.4 and Figure 3.5. For design and experimental purposes, the thermodynamic state variables can either be chosen by the designer to achieve a desired system, or retrieved from measurements, with a requirement of only two known state variables to be able to determine the entire system at the specific point as was seen in the plots in section 3.2.1.

To find Q_H, equating the difference of enthalpy between points two and three for the ideal case in Figure 3.4 and points 2' and five for the actual case in Figure 3.5 is done. It should also be noted that the difference between points two and 2' is related to the irreversibility or efficiency of the actual compressor compared to the ideal compressor. So, in other words, the amount of heat energy put into the conditioned space can be found in power form to be:

$$\dot{Q}_{H_{ideal}} = \dot{m}(h_2 - h_3), \dot{Q}_{H_{actual}} = \dot{m}(h_2{}' - h_5)$$

Where the dot above the variable shows the time rate, and $\dot{m}$ is defined as the mass flow rate of refrigerant. Next, to find $\dot{W}_{net,in}$, the difference of enthalpy between points two and one can be used for both scenarios in Figure 3.4 and Figure 3.5 if a design approach is taking place; otherwise, for experimental results, one can just take the electrical power draw of the compressor or the unit (the product of its current draw, I, and operating voltage, E_{in}), resulting in the following values:

$$\dot{W}_{net,in_{design}} = \dot{m}(h_2 - h_1), \dot{W}_{net,in_{experimental}} = EI$$

It should also be realized that the mechanical work-energy input of the compressor is not used over the total work-energy input into the motor because that would give a fictitious heat pump performance and not the true ratio of energy output versus energy input. Lastly, to get a more accurate COP, the real power draw should be used instead of the reactive power of the system, because compressors containing motors have high inductances resulting in reactive power being drawn and discharged.

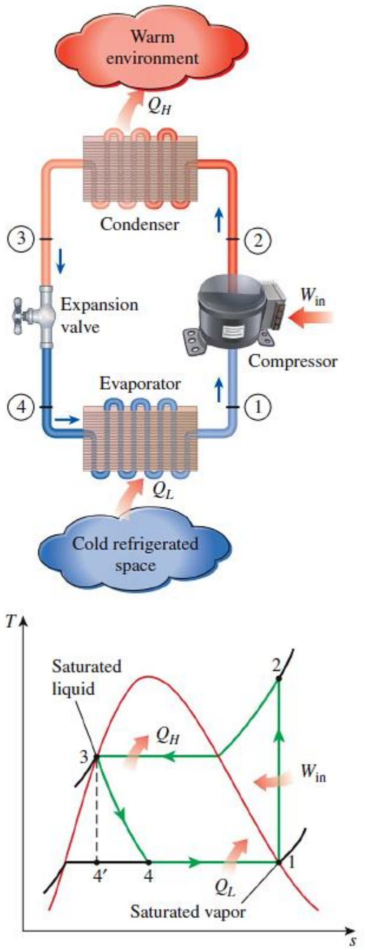
Warm environment
Q_H
Condenser
③
②
Expansion valve
W_{in}
Compressor
Evaporator
④
①
Q_L
Cold refrigerated space
T
Saturated liquid
2
3
Q_H
W_{in}
1
4′
4
Q_L
Saturated vapor
s

Figure 3.4 - Ideal Vapour Compression Cycle

As illustrated in [6], *Fig. 11-3*

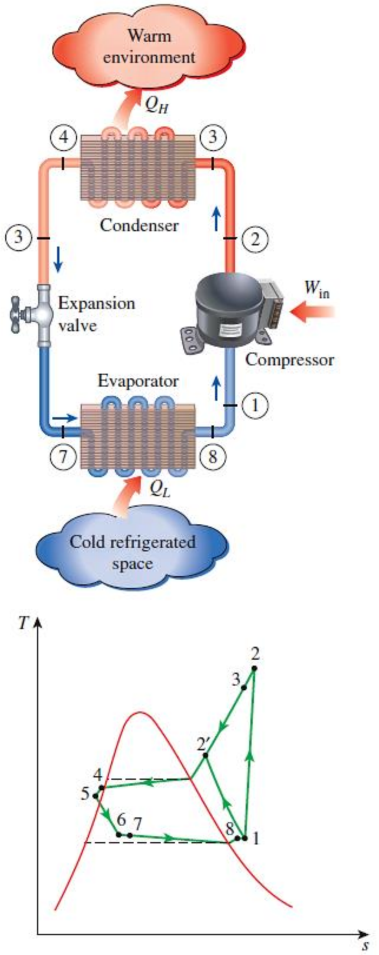
Warm environment
Q_H
④
③
Condenser
③
②
Expansion valve
W_{in}
Compressor
Evaporator
①
⑦
⑧
Q_L
Cold refrigerated space
T
2
3
2′
4
5
6
7
8
1
s

Figure 3.5 - Actual Vapour Compression Cycle

As Illustrated in [6], *Fig. 11-7*

3.2.5 Geo-Exchange Heat Pumps

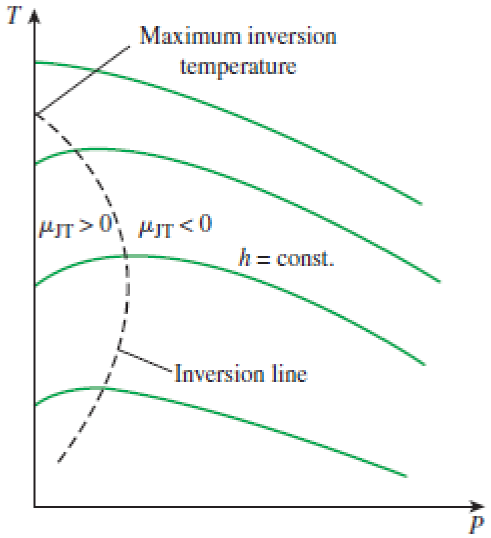

Figure 3.6 - Isenthalpic Throttling Temperature-Pressure Relationship

In conventional geo-exchange systems, the units consist of four main components: The pump (compressor), thermal expansion valve, evaporator coil, and condenser coil, and these are equivalent to the components in the refrigeration cycle. The pump circulates refrigerant through the closed loop, the evaporator coil removes heat from the local environment, the condenser supplies heat to the local environment, and the thermal expansion valve keeps the pressures in both coils at a predetermined level, while also being responsible for the cooling effect when refrigerant throttling takes place at near isenthalpic conditions, and described in greater detail through the Joule-Thomson coefficient, μ_{JT}, shown below in Figure 3.6 as illustrated in [6], Fig. 12-3. Essentially, if the refrigerant temperature and pressure are such that their state is within the inversion line during isenthalpic throttling, then the refrigerant temperature will drop, and vice-versa if the refrigerant temperature and pressure thermodynamic state is outside of the inversion line.

When heating or cooling a space, it is common for the external environment to be the opposite of what the system is trying to accomplish. In warm environments, geo-exchange systems are configured to cool spaces and in cooler environments the function of the system is quite the opposite. To pull a lot of heat out of a cool environment or to put a lot of heat into a warm environment requires a large surface area. This requirement drastically increases the cost of construction for a conventional geo-exchange system.

3.2.6 Boiling and Condensation

From section 3.2.1, it was seen that when heat is added to a saturated liquid, its quality will begin to increase, and vice-versa when heat is removed from a saturated vapour. When looking at the microscopic level of heat transfer rather than the macroscopic level of thermodynamics, one can see that boiling and condensation are both forms of convective heat transfer, but are different “from other forms” in the fact “that they depend on the latent heat of vaporization h_{fg} of the fluid and the surface tension σ at the liquid-vapour interface" [8]. This is because both boiling and condensation involve buoyancy-driven fluid motion due to temperature changes of the fluid, but with the difference that vapour or liquid also move within the liquid or vapour interface, respectively, and are key drivers of convective heat transfer

3.2.6.1 Boiling

Unlike evaporation which can occur at temperatures below the saturation temperature for a liquid when the vapour pressure at the "liquid-vapour interface" is below that of the saturation pressure, boiling only occurs at the saturation temperature of the liquid, T_{sat}, when heat is added [8]. For boiling to occur when heat is transferred to a liquid via a solid, the solid must be kept at a temperature above the saturation temperature of the liquid, T_s, in order to promote heat transfer, and is characterized by Newton's equation of heat transfer:

$$\dot{q} = h(T_s - T_{sat})$$

Boiling is also divided into a passive heat transfer mode called pool boiling (where fluid movement is restricted to natural convection), and a forced heat transfer mode called flow boiling, with both being able to take place with the bulk fluid at temperatures below the saturation temperature, called subcooled boiling, and with the bulk fluid temperature at the saturated temperature called saturated boiling. For subcooled boiling, the vapour bubbles that form at the solid-liquid interface are cooled via heat transfer with the surrounding liquid as they rise and condense and collapse back into a liquid. For saturated boiling, heat transfer between the forming vapour bubbles and the surrounding liquid only takes place due to a temperature gradient between the possibly superheated vapour bubbles and the liquid at the saturation temperature, and, thus, the vapour bubbles do not transfer heat once reaching the saturation temperature and do not condense and collapse back into a liquid.

3.2.6.1.1 Pool Boiling

Pool boiling itself is divided into many regimes and is shown in Figure 3.7 and Figure 3.8 for water, each with their own approximate equations to describe the heat transfer rate. At subcooled bulk fluid temperatures, vapour bubbles only form at the solid-liquid interface but don't make it to the liquid-vapour interface. At saturated bulk fluid temperatures with negligible temperature difference at the solid-liquid interface, no vapour bubble formation is seen due to the liquid only being "slightly superheated in this case … and evaporates when it rises to the free surface" with heat transfer primarily being the same as that of conventional natural convection, and is rightfully named natural convection boiling [8].

When the solid-liquid interface temperature differential increases sufficiently, nucleate boiling takes place and is split into two regions: For smaller temperature differentials, vapour bubbles form at the solid-liquid interface, but don't reach the liquid-vapour interface, and the increase in heat transfer is due to the increased fluid motion of "stirring and agitation caused by the entrainment of the process" from the liquid filling the vacated volume where vapour bubbles rose from [8]; as the temperature differential further increases, continuous columns of vapour bubbles rise from the solid to the liquid-vapour interface and results in much higher heat transfer rates, until reaching a maximum due to a larger fraction of the solid being covered by vapour which acts like an insulator when compared to liquid being in contact with the solid. Due to the higher heat transfer rates and relatively small difference in energy input to heat the fluid, "nucleate boiling is the most desirable boiling regime in practice" [8].

As the fraction of vapour in contact with the solid increases and passes the region of maximum heat transfer, the boiling regime is said to be called transition boiling, and an increased temperature differential between the ever-increasing solid-vapour interface results in a decreased heat transfer rate. This is due to increasing the thickness of the vapour film, and, thus, increasing the thermal resistance between the liquid and the solid because of the decreased thermal conductivity of a gas compared to a liquid.

Eventually, a continuous vapour film at the solid-liquid interface forms, and this regime is called film boiling. Increases in heat transfer by increasing the temperature differential are now only the result of the effects of radiative heat transfer taking place.

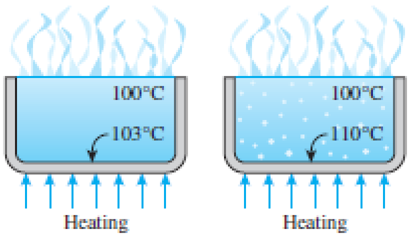

(a) Natural convection boiling

(b) Nucleate boiling

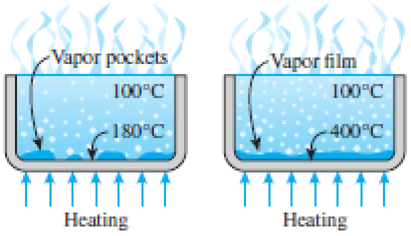

(c) Transition boiling

(d) Film boiling

Figure 3.7 - Pool Boiling Regimes
As illustrated in [8], *Fig. 10-5*

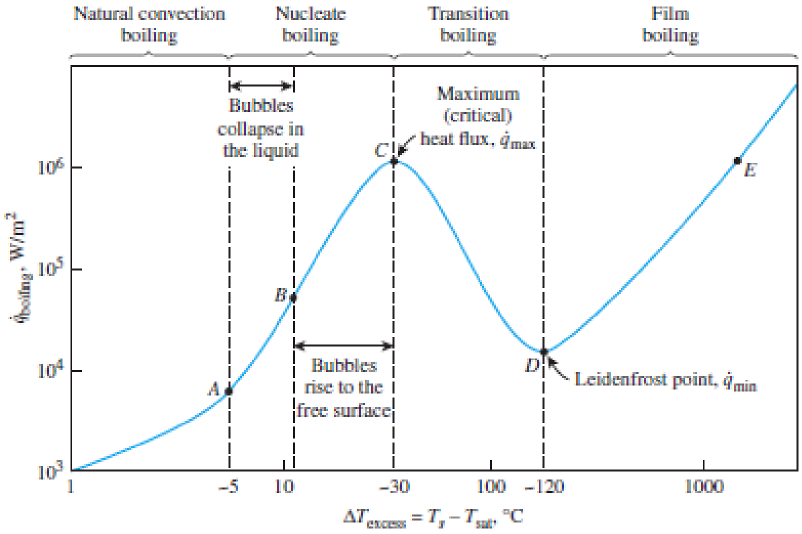

Figure 3.8 - Pool Boiling Regimes versus Heat Transfer
As illustrated in [8], *Fig. 10-6*

3.2.6.1.2 Flow Boiling

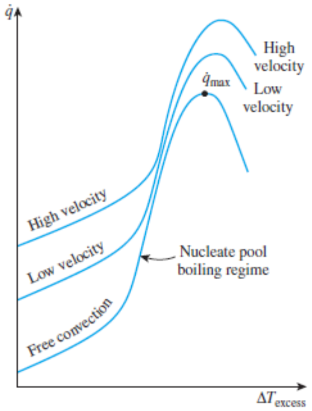

Figure 3.9 - External Flow Boiling
As illustrated in [8], *Fig. 10-18*

Either internal or external, this method of boiling has "combined effects of [forced] convection and pool boiling" [8]. External flow boiling, which can be comprised of pool boiling and forced convection, has its greatest effects during nucleate boiling as can be seen in Figure 3.9, where even a low fluid velocity can have large impacts on the heat transfer throughout different temperature differentials and a large difference for the maximum heat transfer.

Internal flow boiling in tubes, also called two-phase flow, has no free surface, resulting in the liquid and vapour being entrained and flowing together within a tube and complicated proposed correlations for the determination of heat transfer [8]. Figure 3.10 shows the different stages of flow boiling as the temperature differential between the tube and fluid increases; it begins similar to pool boiling with no visible vapour bubble formation, and heat transfer rates comparable to those of internal forced convection. However, as the temperature differential increases, bubble formation around the solid-liquid interface on the internal pipe walls is noticed, with the vapour bubbles being moved with the fluid. This is named bubbly flow due to its appearance. With an increasing temperature differential at the solid-liquid interface, the vapour "bubbles grow in size and eventually coalesce into slugs of vapour … [with up] to half the volume in the tube" being comprised of vapour (resulting in its name being slug flow) and a noticeable enhancement of heat transfer taking place [8]. Further increase in the temperature differential causes the fluid core to become comprised entirely of vapour, while the liquid takes up the remaining outer section, and is named annular flow, and it is in this regime where maximum heat transfer rates can be reached. Similar to pool boiling, the next regime involves the thinning of "the annular liquid layer," and "dry spots" beginning to form on the tube wall, which has the same effect as that of the transition boiling regime in pool boiling in that the heat transfer rate decreases because of the decreased thermal conductivity of vapour compared to that of the liquid and is named transition flow. Once the inner tube walls have become dry and are surrounded by only vapour, the boiling regime becomes mist flow with the only liquid being from suspended droplets in the vapour. From this point onwards, increased heating and temperature differentials result in an increase in the quality of the liquid-vapour mixture until unity is achieved reverting the heat transfer mechanism back to forced convection, but with vapour rather than liquid as the medium through which the process takes place.

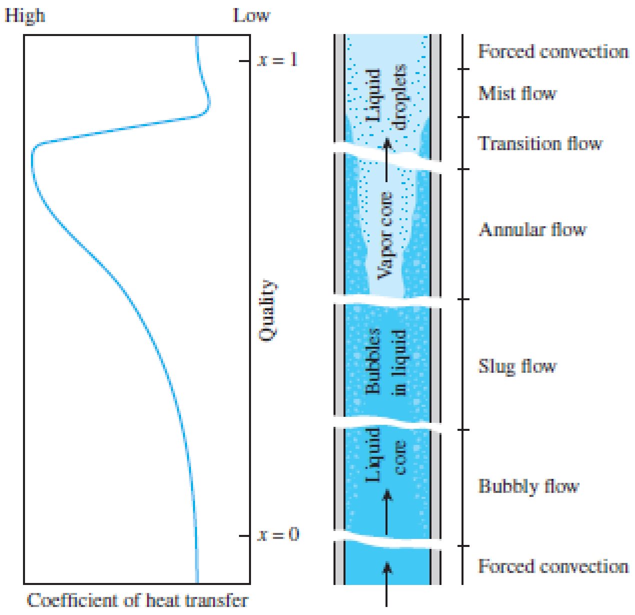

Figure 3.10 - Two-Phase Flow
As illustrated in [8], *Fig. 10-19*

3.2.6.2 Condensation

For condensation to take place, the fluid temperature must be brought below that of its saturation temperature, T_{sat}, for its given pressure. And analogous to boiling, for condensation to occur when heat is transferred to a vapour via a solid, the solid must be kept at a temperature below the saturation temperature of the vapour, T_s, in order to promote heat transfer. However, a difference between boiling and condensation behaviours becomes obvious from two observed forms of condensation: “film condensation and dropwise condensation” [8].

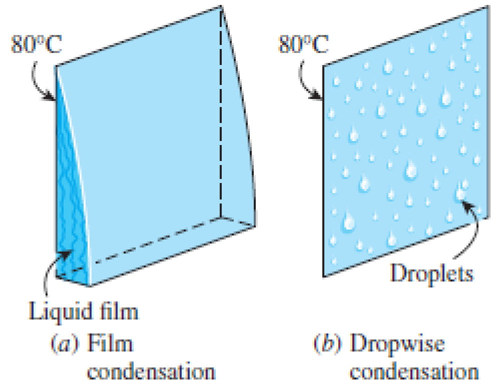

Figure 3.11 - Forms of Condensation
As illustrated in [8], *Fig. 10-20*

As shown in Figure 3.11, film condensation results from when vapour that is being condensed wets the entire cooling surface while running down the surface, thereby impeding heat transfer from the thermal resistance of the liquid and the increased temperature of the liquid in contact with the vapour compared to that of the cooling surface due to the created temperature gradient. Dropwise condensation, on the other hand, results in droplets forming on the cooling surface instead of a film which results in more cooling surface area always being in contact with the vapour that is trying to be condensed [8]; therefore, heat transfer rates for dropwise condensation are higher than those of film condensation, and is a more desirable form, but is very difficult to achieve in practice for prolonged time periods. For this reason, conservative analysis should be implemented using calculations for film condensation rather than dropwise condensation.

3.2.7 Balance point

In addition, to environmental constraints, a geo-exchange system also has thermodynamic constraints. As the external environment becomes cooler there is less heat that can be extracted to heat a dwelling due to the reduced temperature differential between the refrigerant and external environment. Additionally, as the external environment cools, the heating demand grows as now more heat is being lost to the environment. There comes a point where it is no longer physically possible to pull enough heat form the environment to cool the dwelling space. This point is known as a balance point and occurs when the heating output of the evaporator equals the required heating load of the dwelling. For geo-exchange systems, this point is at an external temperature of approximately 0°C. Below this point, geo-exchange systems require supplemental heating sources such as electric heating to assist with conditioning the dwelling space so that a comfortable temperature can be maintained [9].

3.2.8 Heat Transfer through COMSOL Multiphysics

Heat Transfer is the main physics that is used for the COMSOL models. It occurs in the fluids, the solids, and within the pipes.

3.2.8.1 Heat Flux

The heat flux is the flow of energy per unit of area per unit of time. In metric units this is measured in W/m^2. This can also be described as the rate of heat energy that crosses a surface boundary. The heat flux used during the COMSOL simulations is convective heat flux. This is defined as:

$$\dot{q}_0 = h(T_{ext} - T)$$

The heat transfer coefficient can either be defined manually in COMSOL or controlled through selection of the type of convective heat flux that will be used. The convective heat flux that was used for this project was External Natural Convection. This occurred between the tank water and the ground, and between the plate and the tank water.

Natural convection occurs when the fluid motion is created by buoyancy forces induced by density gradients due to the temperature difference in the fluid. These buoyancy forces induce free convection currents. Forced convection is when the fluid is forced to move by an external force. External convections occur over a surface when the fluid is free to move unrestricted.

For the team’s design, natural convection on a vertical wall is used because the ground will heat the water causing it to rise if the water temperature is above 4°C. The plate will also be cooling the water causing it to rise if below 4°C, and pushing the warmer water down.

3.2.8.2 Wall Heat Transfer

Wall heat transfer is the heat exchange that occurs across a pipe wall. COMSOL uses this in the Heat Transfer in Pipes section. The thickness of the pipe wall is defined as the wall layer and multiple layers can be added if the pipe is made up of different materials.

3.2.8.2.1 Heat Transfer Coefficient of Pipe Wall

The heat transfer of the pipe wall is a combination of resistances, which restrict the flow of the heat. The effective heat transfer coefficient is defined as:

$$h_{eff} = \frac{(2\pi)}{\left(\frac{1}{r_0 h_{int}}\right) + \left(\frac{1}{r_N h_{int}}\right) + \left(\frac{\ln(\frac{r_n}{r_n - 1})}{k_{wall,n}}\right)}$$

3.2.8.2.2 Internal Film Resistance

Internal film resistance occurs for all of the pipe lengths. The internal film resistance is the contact resistance that occurs at the atomic level around the inside of the pipe. This resistance occurs between the refrigerant inside the pipe and the copper pipe material. The heat transfer coefficient is defined as:

$$h_{int} = Nu\left(\frac{k}{d_h}\right)$$

3.2.8.2.3 External Film Resistance

External film resistance occurs in the pipe's outer layer that is in contact with the water. Any pipe that is in contact with the plate or the ground does not experience this type of resistance. This resistance is caused by either external natural convection or external forced convection. Fluid velocity is impeded close to the wall and a boundary layer is created, which in turn creates a temperature boundary layer. Because of this, at locations further from the wall, there is both convection and conduction, but closer to the wall only conduction occurs. This resistance to the heat transfer that occurs close to the pipe wall is equivalent to the external film resistance. The heat transfer coefficient is defined as:

$$h_{ext} = Nu\left(\frac{k}{d_h}\right)$$

Chapter 4. Detailed Project Activities and Equipment

4.1 Design Calculations

The following section covers the calculations that were completed to better understand the required heat transfer needed from the design. The full derivations can be seen in Appendix C.

4.1.1 Building Heat Loss

Taking a standard home design for the Vancouver area, and performing heat loss calculations, the total heat loss for the home was found to be:

$$\dot{Q}_{\mathrm{actual}} \cong 10.45\ \mathrm{kW}$$

4.1.2 Heat Transfer through Outdoor Coil (Horizontal)

Next, the theoretical maximum heat transfer through the current outdoor coil was found to be:

$$\dot{Q} \cong 1294.91\ \mathrm{W}$$

$$\therefore \mathrm{n} = \frac{\dot{\mathrm{Q}}_{\mathrm{actual}}}{\dot{\mathrm{Q}}} = \frac{10450\ \mathrm{W}}{1294.91\ \mathrm{W}} \cong 8.07$$

With a required increase in heat transfer, the easier parameter to change to meet demand is the surface area via fins or increasing the length of the tubing in the outdoor coil. Surface area makes more sense because increasing pipe length results in changes of refrigerant pressure via frictional losses, changes to the mass of refrigerant in the system, and more in-depth study into the current refrigeration design.

$$\text{Current Surface Area} = \mathrm{A_s} = \pi \mathrm{DL} \cong 0.2675\ \mathrm{m}^2$$

$$\text{Required Surface Area} = \mathrm{A_s}' = \mathrm{nA_s} \cong 2.1831\mathrm{m}^2$$

4.1.3 Energy & Power Capacity in Tank

Ignoring heat transfer through the ground and tank into the water, the amount of time that heat can be provided by the geo-exchange system by just using sensible heat from the water is:

$$\Delta t_S \cong 0.8042h$$

Similarly, the amount of time that heat can be provided by the geo-exchange system by just using latent heat from the water is:

$$\Delta t_L \cong 15.8974h$$

Adding the calculated times that the tank can provide sensible heat and latent heat of fusion results in a total time of:

$$\text{Total Time} = \Delta t_S + \Delta t_L \cong 16.7016\ hr$$

Meaning, that if all the water in the tank could be frozen via heat transfer, it would be able to provide continuous heat for over 16 hours if heat were to be extracted from the tank at a rate of approximately 10,567 watts. Realistically, though, it would be difficult to freeze the entire geo-exchange tank without first locking out the heat pump due to liquid refrigerant being sent back to the compressor from inadequate heat transfer.

4.1.4 Pipe Losses through Outdoor Coil

This calculation will need to be updated after the system has been run to get accurate pressure and temperature readings from the high-pressure and low-pressure sides of the heat pump, but, at the moment, the pressure loss through the outdoor coil is calculated to be:

$$\Delta p_L \cong 56.182\ kPa$$

This was completed assuming a straight pipe, and this value will have to be updated to take into account any bends that are needed for the final design, with the full calculation shown in Appendix C.4.

4.1.5 Changing Heat Capacity and Freezing Point of Fluid

If a five percent by mass ethylene-glycol-to-water ratio is used in the tank:

$$Q_s \cong 44.452\ MJ \text{ and } \Delta t \cong 1.169h$$

If a ten percent by mass ethylene-glycol-to-water ratio is used in the tank:

$$Q_s \cong 49.487\ MJ \text{ and } \Delta t \cong 1.301h$$

With these values, optimization of the amount of anti-freeze added to the tank can be found. However, as noted earlier, the addition of anti-freeze into the system can pose environmental risks and would require more vigorous design to prevent any leaching into the surrounding soil.

4.1.6 Refrigerant Volume

To determine the required amount of refrigerant that the geo-exchange system will use, desired indoor and outdoor coil temperatures must be chosen, and is a problem of optimization. On the one hand, a lower outdoor coil temperature can result in an increased heat transfer rate; on the other hand, lowering the outdoor coil temperature by decreasing its respective refrigerant pressure will result in a cooler indoor coil as well, which will result in a decreased heat output into the conditioned space. Looking over criteria, the team decided that a greater temperature differential between the outdoor coil and surrounding fluid was more important for this specific project. Therefore, an outdoor refrigerant design temperature of $-10°C$ was chosen with its equivalent pressure of $68.3\ psig$ or approximately $470.9\ kPa$. However, after talking to the refrigeration mechanic, it was found that the system design might not work as intended if coil temperatures were changed, and so the original outdoor coil temperature of $-2°C$ was kept. This resulted in the system being filled with 1 pound and 14 ounces to meet the operating conditions of the compressor.

4.2 Design Approach

The following section covers the steps that were taken to create the end design.

4.2.1 Incumbent Design

The incumbent design was selected by the previous design team, from the 2016-2017 design project, for its scalability for future loops as well as its ease of manufacturing, and this pipe configuration can be seen in Figure 4.1 below.

The previous design team did not utilize fins or additional methods to increase the heat transfer. Also, the design was only able to form ice around the lower coil, therefore, implying that only one coil was effective at transferring heat, and only one of the two coils remove the latent heat of the water. This significantly lowered the available heat energy that could be extracted. With this coil design, the system was only able to achieve slightly over two hours of continuous operation—an amount deemed insufficient for the design criteria.

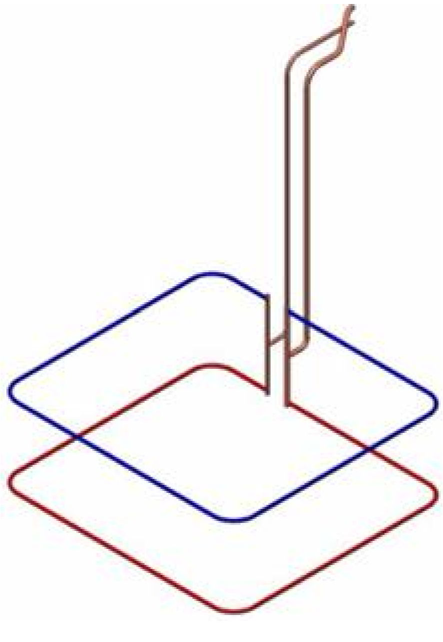

Figure 4.1 - Incumbent Pipe Configuration

As illustrated in [10], *Fig. 8-1*

4.2.2 Calculations

The calculations that were described in Section 4.1 were used to determine what was needed in the new design so that this heat exchanger could maintain set point temperature in a standard home design for the Greater Vancouver area. The building heat loss was calculated and then the theoretical maximum heat transfer through the outdoor coil for the incumbent design was calculated. This showed the team that the new design required approximately 8.07 times the heat transfer that is currently being created.

The team decided to achieve the additional heat transfer through increasing the surface area of the components where the heat transfer will take place. This was decided because the surface area is an easier parameter to change to meet demand. This change can be done using an increased length or by adding fins. The designs that the team moved forward with were the helical design, fin design using a helical coil or serpentine coil, and, finally, the late designs, either horizontal or vertical. These designs are narrowed down in Section 4.3.

4.3 Design Selection

The following section covers the various designs that were created for the pipe configuration to increase surface area and meet the required heat transfer.

4.3.1 Helical Design

When doing research to determine ways to enhance the heat transfer, it was found that heat transfer could be increased via the introduction of turbulence to the system either through surface roughness, using insets inside the pipe, or a helical design. The helical design being easy resulted in further investigation into the increase of heat transfer due to the resulting centrifugal forces on the fluid being moved [11].

The helical design shown in Figure 4.2 is used in many applications in industry because a secondary flow is induced by the centrifugal forces that consists of a pair of longitudinal vortices that result in highly non-uniform local heat transfer coefficients [11]. However, this results in an increase of not only the heat transfer rate, but also frictional losses. Therefore, the main issues that were found with this design were the space management due to the large height required to reach the needed 22 ft. of equivalent piping length, and pressure drop across it.

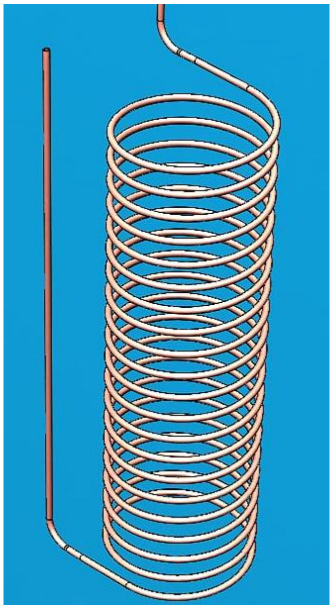

Figure 4.2 - Helical Design for Pipe Configuration Selection

4.3.2 Fin Design

The use of fins, as seen in Figure 4.3 and Figure 4.4, is a design that would increase the heat transfer rate dramatically. However, the main issues in this type of design is the increase in manufacturing complexity, most probably not manufactured in-house, if anything but straight piping is sought, and it would still be expensive to buy off the shelf and assemble. For this reason, the team decided that this design would not be followed through.

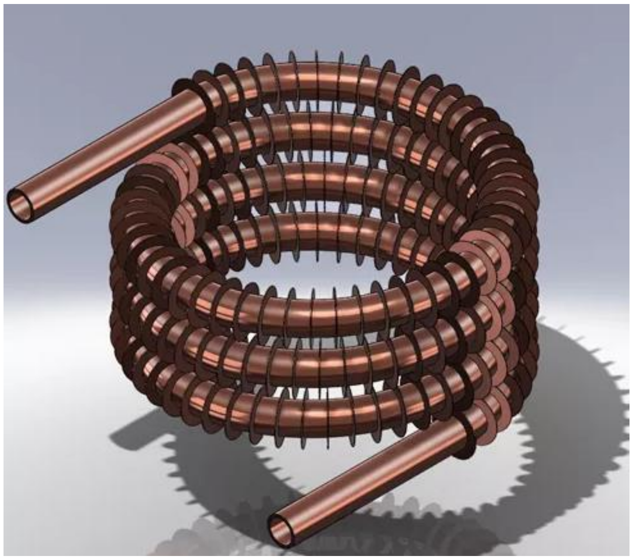

Figure 4.3 - Helical Fin Design for Pipe Configuration Selection [12]

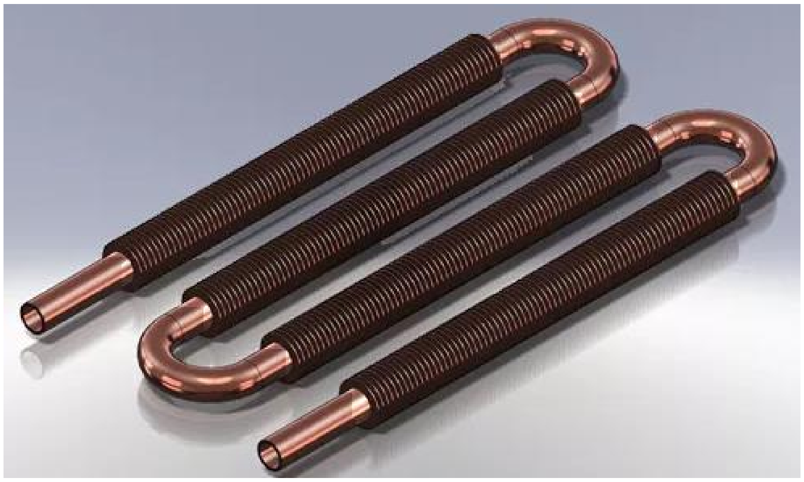

Figure 4.4 - Serpentine Fin Design for Pipe Configuration Selection [12]

4.3.3 Flat Plate Design

The initial flat plate design used two horizontal aluminum plates that would be formed around the piping and use heat conductive paste to further increase the heat transfer, and this design can be seen in Figure 4.5. The team realized the potential in this design because of the push to decrease the complexity of manufacturing, as well as decreasing the need for expensive and custom parts.

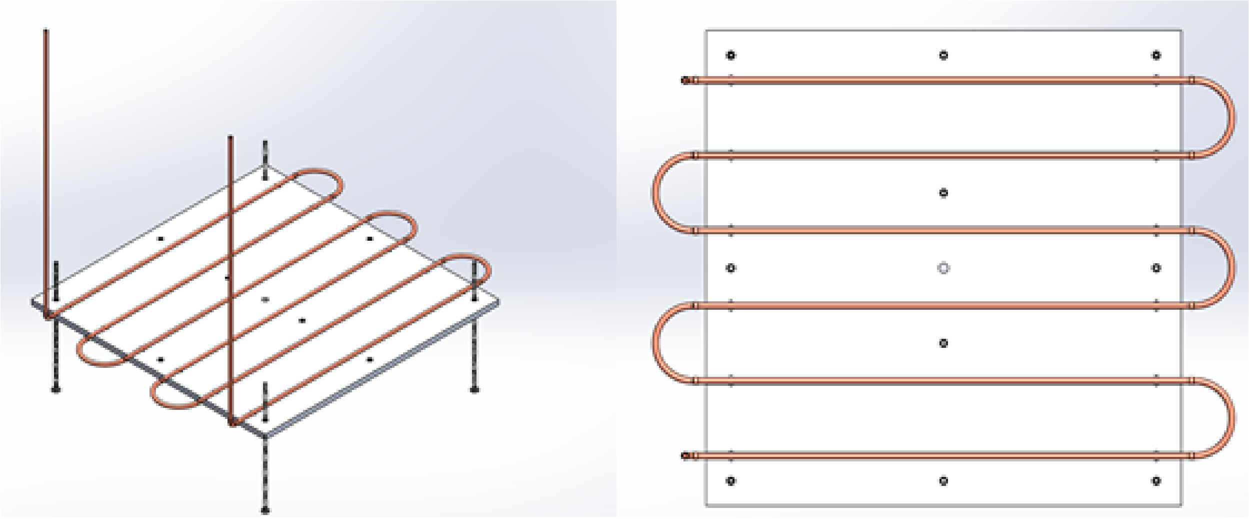

Figure 4.5 - Horizontal Plate Design for Pipe Configuration Selection

4.4 Final Design

The final design can be seen in Figure 4.6 below. The team kept the formed sheet metal design for increasing the surface area, but the plate orientation was changed to vertical to enhance the heat transfer rate: Placing the plates vertically allows the system to take greater advantage of the increased heat transfer due natural convection due to the changes in buoyancy in the water when temperature changes occur. The pipe configuration will have four runs across each of the plates and three 180-degree bends. The inlet line will split horizontally, and the refrigerant flow rate will be balanced resulting in an equal amount to each plate. If the design is done correctly, the refrigerant will be fully evaporated when it leaves the flat plates allowing the pump to more easily lift and move it to the suction line.

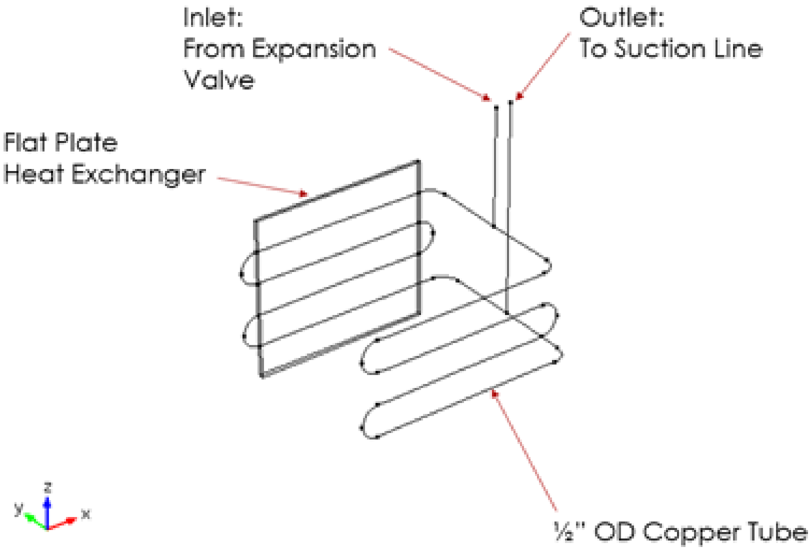
Inlet:
From Expansion
Valve
Outlet:
To Suction Line
Flat Plate
Heat Exchanger
½" OD Copper Tube
z
y
x

Figure 4.6- Vertical Plate and Piping Configuration

This fin configuration was then slightly updated after a meeting with Dr. Vahid Askari on March 23rd, 2018: The configuration changed to include secondary tubular fins snap fitted to the formed plate bends. All other dimensions were kept the same. This change will increase the useful contact area between the pipe and the fin, in turn increasing the heat transfer between these surfaces, with this addition illustrated in Figure 4.7.

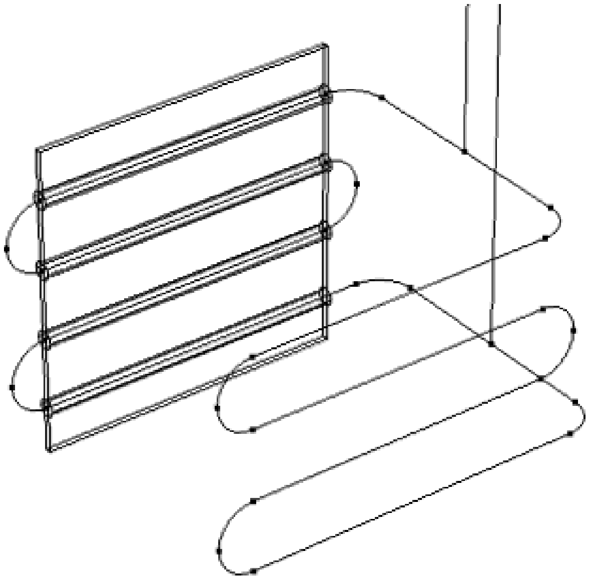

Figure 4.7 - Vertical Plate with Tubular Fins and Piping Configuration

4.5 COMSOL

The following section covers the process of creating a COMSOL model that can be used to determine parameters needed for the installation of the designed heat exchanger in areas around the world. This model focused on testing the geometry that the design team chose, the system parameters, and the needed initial temperatures to obtain the required heat transfer.

4.5.1 COMSOL Practice

For the design team to better understand the COMSOL Multiphysics software, various tutorials were completed. These tutorials focused on heat transfer in both fluids, pipes and solids, and pipe flow and buoyancy. This practice was ongoing throughout the project until March 16th, 2018 when the boundary conditions were determined, and the final models could be constructed.

4.5.2 COMSOL Models

The following section covers the COMSOL models that were used for this project.

4.5.2.1 Incumbent Design

Due to time constraints, a COMSOL model for the incumbent design was not created. This model would have been used to compare against the results gathered from the incumbent design for verification, but as it was already determined that that design was unsatisfactory due to low run time, the design team did not create the COMSOL model.

4.5.2.2 Geometry Models

The geometry models were created so that various simulations could just input the geometry instead of requiring a recreation each time. The two geometry models that were created were one for the final plate design and the other for the final plate design with the additional tubular fin attachments. The geometry that was created was shown in Section 4.4 in Figure 4.6 and Figure 4.7.

4.5.2.3 Vertical Plate Design

There were two final COMSOL models that were created. One being the simple vertical plate design and the other having the added tubular fins. These were used to compare the difference between the two designs and more accurately determine which would provide the ideal heat transfer. The results of running these simulations is documented in Section 5.1.

4.5.2.3.1 Original Vertical Plate Model

The original vertical plate model uses the geometry imported from the geometry models. The pipe and the plate geometry are imported twice. They are imported once, and then a difference is taken between them and the tank geometry. This creates a block of water the size of the tank with holes for the pipe and the plate. The pipe and the plate geometry are then imported once more to fill those holes, and, therefore, there is no overlap between the water and the metal objects.

The physics for this model uses Multiphysics for Heat Transfer in Fluids, in Solids, and in Pipes, as well as Pipe Flow.

Heat Transfer in Fluids uses two convection Heat Flux sections. The first affects the outside of the tank with a constant external temperature set to the ground temperature, T_g. The second heat flux is along the plate walls and edges and has a changing external temperature set to the dependant variable, T, of the Heat Transfer in Solids physics. This is equal to setting the water temperature directly around the plate to the external temperature of the plate so that the plate temperature affects the water temperature.

Heat Transfer in Solids used a single heat flux that uses external natural convection on a vertical wall. It has the external temperature set to the dependant variable, T_3, of the Heat Transfer in Fluids physics.

Heat Transfer in Pipes needed three separate Wall Heat Transfers. Two of the heat transfers needed a Wall Layer and an Internal Film Resistance. These two being the pipes within the plate and the pipes that sit above the water level. The last heat transfer, for the pipes exposed to the water, also requires an External Film Resistance to simulate the external natural convection between the pipes and the water.

Pipe Flow is needed to simulate the motion of the fluid within the pipe, so this motion effect of the heat transfer will be accounted for. Two T-Junctions are used at the nodes for the connection between the right and left plates. A Volume Force is also added to simulate the effect of gravity as the fluid flows downwards in the system.

The study for this model is a time dependent study with a physics-controlled mesh that collects data for fluid velocity, temperatures of the pipes, the plates, and the filled tank, and, also, pressure in the pipes. The simulation returns the temperature and pressure of the inlet and outlet pipes and animations of the full system over the desired time step.

4.5.2.3.2 Vertical Plate Model with Added Tubular Fins

The geometry is imported just as documented in the previous section. A difference is taken between the pipe and plate geometries and then they are both re-imported. The only difference in this model is that the geometry of the plate now includes the tubular fin attachments.

The physics and the study settings for this model are kept the same as the previously discussed model. These similarities allow the design team to run the simulations for the same conditions so that they can be easily compared.

4.5.3 Future Prototype Testing

The new heat exchanger design can increase its heat transfer even more by implementing changes to the parameters of the water or by adding other sources of heat as well as the use of the ground.

4.5.3.1 Addition of Anti-Freeze into the Tank

By adding anti-freeze to the tank (with Glycol used for data collection), the new anti-freeze-water mixture will have unique thermodynamic properties differing to a certain extent compared to that of water; of interest to this project, is that of a lower freezing temperature of the fluid, and that of a decreased specific heat capacity. Since there is a trade off between the two properties of interest, an optimization between the two must be made. According to Dr. Joseph Cheung, the recommended percentage of anti-freeze in water by mass in chilled water refrigeration systems (such as water-source geo-exchange systems) is five percent. At five percent by mass ethylene-glycol to water, the freezing temperature drops to $T = -2$°C [13], and the specific heat capacity drops from

$C_P = 4.202\ kJ/kg \cdot K$ to $C_P \cong 4.088\ kJ/kg \cdot K$ for a temperature of $T = 5°C$ [14]. This could be implemented into the COMSOL model by changing the tank water properties to match those of the mixed water-antifreeze solution.

4.5.3.2 Addition of Waste Water Source

Through research that was completed, the team decided that using waste water had the potential to increase the available heat available in the tank without requiring greater power input to the system. Using waste water heat recovery involves passing the building sewage through a simple heat exchanger (to prevent sewer blockage issues related to more complex passages) within the geo-exchange system tank to remove as much thermal energy as possible from the sewage. Aside from water used for toilets, the majority of all other fluids leaving a building sewer are at temperatures above that of the ground and the water in the heat-exchanger tank—and sometimes much higher. This is because sewage coming from kitchens sinks and dishwashers, showers, bathroom sinks, and laundry can be at temperatures ranging from $40°C - 60°C$; that is a very large amount of energy that is wasted—which this project could potentially tackle to recover a portion of that energy. This will be accomplished by modelling a straight pipe through the tank with fins on the underside of the pipe, and cleanout access on the upstream side of the tank.

4.6 Physical Prototype Manufacturing

The following section covers the manufacturing that was completed to create the final prototype.

4.6.1 Incumbent design

The incumbent design, which can be seen in Figure 4.1, needed to be removed from the tank so that the new design could be implemented. The removal of the incumbent design occurred after various test runs were completed. Before the test runs were completed, the agitator was reconnected using a separate DC power supply. The tests are documented in 0. The overhead struts were then removed, the refrigerant evacuated, and the lines disconnected.

4.6.2 Modifications

The modifications that were implemented to the incumbent design were two sets of fins and a new pipe configuration as shown in Figure 4.7. There will be a vertical plate fin as well as an attached tubular fin design. These two fins add surface area that contacts the water and will increase the heat transfer. This design is hypothesized to provide the needed heat transfer to heat the typical 2,000 square foot home in the greater Vancouver area. There was no modification done to the heat pump system that was purchased during the project that was completed in the 2016-2017 school year.

4.6.2.1 Vertical Plate

The following section outlines the manufacturing processes that were used to create the vertical plates. The vertical plate was constructed out of 24-gauge aluminum sheets that were cut to 26 by 25 inches. The plates require four half circle bends to be created that will form around the piping. To create the bend design seen in Figure 4.8, a wood mold was created.

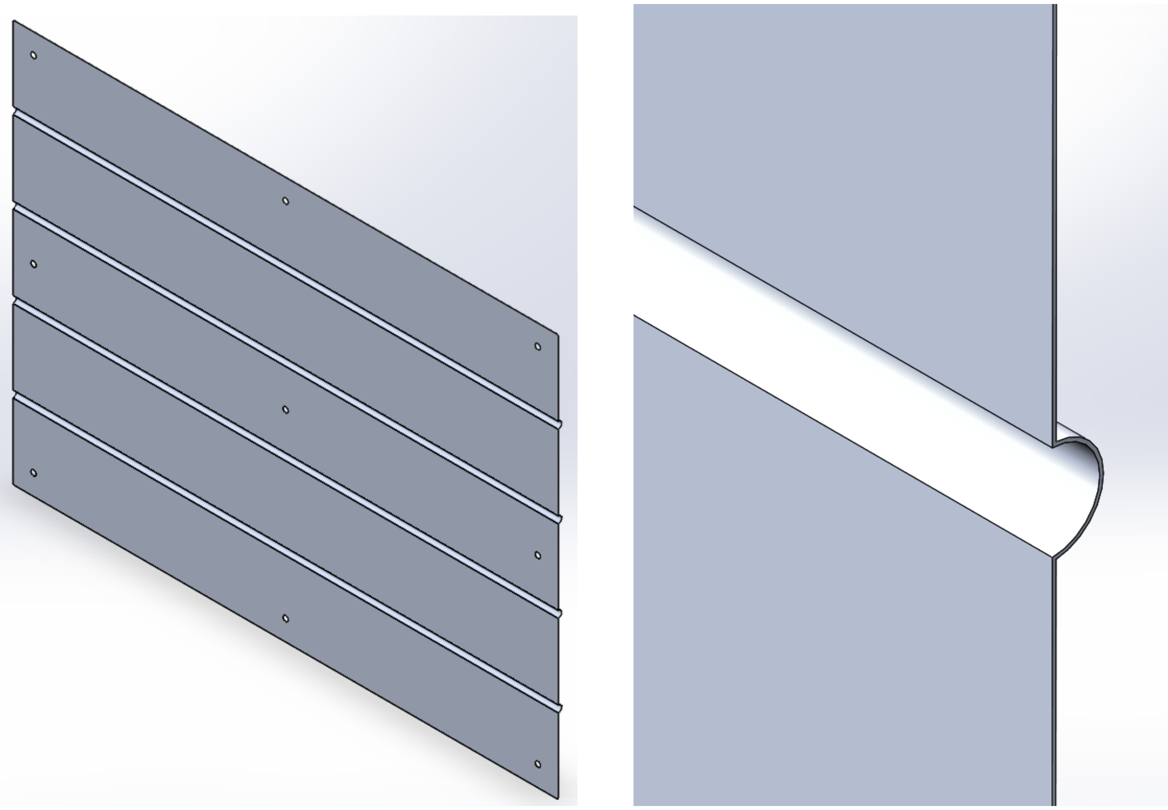

Figure 4.8 - Vertical Plate Bend Design

4.6.2.1.1 Wood Mold for Sheet Metal Bending

The bends were created using a wood mold and the mechanical press in BCIT's wood shop. Various methods for the bending of the sheet metal were looked at before landing on the wood mold. These methods included using the break press, the sheet metal roller, or the English wheel from BCIT's metal shop. These all required a custom die to be made so the wood mold was chosen for simplicity.

The first stage of creating the wood mold was to use the wood mill to test various depths. This process can be seen in Figure 4.9.

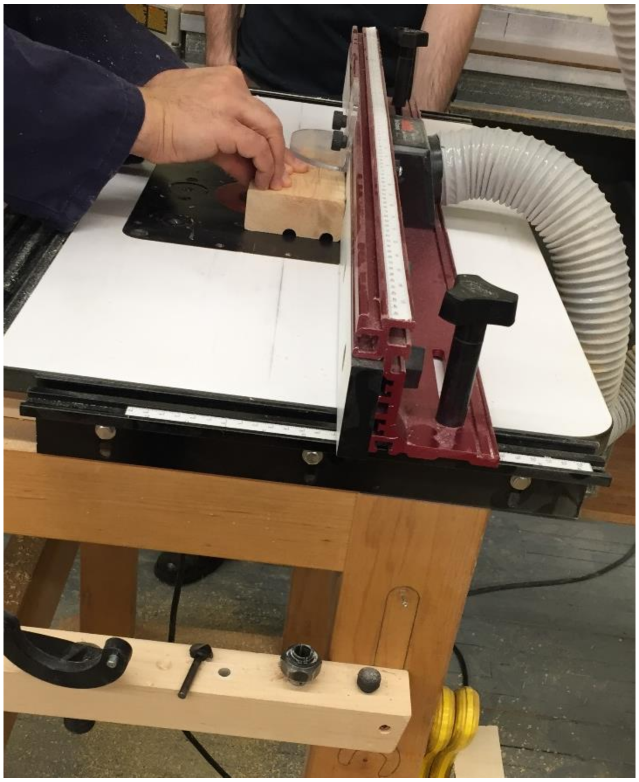

Figure 4.9 - Wood Milling to create Test Bend Block

The bottom of the wood mold was cut so that half of the tube sat inside it and then the smaller block had various depth cuts that were tested. This can be seen in Figure 4.10 compared against the final mold.

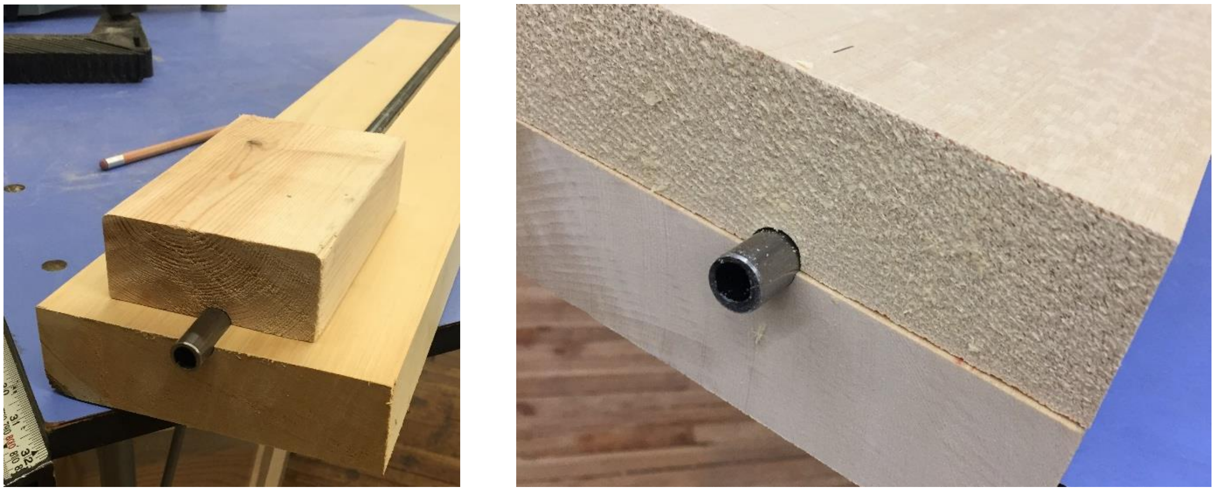

Figure 4.10 - Test Bend Block and Bend Mold Clearance

Using small pieces of sheet metal, the test bend block was used to find the size that creates the tightest clearance. This was done using the hydraulic press in BCIT's mechanics shop. The same method was then used to confirm the tolerance of the full mold which can be seen in Figure 4.11. The clearance created by the final wood mold can be seen in Figure 4.12.

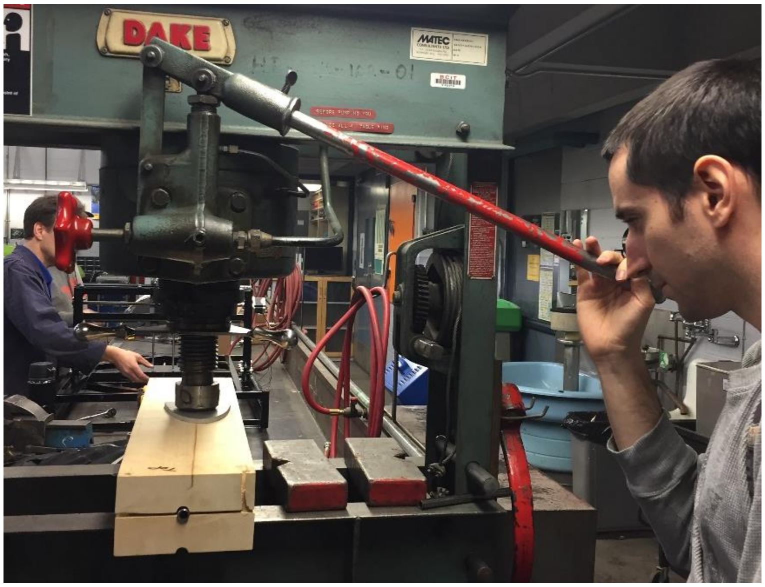

Figure 4.11 - Hydraulic Press used for Test Bends

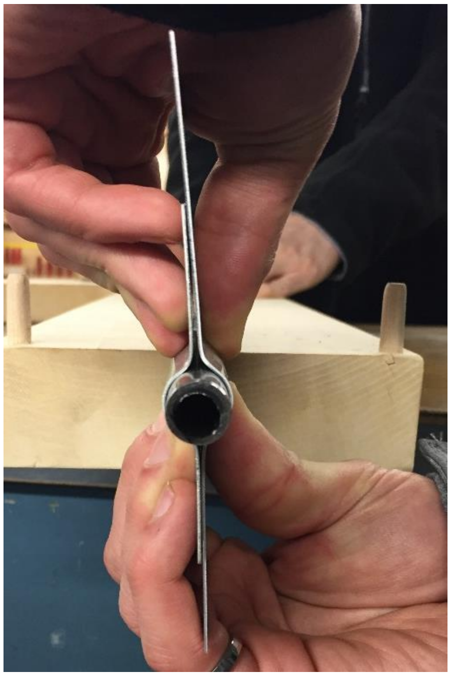

Figure 4.12 - Clearance around Pipe using Bend Mold and Light Gauge Stainless Steel

Using the mold, the four aluminum sheet metal plates were bent to have four half circle geometries. Two plates were then connected that fit over the piping. Before the plates were bent, the design team did practice bends using the wood press and scrap strips of 24-gauge aluminum. This practice set up can be seen in Figure 4.13.

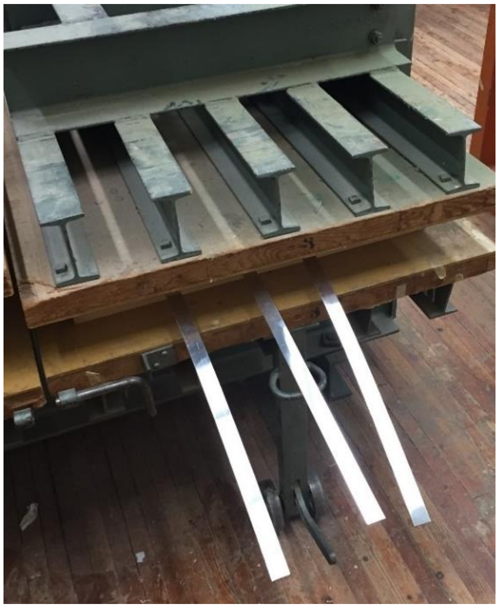

Figure 4.13 - Practice Bends using the Wood Press

The wood mold design was altered on April 24th, 2018 due to the inability of the first design to locate the bends, keep the bends straight and maintain a constant distance between them. The result of the first bend test using this mold can be seen in Figure 4.14.

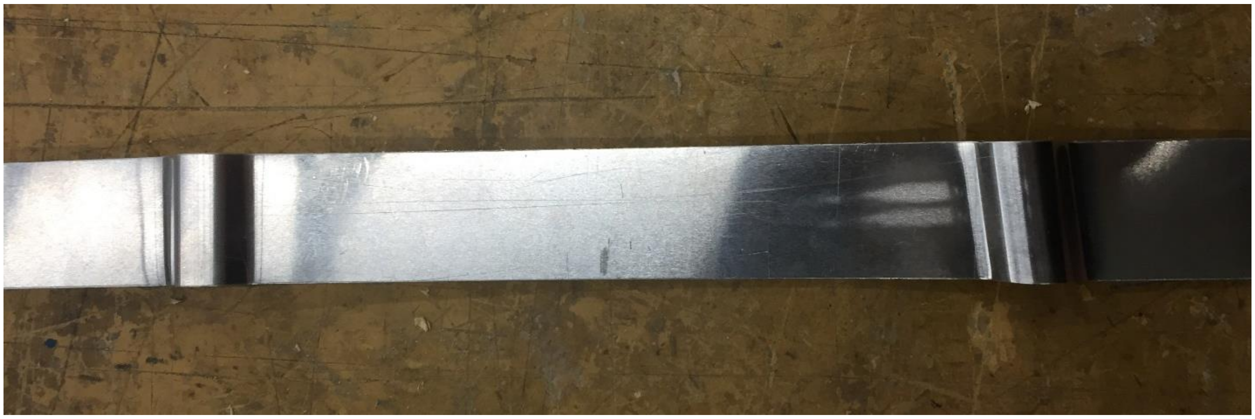

Figure 4.14 - Crooked Bends from the First Wood Mold Design

The new design used a second piece of wood with a grove cut into it that was the same size as the bending grove and can be seen in Figure 4.15. The new design allowed the team to move forward with bending the 26” x 25” aluminum sheet metal.

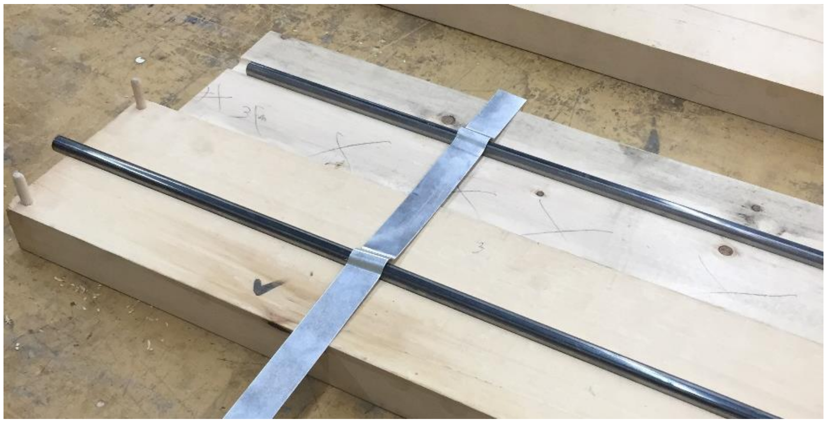

Figure 4.15 - New Wood Mold with Locator

4.6.2.1.2 Sheet Metal Bending

For the first bend, because it was unable to use the locator, the team added screws into the plate and the mold so that no movement or shifting would occur and the bend would be consistent for all four sheets. In Figure 4.16, one can see the two mold pieces which were clamped together and the two screws that are holding the plate in place. The holes that have been added to the plate will be used for supporting the plate when installed.

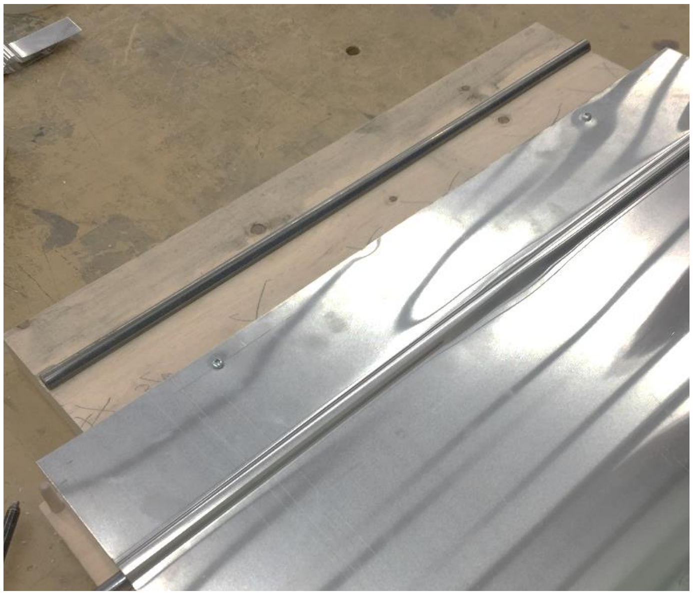

Figure 4.16 - Screws for First Bend

The following three bends used the locator and no additional holes were needed. The final plates and their clearance around the pipe can be seen in Figure 4.18.

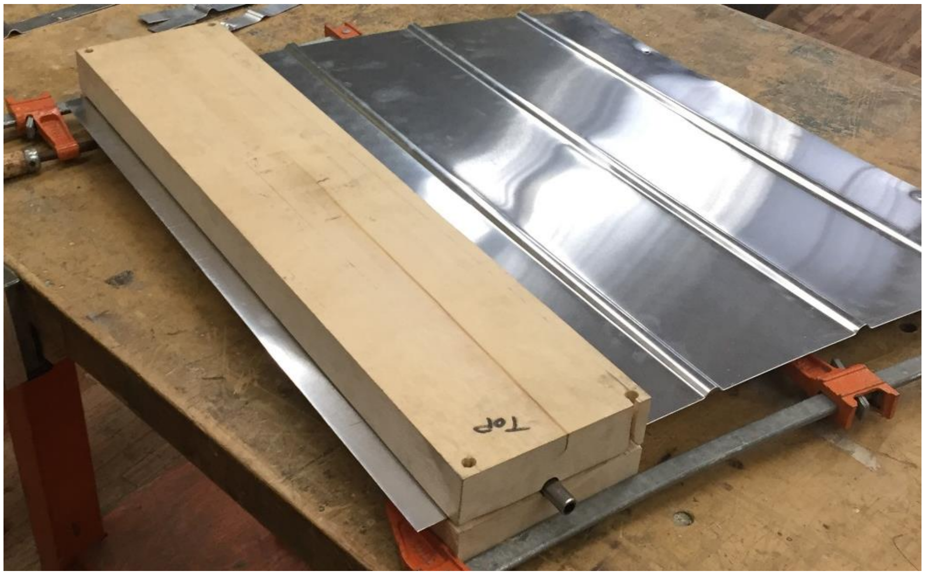

Figure 4.17 - Bending of the Aluminum Sheet Metal

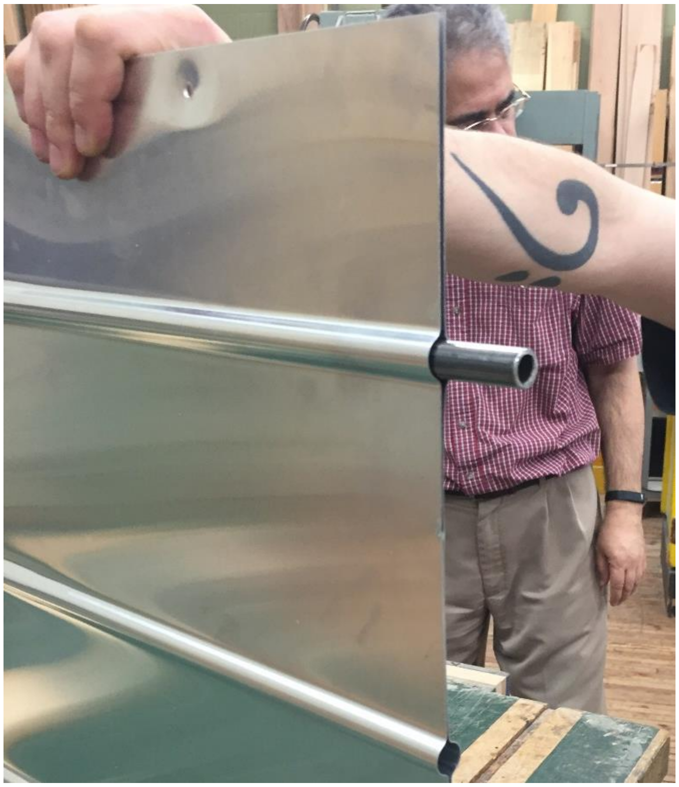

Figure 4.18 - Two Plates after Bending

4.6.2.2 Pipe Configuration

The final design for the pipe configuration is discussed in Section 6.4 and can be seen in Figure 4.6 and Figure 4.7. The pipe configuration did not change when the tubular fins were added to the design. The pipes that were used to create the heat exchanger were ½" OD type 'ACR' copper and were brazed together using silver solder. The spacing between the pipes needed to match the spacing between the bends in the plate exactly to maximize the contact area so the 180-degree bends were created using two long-radius 90-degree bends and straight links of pipe. This allowed the bends to match relatively close to the plate geometry, and the bends can be seen in Figure 4.19.

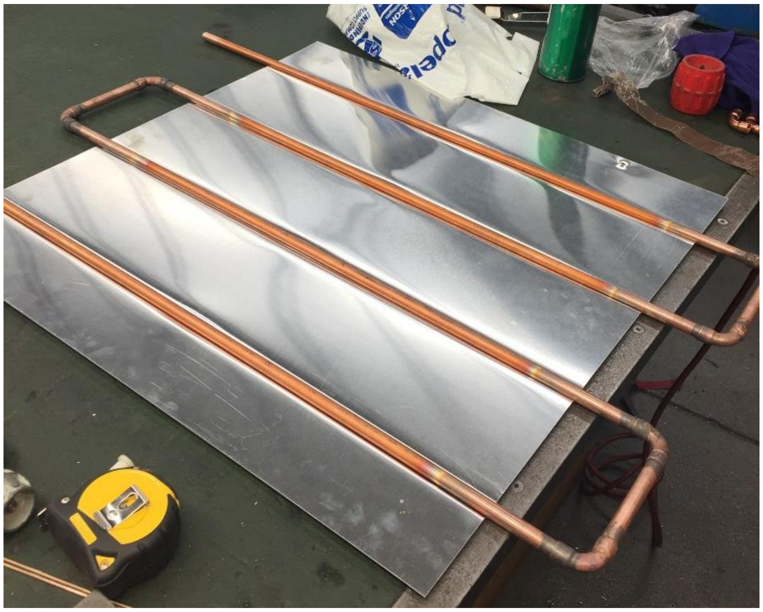

Figure 4.19 - Brazed Pipe set in a Single Plate

The clearance between the plates and the pipe is the smallest around the edges of the plate, as the mold in the wood press was able to place more pressure at the sides. This was corrected by placing the bent plates back into the mold and using the hydraulic press in BCIT's mechanics shop to apply centralized pressure to the middle of the mold. The final pipe configuration between the plates is shown in Figure 4.20.

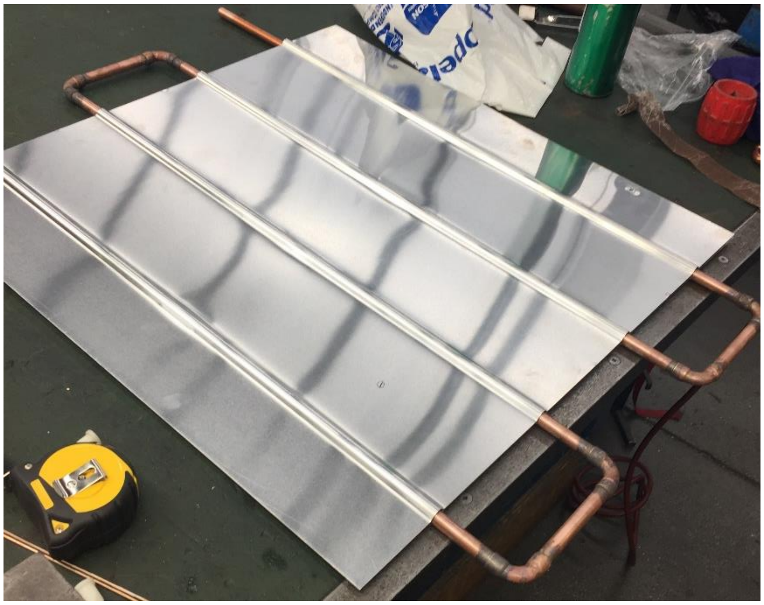

Figure 4.20 - Brazed Pipe between Two Plates

4.6.2.3 Round Fin Attachment

In order to add round fins to the heat exchanger, 3/8" OD schedule 40 aluminum pipe was cut in half in the longitudinal direction, and then its inner wall milled to create a tight tolerance fit between it and the flat plate heat exchanger. In order to ensure, the fit would not become loose over time, gear clamps were added between the two pipe halves on the sections just outside the flat plate heat exchanger. However, the manufacturing technique used was not able to reach the correct tolerances, and, so the design was not connected to the final prototype.

4.6.2.4 Prototype Attachment

The prototype was attached by Ian Winning from Control Temp Ltd. on May 7th, 2018. This involved evacuating the incumbent design of refrigerant and removing the old piping for the outdoor heat exchanger, brazing the plate design to the liquid and suction lines, and charging the plate design with refrigerant. The installed plate design can be seen in Figure 4.21.

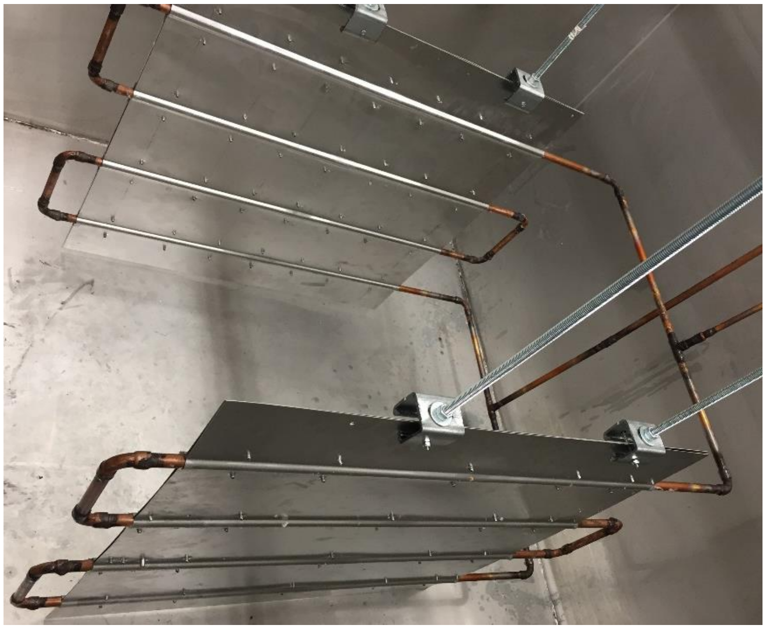

Figure 4.21 - Installed Plate Design Prototype

The plates are held up by strut channel that was cut into sections so that each had a single hole on the top. This was then connected to ready rod that was attached to the top strut channel. This connection is shown in Figure 4.22.

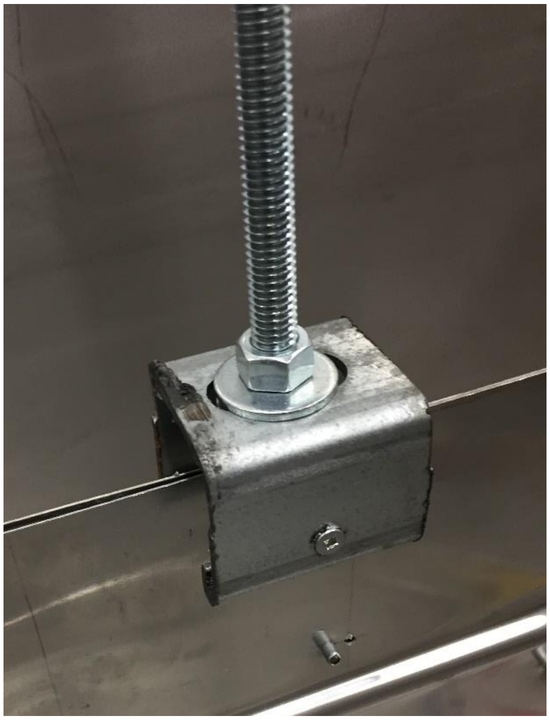

Figure 4.22 - Plate Support Connection

Chapter 5. Discussion of results

5.1 COMSOL Results

The following section documents the results gathered from the COMSOL simulations.

5.1.1 300 Second Time Interval Test using Water

The following section covers the results of the first simulation run for the two COMSOL models using water as the fluid inside the pipes. The results for this test are the outlet temperature and the change in temperature for the full pipe and plate configuration over the 300 second time interval.

5.1.1.1 Vertical Plate Design

Initially the simulation was run for 300 seconds, and then the outlet, pipe, and plate final temperatures were observed. The outlet temperature over the time interval is shown in Figure 5.1. With the parameters that were used shown in Table 5.1.

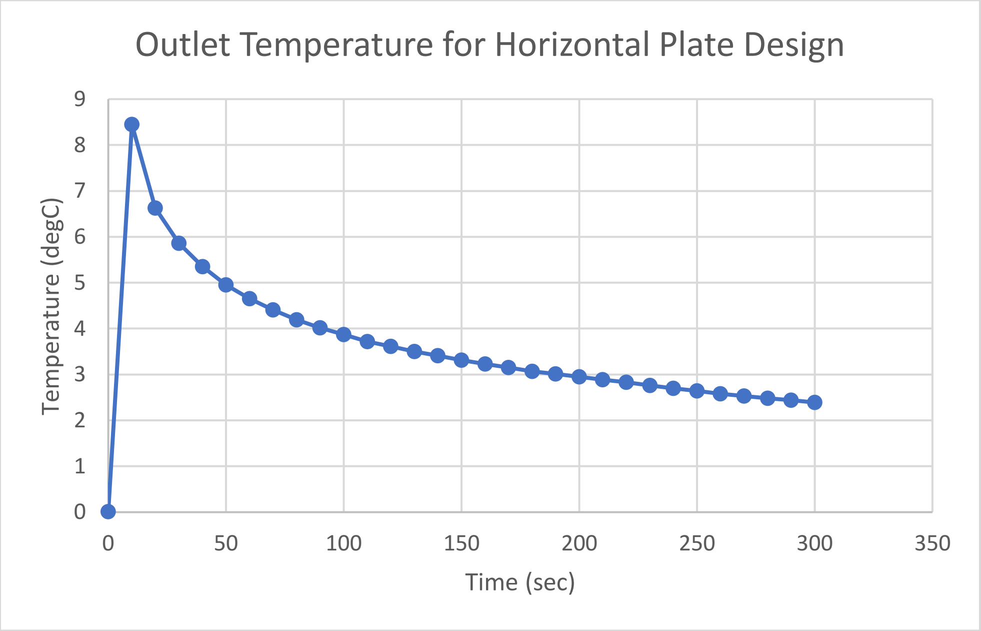

Figure 5.1- Outlet Temperature for Horizontal Plate Design over 300 seconds

Table 5.1 - Parameters for Horizontal Plate Design over 300 seconds

Parameter	Value
Constant Inlet Temperature, T_{in} [°C]	-10
Initial Pipe Fluid Temperature, T_0 [°C]	0
Tank Water Temperature, T_w [°C]	20
Ground Temperature, T_g [°C]	25

The pipe and plate final temperatures are shown in Figure 5.2 and Figure 5.3 respectively.

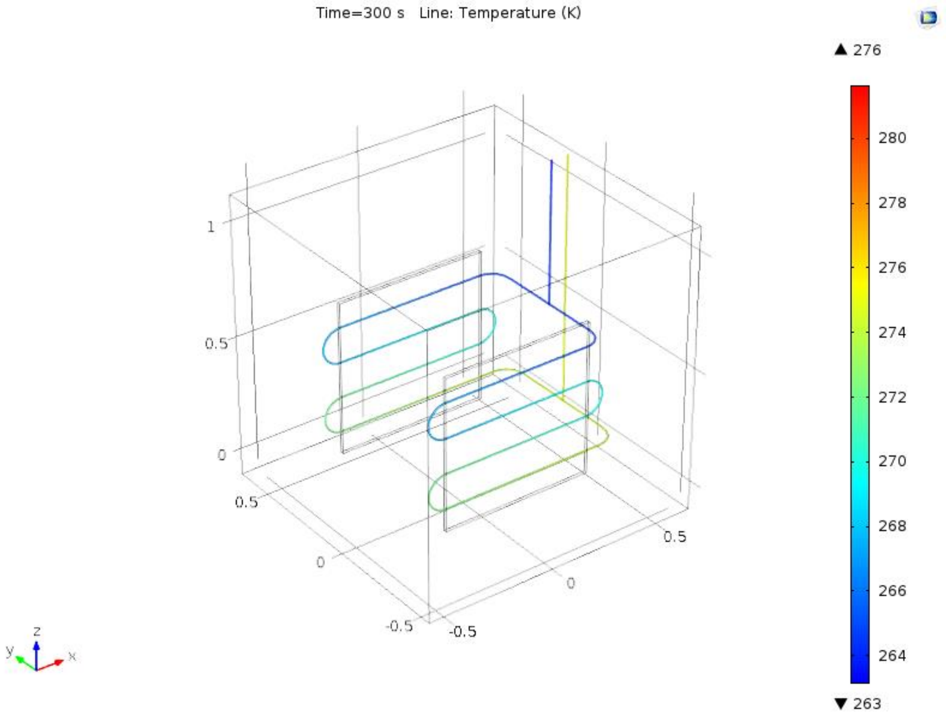

Figure 5.2 - Final Pipe Temperature for Horizontal Plate Design over 300 seconds

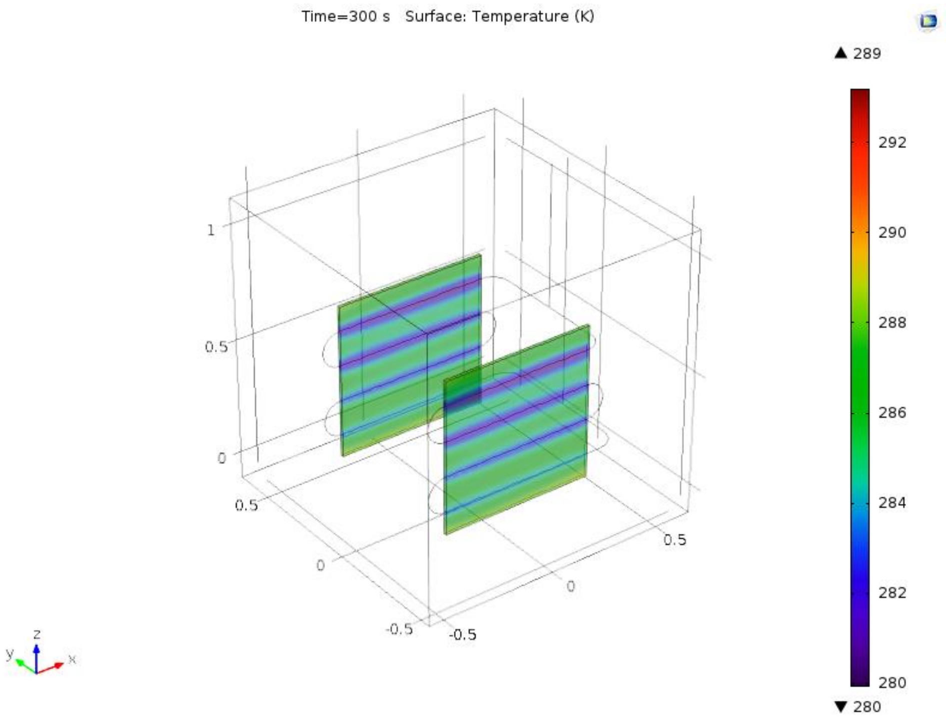
Time=300 s Surface: Temperature (K)
▲ 289
292
290
288
286
284
282
280
▼ 280
1
0.5
0
0.5
0
-0.5
-0.5
0
0.5
z
y
x

Figure 5.3 - Final Plate Temperature for Horizontal Plate Design over 300 seconds

5.1.1.2 Vertical Plate Design with Added Tubular Fins

This simulation was also run for 300 seconds which could then be compared to the design without the fin attachment. The outlet, pipe, and plate final temperatures were observed. The outlet temperature over the time interval is shown in Figure 5.4, with the parameters equal to those in the previous 300 second test and can be seen in Table 5.1.

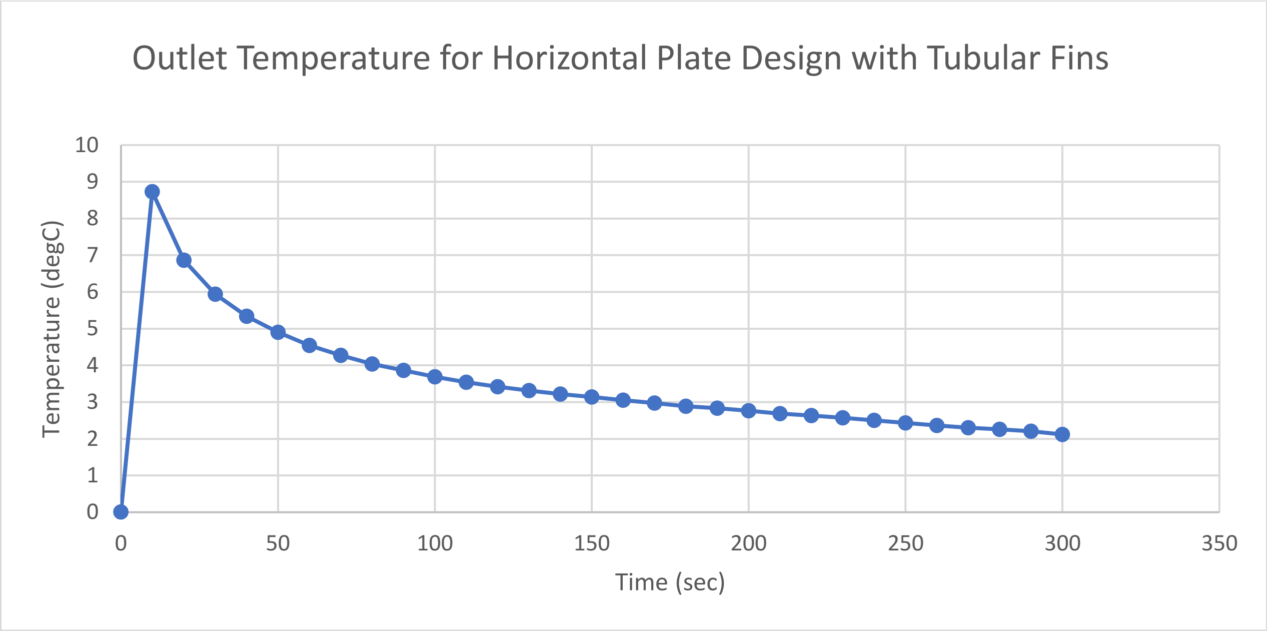

Figure 5.4 - Outlet Temperature for Horizontal Plate Design with Tubular Fins over 300 seconds

The pipe and plate final temperatures are shown in Figure 5.5 and Figure 5.6 respectively.

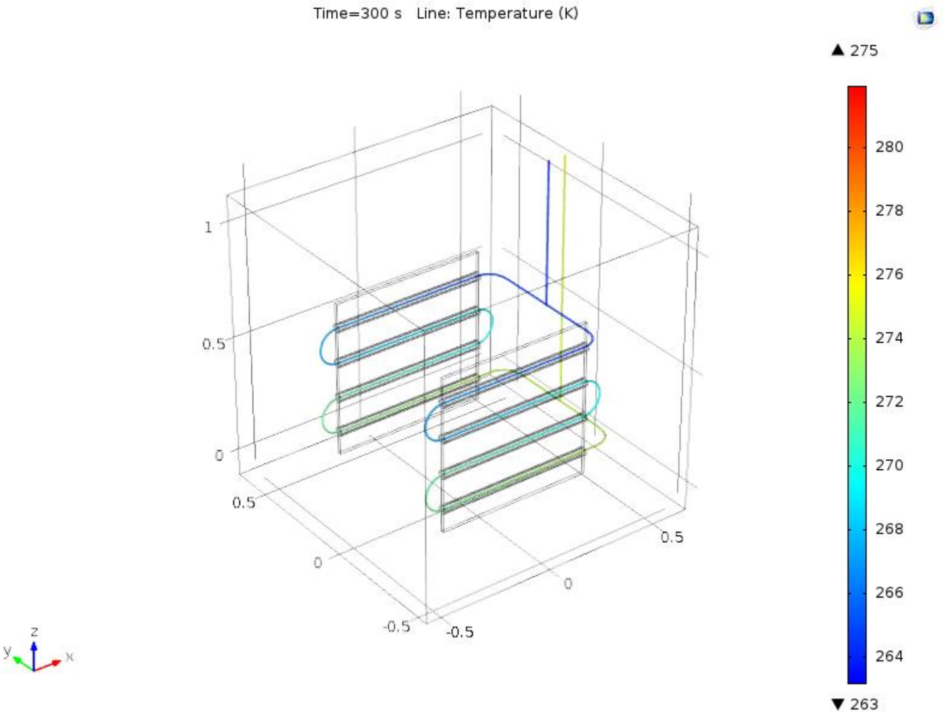
Time=300 s Line: Temperature (K)
▲ 275
280
278
276
274
272
270
268
266
264
▼ 263
1
0.5
0
0.5
0
-0.5
-0.5
0
0.5
z
y
x

Figure 5.5 - Final Pipe Temperature for Horizontal Plate Design with Tubular Fins over 300 seconds

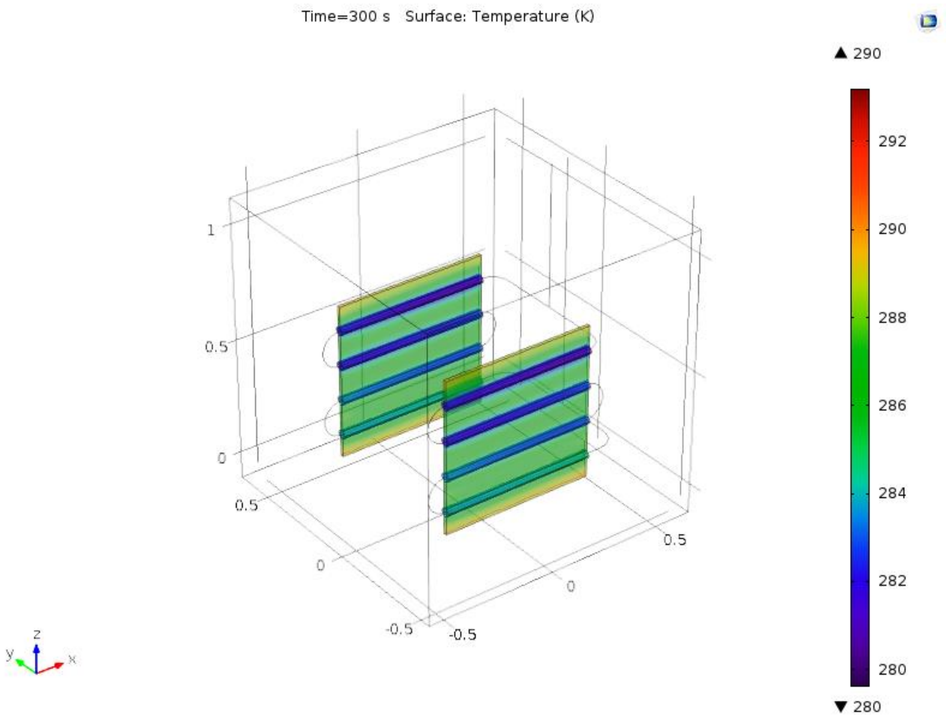

Figure 5.6 - Final Plate Temperature for Horizontal Plate Design with Tubular Fins over 300 seconds

5.1.1.3 Discussion of Results

The 300 second test was important in determining if the results that were being output made sense conceptually. The outlet temperature is decreasing slightly over time for the simulations with and without fins, which is due to the decrease in temperature difference between the fluid entering the pipe and the water in the tank. The water in the tank decreases, and, therefore, less heat transfer takes place between the fluid in the pipe and the plate. The difference between the two simulations is minimal. The outlet temperature, for the simulation with the tubular fins decreases slightly faster reaching 2.12 degrees while the other simulation only reaches 2.39 degrees. This makes logical sense because the heat transfer that occurs between the tank and the plate should occur quicker, which will cause the tanks temperature to decrease faster. The difference between the simulations is very small so the simulations were then run for two hours (7200 seconds).

5.1.2 7200 Second Time Interval Test Using Water

The following section covers the results of the two-hour simulation, run for the two COMSOL models using water as the fluid inside the pipes. This simulation was used to better understand the differences between the designs that wasn't gathered from the 300 second test, and, also, to see the changes that occur over a larger time interval.

5.1.2.1 Vertical Plate Design

The simulation was run for two hours or 7200 seconds, and then outlet temperature, pipe, and plate final temperatures were recorded. The outlet temperature over the time interval is shown in Figure 5.7. The parameters were kept the same as those used in the 300-second tests and can be seen in Table 5.1.

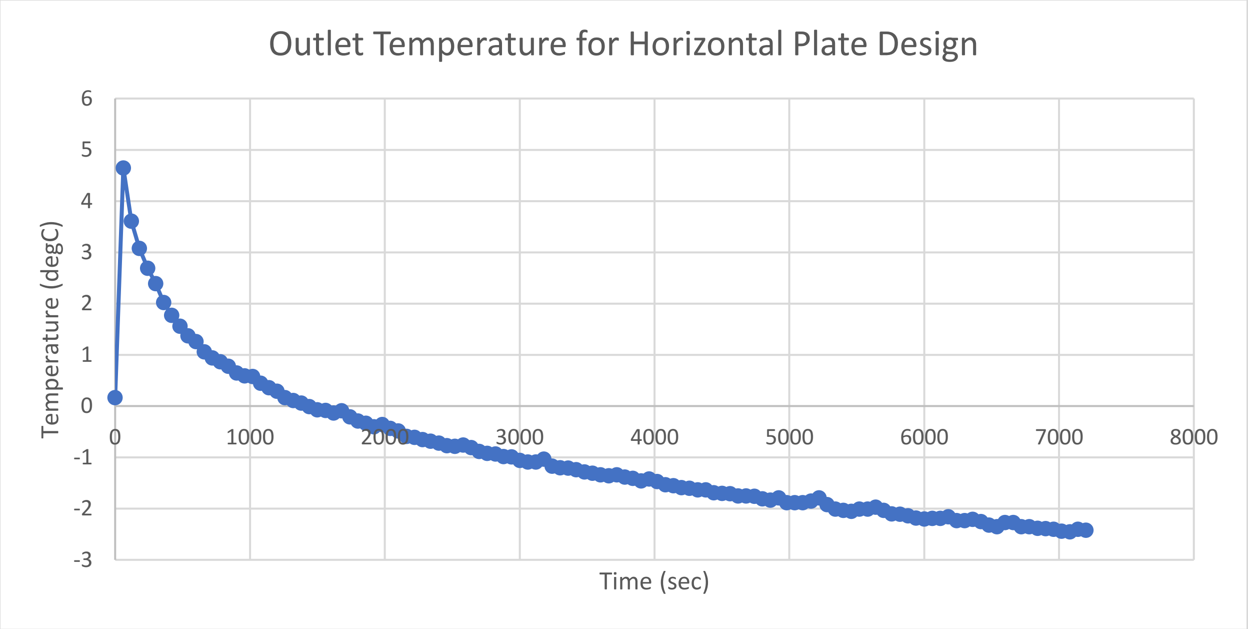

Figure 5.7 - Outlet Temperature for Horizontal Plate Design over 7200 seconds

The pipe and plate final temperatures are shown in Figure 5.8 and Figure 5.9, respectively.

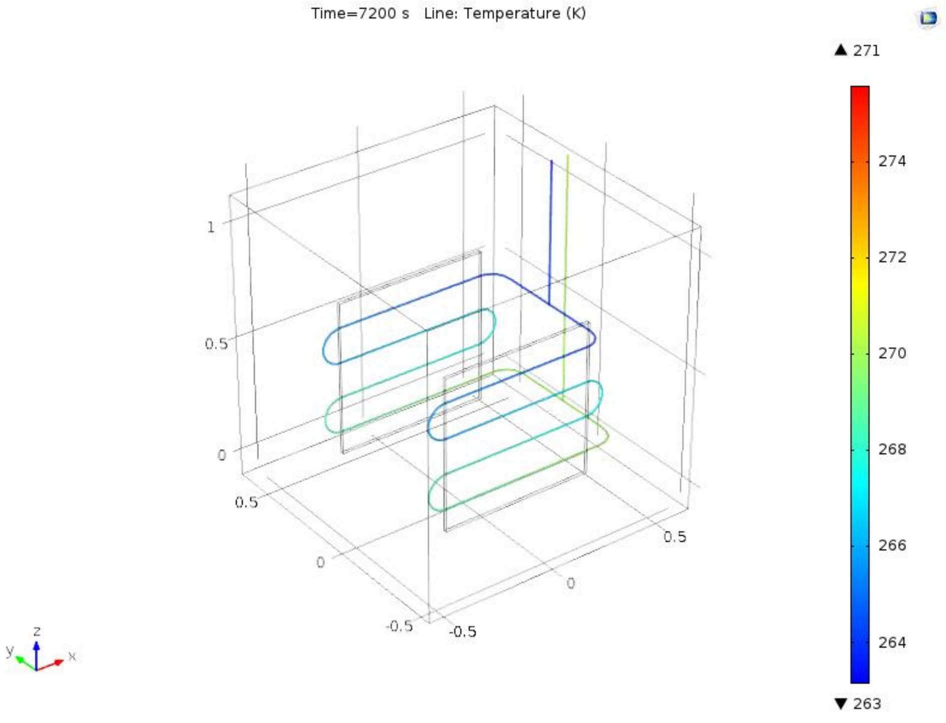

Figure 5.8 - Final Pipe Temperature for Horizontal Plate Design over 7200 seconds

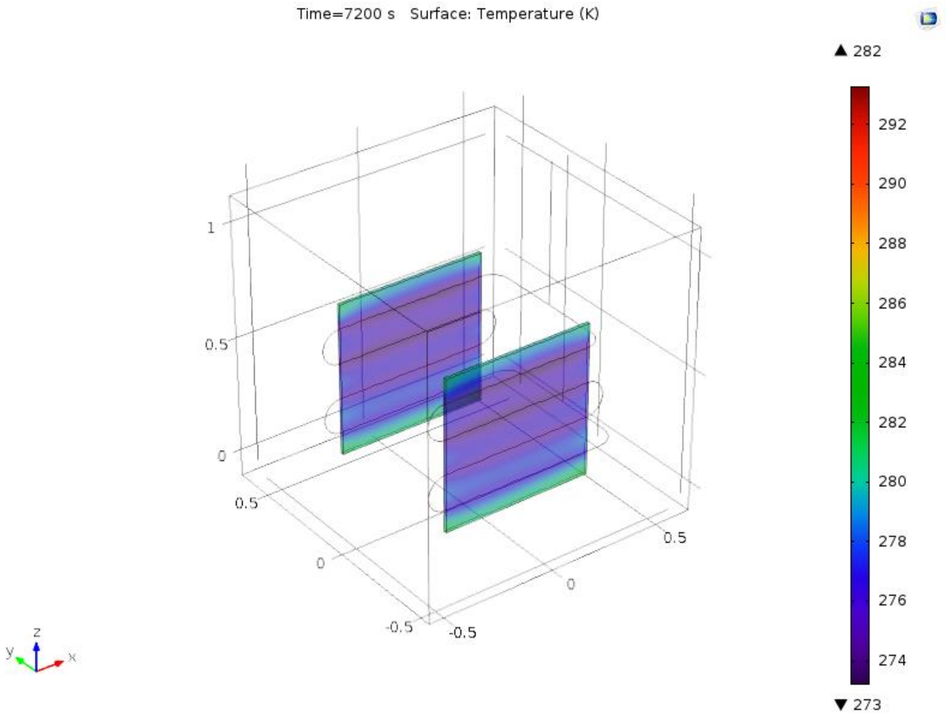

Figure 5.9 - Final Plate Temperature for Horizontal Plate Design over 7200 seconds

5.1.2.2 Vertical Plate Design with Added Tubular Fins

The simulation was run for two hours or 7200 seconds, and then outlet temperature and the pipe and plate final temperatures were recorded. The outlet temperature over the time interval is shown in Figure 5.10. The parameters were kept the same as those used in the 300-second tests and can be seen in Table 5.1.

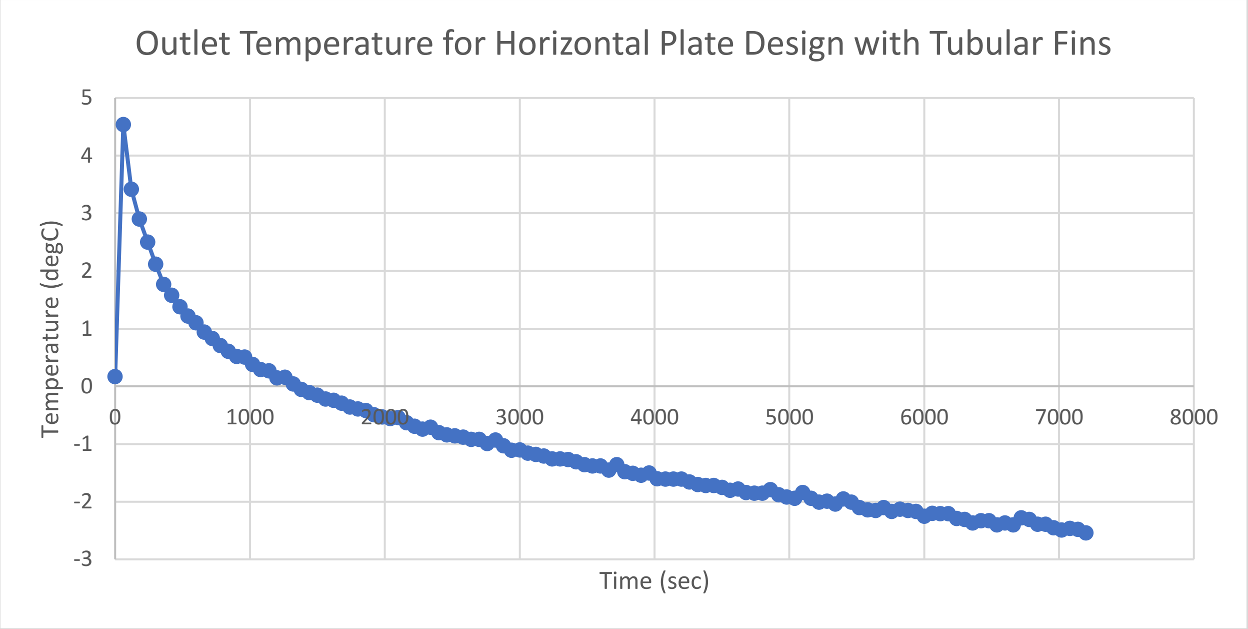

Figure 5.10 - Outlet Temperature for Horizontal Plate Design with Tubular Fins over 7200 seconds

The pipe and plate final temperatures are shown in Figure 5.11 and Figure 5.12 respectively.

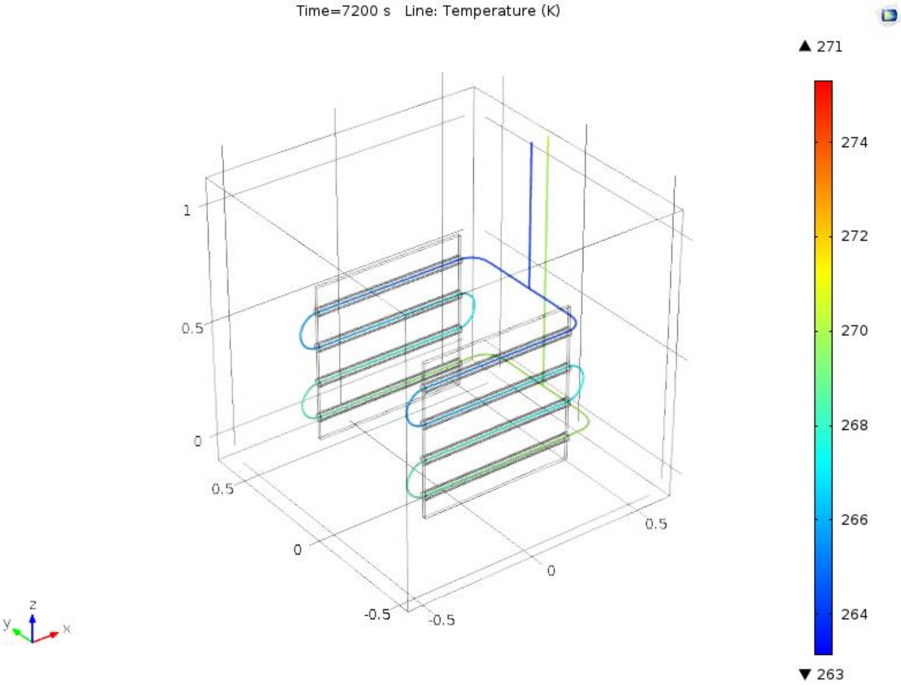

Figure 5.11 - Final Pipe Temperature for Horizontal Plate Design with Tubular Fins over 7200 seconds

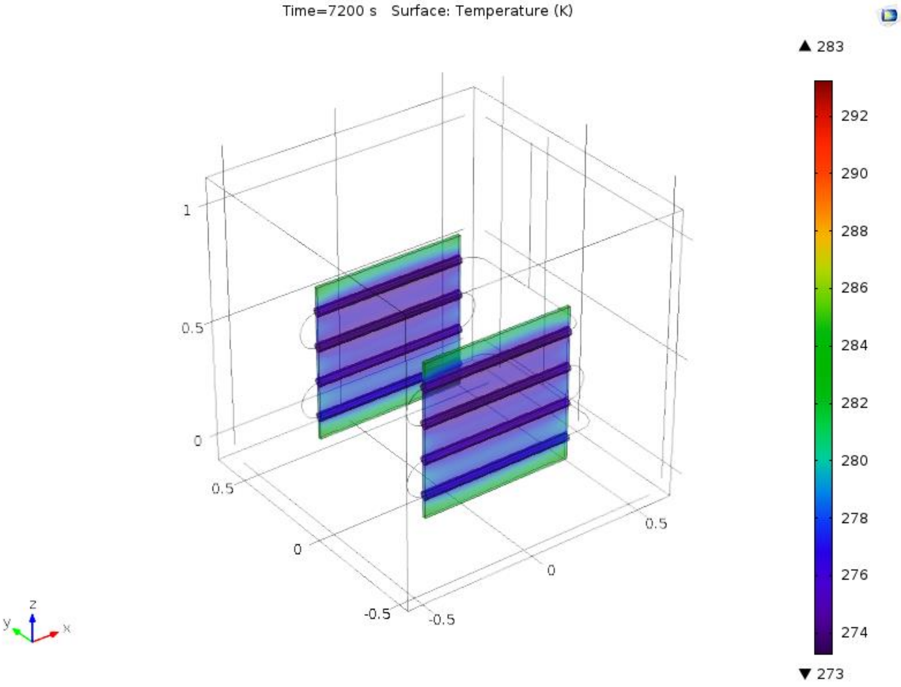

Figure 5.12 - Final Plate Temperature for Horizontal Plate Design with Tubular Fins over 7200 seconds

5.1.2.3 *Discussion of Results*

The results between the tubular fin and no-tubular fin simulations show that the fins add very little to the overall plate and pipe temperatures as well as the outlet temperatures. The behaviour of the graphs is equal to those in the 300-second test. The system being allowed to run longer, reaches a negative outlet temperature because of the decrease in temperature of the plate which can be seen in Figure 5.9 and Figure 5.12.

5.2 Verification of COMSOL Model

The complexity of implementing refrigerant in COMSOL Multiphysics provided a challenge to the design team. The data from the water run COMSOL tests needed to be able to be compared to the refrigerant run prototype tests. This was completed by using the heat energy transfer rate, $\dot{Q}$, with the equation as follows;

$$\dot{Q} = \dot{m}C_p(T_{out} - T_{in})$$

and the mass flow rate was determined using:

$$\dot{m} = \rho v A$$

5.2.1 COMSOL Simulation

The COMSOL parameters were obtained and can be seen in Table 5.2.

Table 5.2 - COMSOL Parameters for Energy Calculation

COMSOL Parameter	**Value**
Inlet Velocity $[m/s]$	-1.5
Outlet Velocity $[m/s]$	1.5
Inlet Velocity (at T) $[m/s]$	-0.5
Outlet Velocity (at T) $[m/s]$	0.5
Inlet Temperature, T_{in} $[K]$	263.15
Outlet Temperature, T_{out} $[K]$	Non-Constant
Internal Pipe Area, A $[m^2]$	$7.1256 \cdot 10^{-5}$
Mass Flow Rate, $\dot{m}$ $[kg/s]$	0.10730
Specific Heat, C_p $[J/kg \cdot K]$	4216.3

The calculated power in the form of heat, $\dot{Q}_L$, can be seen in Figure 5.13 below.

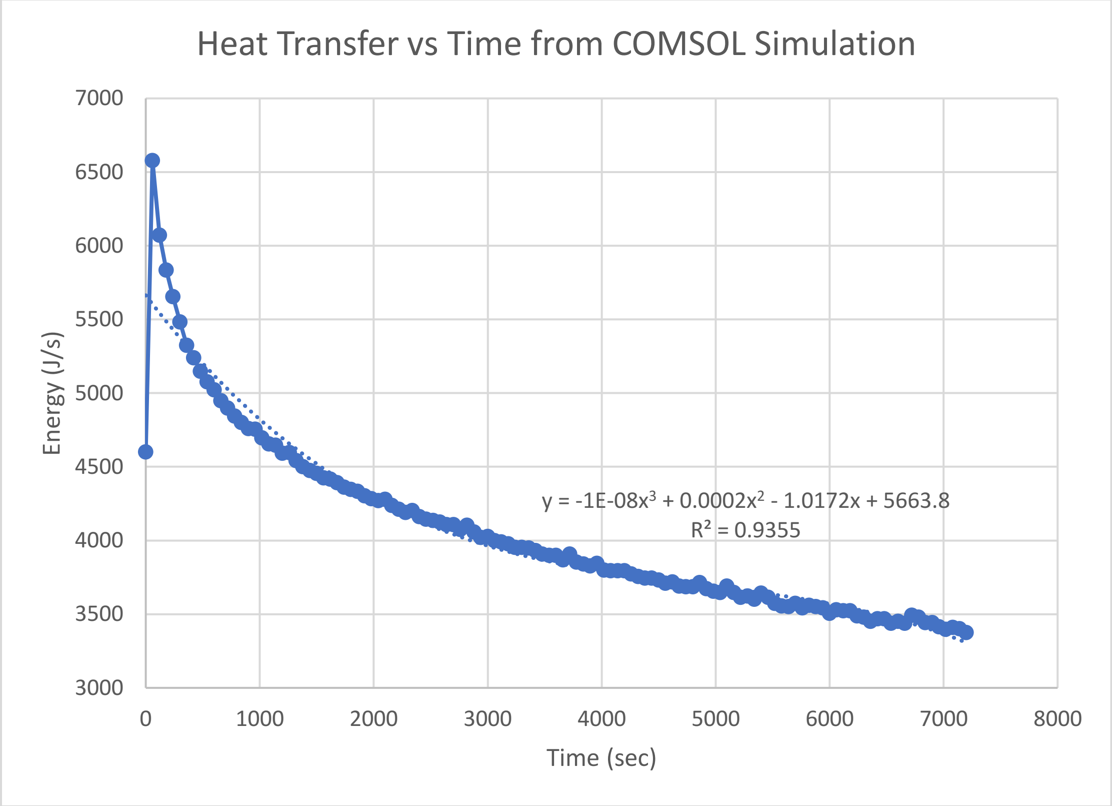

Figure 5.13 - Heat Transfer from COMSOL Simulation

Using the trend line, with the accuracy confirmed using the R Squared value, the average $\dot{Q}_L$ value was determined. This value was determined to be approximately 4500 watts. Both the initial heat transfer and this average value are to be compared to the physical results.

5.2.2 Physical Prototype

To be able to interpret heat pump performance and effectiveness, data must be gathered for the refrigerant temperature and pressure at the points of interest on the heat pump; the air inlet and outlet temperatures via temperature sensors; the volume flow rate of the air on the system indoor coil through the use of a balometer. With this data, it becomes possible to find all the parameters of interest for the system: The heat transfer rate of the outdoor coil can be found by using the equation below.

$$\dot{Q}_H = \dot{m}_{air} c_{p_{\text{avg}}} \Delta T$$

The results from the balometer and measured temperature difference across the heat exchanger can be used to find the mass flow rate by converting the measured standard cubic feet per minute (SCFM) to the equivalent mass flow rate for a given temperature with the recorded values for the unit shown below in Table 5.3.

Table 5.3 - Recorded Values for Indoor Heat Exchanger

Parameter	**Value**
Volume Flow Rate, $\dot{\mathcal{V}}$ $[SCFM]$	590
Return Air Temperature, T_R [°F, °C]	67, 19.444
Supply Air Temperature, T_S [°C]	35

With the assumption of dry air, and with temperatures between $-10°\mathrm{C} \leq T \leq 50°\mathrm{C}$, the specific heat capacity of air can be taken to be $c_p = 1.005\ kJ/kg \cdot K$, and an ideal gas assumption holds to an error below 0.2 percent [6]. With this assumption, standard air conditions can be used that give specified values for air temperature, density, specific heat capacity, and humidity—greatly simplifying the calculations. This results in the following conversion and calculation:

$$\dot{m}_{air} = \rho\dot{\mathcal{V}} = \left(1.225\frac{kg}{m^3}\right)(590\ SCFM)\left(0.0283168\frac{m^3}{ft^3}\right)\left(\frac{1min}{60s}\right) \cong 0.341\frac{kg}{s}$$

$$\dot{Q}_H = \dot{m}_{air}c_{p_{avg}}\Delta T$$

$$\dot{Q}_H = \left(0.341\frac{kg}{s}\right)\left(1.005\frac{kJ}{kg \cdot K}\right)(35°\mathrm{C} - 19.444°\mathrm{C}) \cong 5.33\ kW$$

With the heat transfer rate across the indoor coil calculated and using the relationship between the work input rate (namely, the product of the potential voltage difference and the rated current draw for the unit, found in section 1.3.4), the unit COP is found as follows.

$$COP_H = \frac{\dot{Q}_H}{EI} = \frac{5.33kW}{(240V)(6.04A)} = \frac{5.33kW}{1449.6W} \cong 3.679$$

Now, for the heat transfer rate on the indoor coil, the correlation between the heat transfer rates of the two coils is used to find its value and is shown below.

$$\dot{Q}_L = \dot{Q}_H - \dot{W}_{net,in} = 5.33kW - 1.4496kW \cong 3.883kW$$

This parameter data can then be used to further design, optimize, and iteratively improve the geo-exchange system via the virtual model. Focusing on the heat energy transfer rate on the outdoor coil, $\dot{Q}_L$, one can compare the virtual results of water flowing through the piping setup instead of refrigerant and compare it to the actual results with an assumed decent accuracy. Errors would come in the way of the difference in thermal conductivity, thermal diffusivity, and specific heat capacity for water and refrigerant.

5.2.3 Discussion of Results

Comparing the heat transfer rates for the outdoor heat exchanger for the virtual mode and physical prototype results in a percent error shown below.

$$\%Error = \frac{\left|\dot{Q}_{L,real} - \dot{Q}_{L,virtual}\right|}{\dot{Q}_{L,real}} \cdot 100\% = \frac{|3.883kW - 6.60kW|}{3.883kW} \cdot 100\% \cong 69.97\%$$

It should be noted however that this value only represents the percent error during the initial conditions of the system start up, and data collection for the supply and return air temperatures would be needed throughout the entire system run time in order to reach more conclusive results.

Sources of error include, but are not limited to,

- the use of water as the fluid in the piping in the virtual model instead of refrigerant, causing errors related to differences in thermal conductivity, and diffusivity,
- contact resistances as a result of tolerancing issues in the manufacturing of the plates,
- the lack of enough heat conductive paste used for the flat plate heat exchangers,
- measurement errors from the instrumentation used to gather data, and
- the COMSOL simulation not accounting for gravity or buoyancy forces.

Therefore, even with all these errors, it is likely to conclude that the agreement between the physical prototype and virtual model within twenty percent was not met.

When the average value for the COMSOL results is used, the error is below the desired agreement, equalling approximately 16 percent. Because of this result, it is recommended that a time-based heat transfer rate be physically measured in future tests. With a time-based study, the COMSOL simulation and the physically results could be more accurately compared because an error for each time step could be determined as well as an error between both average results. With this the recommended agreement, the error could be confirmed along the full run time.

Similarly, the mass flow rate of the refrigerant should not be experimentally found until data for the supply and return air temperatures are collected at each time step to ensure more accurate results. However, to find their values, a simple formula can be used by relating outdoor coil heat transfer rate to the following equation.

$$\dot{Q}_L = \dot{m}_{refrigerant}\Delta h_L \Rightarrow \dot{m}_{refrigerant} = \frac{\dot{Q}_L}{\Delta h_L}$$

5.3 Physical Results

The physical testing was split into two sections. These included the incumbent design and the plate design. Both were run various times to test the system and allow comparison to the COMSOL model. The high temperature side sensor was placed after the compressor and the low temperature side sensor was placed before the outdoor heat exchanger.

5.3.1 Incumbent Design

This section contains all the data that was gathered from the incumbent design for comparison to the new design.

5.3.1.1 Incumbent Design without the Agitator

The following section is for when the system was run without the agitator. This is to test various tank water properties and its effect of the running time by adding antifreeze or pure ethylene-glycol to the tank.

5.3.1.1.1 Tank with Water

Approximately 874.84 liters of water was placed into the tank and the system was run. The starting temperature of the tank was approximately 20 degrees and the inlet and outlet temperatures were approximately room temperature (24 degrees). The data that was gathered is displayed in Figure 5.16.

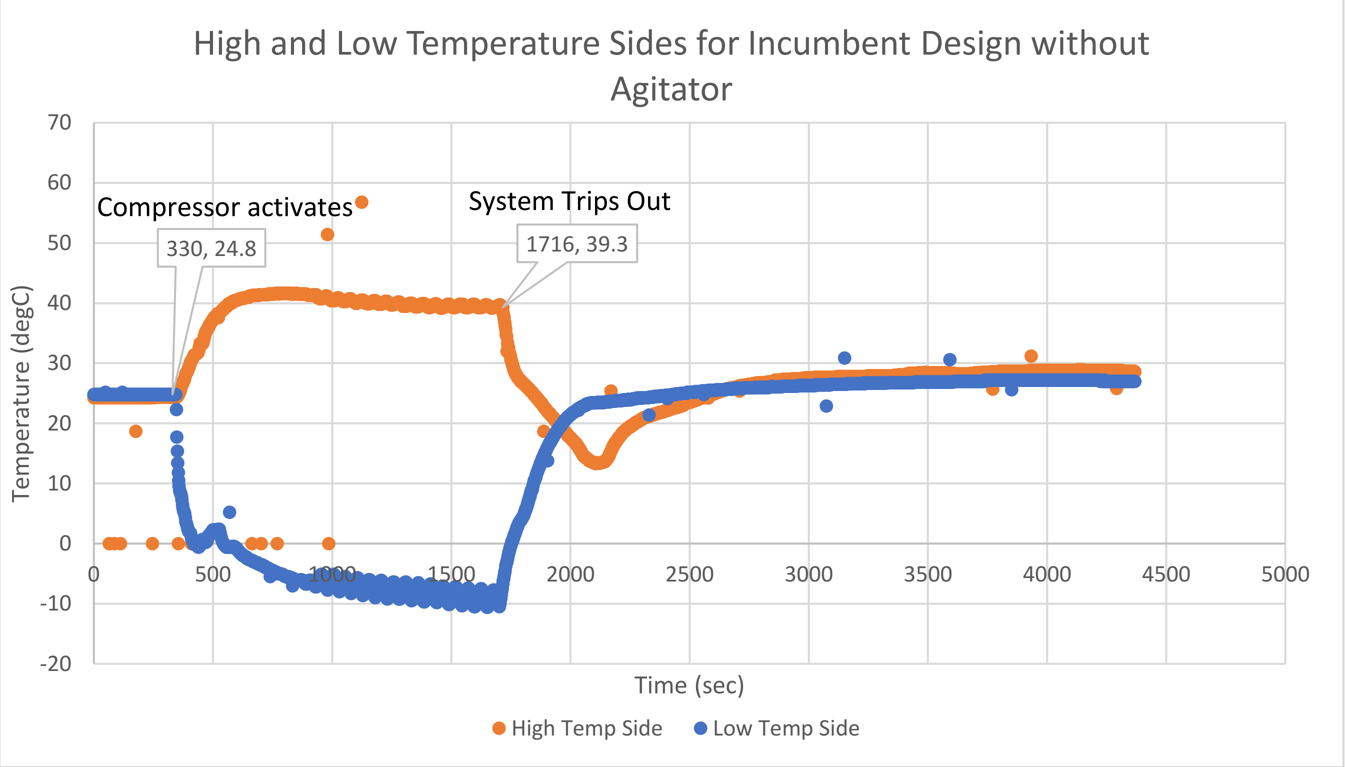

Figure 5.14 - High and Low Temperature Sides for Incumbent Design without Agitator

The high side increases to above 40 degrees while the low side decreases to 0 degrees Celsius when the system is initially turned on. The system is then able to run for 1716 seconds starting at 330 seconds when the compressor is activated, or approximately 23 minutes of run time before the compressor locks out due to the liquid refrigerant entering the compressor.

5.3.1.1.2 Tank with Water and Plumbing Antifreeze

3.78 litres of Plumbing Antifreeze were added to 874.84 liters of water inside the tank. The agitator was turned on to mix the new fluid and then the system was turned on without the agitator. The starting temperature of the tank was approximately 14 degrees and the inlet and outlet temperatures were at approximately 20 degrees. The data that was gathered is displayed in Figure 5.15.

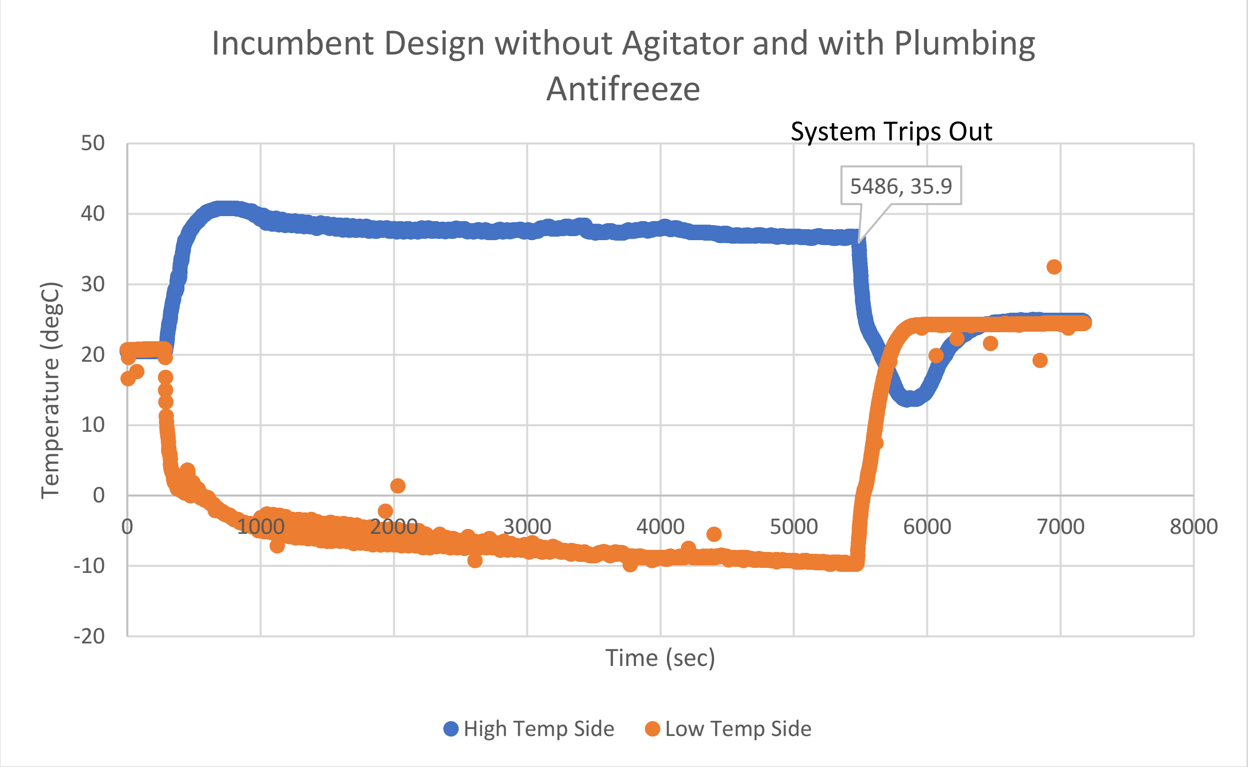

Figure 5.15 - High and Low Temperature Sides for Incumbent Design without Agitator and with Plumbing Antifreeze

Even though the starting temperatures of the components were lower, the compressor status was able to be maintained longer with the addition of antifreeze. The system ran for 5486 seconds or approximately 1 hour and 30 minutes. One hour longer then the previous run.

5.3.1.2 Incumbent Design with the Agitator

For this test the starting temperature of the tank was approximately 20 degrees and the inlet and outlet temperatures were approximately room temperature (24 degrees). The data that was gathered is displayed in Figure 5.16.

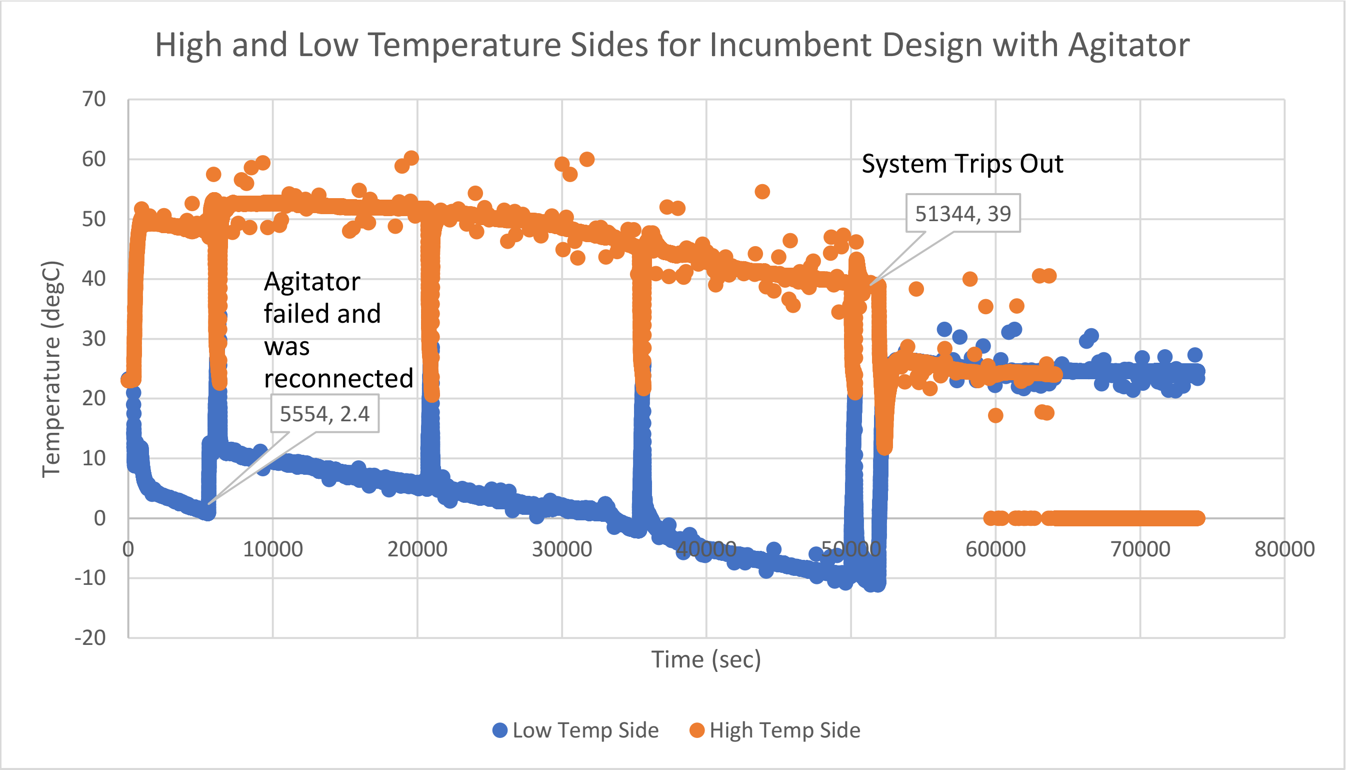

Figure 5.16 - High and Low Temperature Sides for Incumbent Design with Agitator

The first section, up to approximately 5000 seconds was not running with the agitator due to it becoming unplugged. This explains the quick drop in temperature for both the high and low sides of the system and the quick failure of the system. At around 1.5 hours or 5400 seconds, the agitator was reactivated.

The system trips out at various intervals during the test process, and this can be seen by the two temperature plots converging on the vertical lines. This is because once the compressor is turned off the pressure equalizes across the entire system and an even temperature is established.

The system stopped working at approximately 50000 seconds or 13.8 hours. This is theorized to be due to the two faults that occurred consecutively due to the -10℃ low temperature side refrigerant that was not being evaporated.

5.3.2 Vertical Plate Design

This section contains all the data that was gathered from the vertical plate design for comparison to the new design.

5.3.2.1 Vertical Plate Design without the Agitator

The following section focuses on when the newly implemented system was run without the agitator, testing the system performance to determine if the required ten hours of continuous run time for home heating would be met.

With similar amounts of water added to the tank, ensuring the flat plate heat exchangers were fully submerged in water, the results shown in Figure 5.17 were found.

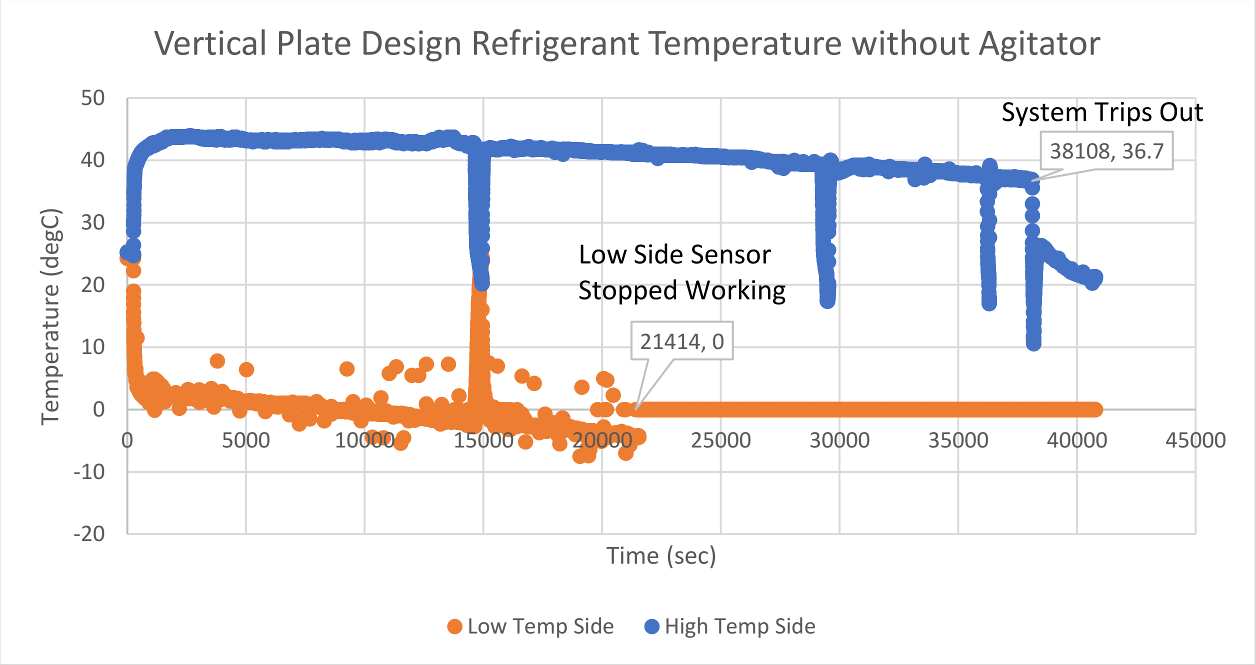

Figure 5.17 - High and Low Temperature Sides for Vertical Plate Design without Agitator

These results show the system running in excess of 10.5 hours before locking out the compressor due to liquid refrigerant entering the compressor. With the low side sensor failing prematurely, it is hard to interpret all data, but by considering the relationship between the high-side temperature and low-side temperature, a slow decrease in refrigerant temperature can be observed throughout system run time. Again, the data points on vertical lines that converge are the result of the compressor temporarily shutting down and equilibrium temperature and pressure conditions being reached throughout the system.

5.3.2.2 Vertical Plate Design with the Agitator

The following section focuses on when the newly implemented system was run with the agitator, testing the system performance at a low starting temperature to more accurately compare the system to ground implementation. The data that was collected during this test can be seen in Figure 5.18.

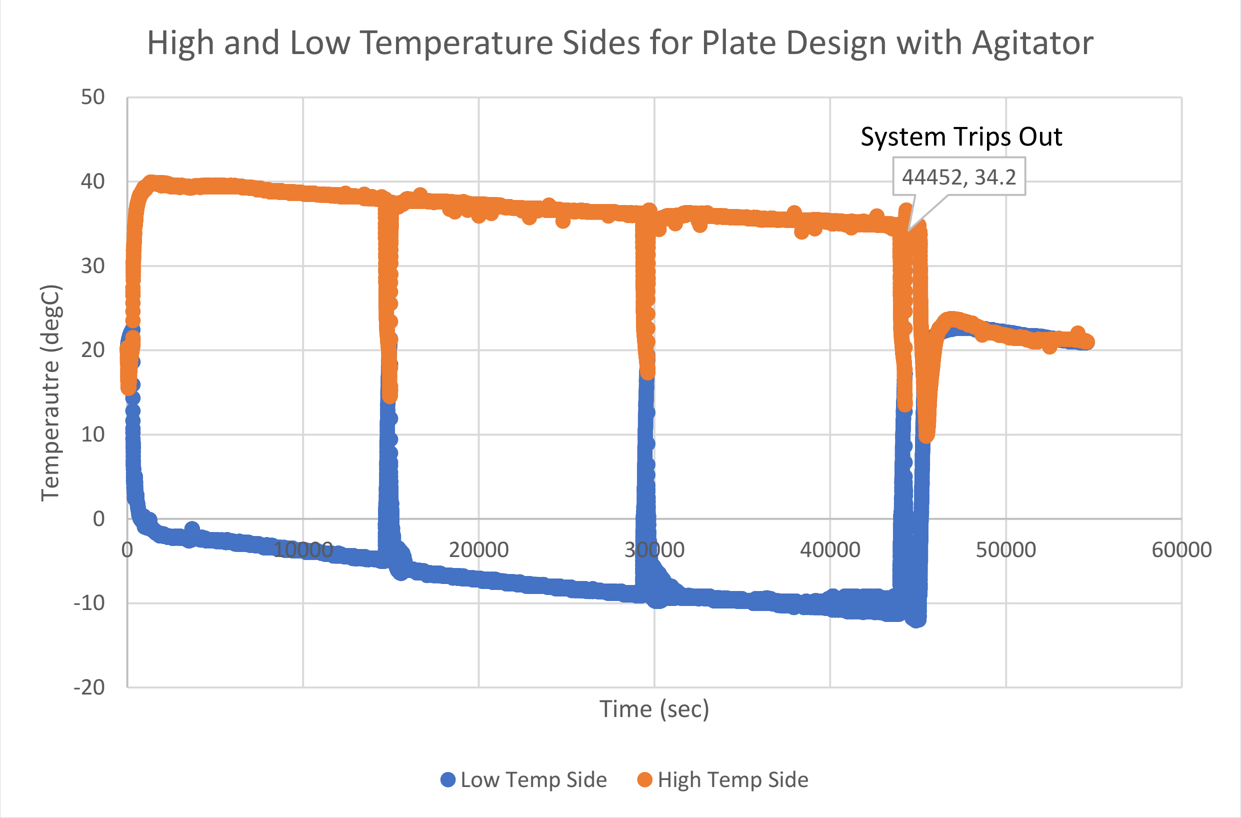

Figure 5.18- Vertical Plate Design with the Agitator

The system with the agitator was able to run for approximately 12.4 hours. This test had a starting tank temperature of between zero and four degrees. There was this slight variance in the water temperature because the team was unable to bring the full tank to the average Vancouver ground design temperature of two degrees. The average temperature of the tank was able to meet this parameter.

With this starting temperature, the team could more accurately determine if the system could meet the required ten hours that was needed to heat the standard home to a comfortable room temperature. This test, however, was not able to simulate the heat transfer that would occur between the ground and the tank because the system still had to remain in BCIT's Plastics Lab.

With this starting temperature the plate design was able to meet the required run time. This better confirms the validity of this concept.

5.4 Comparison of Incumbent with Plate Design

The following section covers the comparison between the previous incumbent design and the team's plate design. This will cover the tests that were run with and without the agitator. All of the tests were compared against the required run time given to the team by Joe Cheung, one of the team's faculty sponsors. This is the longest time that a heat pump must be active because it is the average time it takes to heat a standard home from before any heating has taken place to warm a space to a comfortable room temperature.

5.4.1 Results without Agitator

The following section covers the comparison of the tests that were completed without the addition of the agitator.

5.4.1.1 Comparison with Water as Tank Fluid

When the agitator was not used, the previous incumbent design was able to run for only 23 minutes, as discussed in section 5.3.1.1.1. This was much lower than the required run time of 10 hours. This confirms the need for the team's new heat exchanger design.

The plate design was then implemented, and the discussion of the full results is in section 5.3.2.1. These results show the system running in excess of 10.5 hours which means the required run time was able to be met without any additional equipment, if the initial tank water temperature is ignored

5.4.1.2 Comparison with "Water and Ethylene-Glycol" mix as Tank Fluid

The system was only run with Propylene-Glycol when the previous incumbent design was implemented, as discussed in section 5.2.1.1.2. This is because the team deem the results to be conclusive enough to determine the validity of changing the parameters of the water to increase the run time. The plate design also met the required run time without any additions such as the agitator and anti-freeze so the decrease in freezing temperature was unnecessary. The ethylene-glycol was also deemed to be too harmful to the environment if there were to be leaks in the tank. With these conclusions, the team decided to continue to use just water in the tank.

5.4.2 Results with Agitator

The following section covers the tests that were completed with the addition of the agitator. The agitator causes motion in the water which changes the convective heat transfer mode between the tank water and the plate from natural convection to forced convection. The hypothesis was that with this addition the agitator would slow down the formation of the ice around the exposed tubing and the plate areas because of the increased heat transfer and mixing of the tank water. This in turn would increase the run time of the system.

5.4.2.1 Incumbent Design with Water as Tank Fluid

The agitator tests were only completed on the system when only water was present in the tank, and not with any anti-freeze water mixture. This is due to the same reasons as discussed previously in section 5.4.1.2, which included the improvements of the design by using the plates and also the possible environmental impacts of the use of ethylene-glycol.

When the previous incumbent design was run using the agitator, it was able to run for approximately 13.8 hours, as discussed in section 5.3.1.2. This showed how drastic the improvements are with the addition of forced convection to the system. The agitator also allowed the system to maintain a more uniform temperature within the tank which also slowed the formation of ice. With the decreased rate of ice formation, the system was able to maintain heat transfer because there was less insulation caused by this ice build-up early on.

5.4.2.2 Plate Design with Water as Tank Fluid

The test that was completed for the plate design with the addition of the agitator is not directly comparable to the incumbent test. This is because the team decided to run the test with a starting temperature closer to the ground temperature that is observed in the Vancouver area. This being an average starting temperature of two degrees. During this test the system was able to run for approximately 12.4 hours, as discussed in section 5.3.2.2. This is a little more than an hour less than the other agitator test.

This result still proves that the plate design has met the required deliverable of being an improved geo-exchange system. This is because there was almost a twenty-degree difference in the starting temperature of the system, with the incumbent tank water starting at room temperature, but only an hour difference in run time.

This test also confirms the viability of the concept and need for future testing of this system.

Chapter 6. Conclusion

The project was successful at proving the proof of concept for using the latent heat of water in addition to the high heat capacity of the sensible heat of water to provide heating to homes. The vertical plate system has a COP of 3.7, and is capable of running for 12.4 hours with an average initial water temperature of 2°C. This is a considerable improvement over the incumbent system. The vertical plate system produced significantly more ice than the incumbent system—while still continuing to run—further demonstrating the increase of the amount of heat that was removed from the tank. These positive results are only a small portion of the possibilities for this system. The addition of glycol tripled the available heat in the incumbent system. This method could be used to further improve the final design with ease but is still seen as a risky solution to increase total heat transfer because of the possibility of fluid leaching from the tank into the environment. The increase of surface area was the only parameter that was altered from the incumbent design. An in-depth sensitively analysis and additional data collection could be done to investigate the optimization of system parameters. Many lessons were learned in the manufacturing of the vertical plate and can be further improved upon. The next vertical plate system prototype could be further improved by using sufficient heat conducting paste as well as reducing the amount of bare pipe and creating tighter tolerances through more in-depth manufacturing design and processes.

For these reasons mentioned above, the project was a success. But still has significant room for improvement and investigation.

Chapter 7. Lessons Learned

With many challenges overcome throughout the project, valuable lessons provided insight into how the project could be streamlined and finished with greater efficiency and effectiveness. Firstly, the typical issue of time constraints was found throughout the project, and better organization and devotion of time in the early portion of the project would have resulted in vast improvements in the latter portion of the project. Similarly, following a more formal approach in the early stages with respect to research would have been beneficial in the functional matrices for deciding on components to be used in the system. For example, a more in-depth heat exchanger theory investigation would have helped with the decision of which heat exchanger to use and optimization of the heat exchanger design. In other words, a more rigorous first-principles approach, although slower in the design stage, would have improved and saved time in the final design and manufacturing stage.

Now focusing on the manufacturing side, a key lesson was learned with respect to material ordering, as a key component in the heat conductive paste stalled the assembly of the heat exchanger and resulted in less time for the analysis and interpretation of the results. Also, when the paste did arrive, the quantity was insufficient and had reached a time where it was too late to order more—decreasing the overall effectiveness of the design.

A last key lesson that was found in working on this project was the importance of maintaining near-constant operating conditions for data collection to be able to get valuable and realistic comparisons between different setups and experimental tests. For this set of particular tests, using a tank water temperature of approximately 4°C would have been ideal to simulate realistic temperatures encountered in the ground and get more valid data.

Chapter 8. Bibliography

[1] F. BC, "Fortis Home Page," Fortis, 07 Jan 2018. [Online]. Available: https://www.fortisbc.com/NaturalGas/Homes/Switchtonaturalgas/Pages/Southern-Interior.aspx.

[2] "History of Refrigeration," [Online]. Available: http://www.historyofrefrigeration.com/. [Accessed 14th January 2018].

[3] E. Palermo, "Live Sciene," 14 May 2014. [Online]. Available: https://www.livescience.com/45268-who-invented-air-conditioning.html. [Accessed 14 January 2018].

[4] "New World Encyclopedia," [Online]. Available: http://www.newworldencyclopedia.org/entry/Geothermal_energy.

[5] Western Pennsylvania School For the Deaf, "WPSD Geothermal," [Online]. Available: http://www.wpsd.org/wp-content/uploads/WPSD-Geothermal.pdf. [Accessed 26 04 2018].

[6] Y. A. Cengel and M. A. Boles, Thermodynamics: An Engineering Approach Eighth Edition, New York: McGraw-Hill Educaion, 2015, p. 610.

[7] Natural Resources Canada, "Government of Canada," 27 March 2017. [Online]. Available: https://www.nrcan.gc.ca/energy/publications/efficiency/heating-heat-pump/6831. [Accessed 26 April 2018].

[8] Y. A. Cengel and A. J. Ghajar, Heat and Mass Transfer: Fundamentals and Applications Fifth Edition, New York: McGraw-Hill Education, 2015.

[9] Green Match , "Types of Ground Source Heat Pumps," [Online]. Available: https://www.greenmatch.co.uk/heat-pump/ground-source-heat-pump/types-of-ground-source-heat-pumps. [Accessed 26 04 2018].

[10] D. Li, B. Lam and P. Dela Masa, "Geothermal Ice Bank Heat Pump," BCIT, Burnaby, 2017.

[11] T. L. BERGMAN, A. S. LAVINE, F. P. INCROPERA and D. P. DEWITT, Introduction to Heat
Transfer, John Wiley & Sons, Inc. .

[12] Finned Tube, "FTBC BENT FINNED TUBE," [Online].
Available: https://www.finnedtube.com/product/bent-finned-tubes/.

[13] Temperature Corporation, "Temperature Corporation," [Online]. Available: http://www.temperaturecorporation.com/pdf/glycolconcentrationrequirements.pdf. [Accessed 25 April 2018].

[14] MSDS, "MSDS Search," [Online].
Available: http://msdssearch.dow.com/PublishedLiteratureDOWCOM/dh_010e/0901b8038010e413.pdf?filepath=/heattrans/pdfs/noreg/180-01190.pdf&fromPage=GetDoc. [Accessed 25 April 2018].

[15] "Finned Tube," [Online]. Available: http://www.finnedtube.com/helical-coils. [Accessed February 2018].

[16] greenTEG, "What it Heat Flux," [Online]. Available: https://www.greenteg.com/heat-flux-sensor/about-heat-flux/what-is-heat-flux/. [Accessed 26 04 2018].

[17] G. Leisgang, "Tri-County Heatin," 13 August 2013. [Online]. Available: http://www.tricountyheatingandcooling.com/home/heating_cooling_cincinnati/insights/post/20130807_the_heat_pump_balance_point_--_what_it_is_and_why_it_matters.html. [Accessed 27 April 2018].

Chapter 9. Index

balance point, 28
balometer, 65, 66
COMSOL, 1, 2, 5, 6, 7, 8, 10, 28, 29, 40, 43, 55, 60, 64, 65, 68, 90, 99
External Film Resistance, 10, 29, 41
heat exchanger, v, ix, 1, 2, 5, 6, 13, 15, 18, 19, 35, 40, 42, 43, 50, 52, 68, 79, 107, 110
heat loss calculations, 31
Heat pumps, 1, 19
Heat Transfer in Fluids, 41
Heat Transfer in Pipes, 29, 41
Heat Transfer in Solids, 41
Latent heat, 18
saturated liquid, 17, 19, 22, 112, 121, 122
saturated vapour, 17, 22
standard air, 66
subcooled liquid, 17
superheated vapour, 17, 23
throttling, 22, 111, 113, 121
waste water, 43
wood mold, 44, 45, 46, 48

Appendix A – Request for Proposal

Request for Proposal

NEW HEAT PUMP DESIGN FOR GEOEXCHANGE SYSTEMS

October 24, 2017

Issued by:

Hypocaustum Enterprises

Representative: Les McBurney

L_McBurney@hypocastum.ca

1-604-666-6666

A.1 Introduction & Background

Hypocaustum Enterprises is an HVAC company that operates throughout all of Canada providing high end geothermal energy solutions and is looking to implement a new system that will be able to be used in densely populated areas, at a lower cost. For this reason, Hypocaustum is looking for a new design for a Geo-Exchange system and is accepting proposals to find a qualified firm to provide the design. Our goal with this new Geo-Exchange system is to

1. reduce installation costs,
2. reduce footprint of sink/source loops without vertical drilling,
3. reduce environmental impact, and
4. increase cycle time of existing prototype.

The objective of this RFP is to locate a firm that will provide the best overall value to Hypocaustum Enterprises. More so, we are in search of a firm that will be able to exceed our expectations while meeting time and cost requirements. While price is a significant factor, other criteria will form the basis of our award decisions, as more fully described in the Evaluation Factors section of this Request for Proposal below.

A.2 Submission Guidelines & Requirements

The following submission guidelines and requirements apply to this RFP:

1. First, and foremost, only qualified individuals or firms with prior experience on projects such as this should submit proposals in response to this RFP.
2. Bidders intent on submitting a proposal should so notify the representative identified on the cover page no later than October 25, 2017.
3. Bidders are required to provide examples of previous work of a similar technical expertise and demonstrate how they are related.
4. The technical part of the proposal must be concise and must provide an overview of the proposed solution schedule and milestones, as applicable.
5. The price section of the proposal should indicate the breakdown of fixed cost for the project as well as hourly rates and an estimated total number of hours.
6. Proposals must be signed by a representative that is authorized to commit bidder's company.
7. Proposals must be received prior to November 7th, 2017 to be considered.
8. Proposals must remain valid for a period of 30 days.

A.3 Project Description

Hypocaustum requires an innovative design for a Geo-Exchange system that will be used in densely populated areas and must have a smaller footprint than current systems. The system must run for at least 10 hours, without the suction side pressure dropping below the safety limit. The project will require the creation of a multi physics model of the system that will allow the best material to be chosen, the equipment to be size and for the best pipe orientation to be determined for various environments all over Canada.

A.4 Project Scope

This project is limited to the model and a small-scale prototype. The model should also be verified against a physical prototype. There will be no full-scale testing. The successful bidder will also be responsible for a report created to document the project. It is desired that this report be published.

A.5 RFP Timelines

The Request for Proposal timeline is as follows:

Selection of Top Bidders / Notification to Unsuccessful Bidders	[December 5, 2017]
Start of Negotiation	[December 11, 2017]
Contract Award / Notification to Unsuccessful Bidders	[December 22, 2017]

The need-date for project completion is June 1, 2018. Bidders may propose a date earlier or later and will be evaluated accordingly.

A.7 Budget

Hypocaustum budget for the project is $100,000 but will except student labour at a reduced cost.

A.8 Evaluation Factors

Hypocaustum will rate proposals based on the following factors:

1. Ability to meet to the requirements set forth in this Request for Proposal
2. Relevant past performance/experience
3. Samples of work
4. Total Cost
5. Technical expertise/experience of bidder

Hypocaustum reserves the right to award to the bidder that presents the best value as determined solely by Hypocaustum in its absolute discretion.

Appendix B - Design Review

Geo-Exchange System Heat Exchanger Redesign

Design Review Package

Prepared For:

Johan Fourie

Joseph Cheung

Vahid Askari

Henry Chang

BCIT Mechanical Engineering

Prepared By:

Aaron Rendina

Emily Robinson

Eric Jacobsohn

Date: February 14th, 2018

B.1 Design Review Purpose and Objective

This review will be a combination of a requirements review and a preliminary design review. More so, the purpose of this review will be to ensure that all the requirements for the project have been clearly identified, to critically evaluate the current designs, and to become aware of any flaws or missed opportunities in the design. Lastly, the design review will conclude with the design that best meets the project requirements, as well as current areas of concern.

The objective for this review will be to bring forward any errors that the team has missed in the requirements or design and seek constructive criticism that will improve the design.

B.2 Project Objective

The project objective is to investigate the viability of the Ice Bank Geo-Exchange System, through the creation of a validated and verified software model. This will require that a model that predicts the real-life results within ten percent accuracy is made.

B.3 Deliverables

The deliverables for this project will be the validated and verified CFD and CHT model, and an improved upon outdoor coil for the geo-exchange system that will be manufactured and implemented into the current prototype.

B.4 Constraints

The main constraint for this project is time. The team is required to learn and understand a new software that has previously never been used by the group members. This has required multiple tutorials and many hours of troubleshooting. Another constraint is that COMSOL Multi Physics must be used and no other software because of its availability on campus, and its precision; other types of software are less powerful but have a friendlier and more intuitive user interface. The last constraint is the limitation to current prototype hardware and only redesigning the outdoor coil of the heat pump.

B.5 Calculations

B.5.1 Building Heat Loss

Taking a standard home design for the Vancouver area, the total heat loss for the home was found to be

$$\dot{Q}_{actual} \cong 10.45\ kW$$

B.5.2 Heat Transfer through Outdoor Coil (Horizontal)

Next, the theoretical maximum heat transfer through the current outdoor coil was found to be

$$\dot{Q} \cong 1294.91\ W$$

$$\therefore n = \frac{\dot{Q}_{actual}}{\dot{Q}} = \frac{10450\ W}{1294.91\ W} \cong 8.07$$

With a required increase in heat transfer, the easier parameter to change to meet demand is the surface area via fins or increasing the length of the tubing in the outdoor coil. Surface area makes more sense because increasing pipe length results in changes of refrigerant pressure via frictional losses, and more in-depth study into the current refrigeration design.

$$Current\ Surface\ Area\ =\ A_s = \pi DL \cong 0.2675\ m^2$$

$$Required\ Surface\ Area =\ A_s' = nA_s \cong 2.1831 m^2$$

B.5.3 Energy & Power Capacity in Tank

Ignoring heat transfer through the ground and tank into the water, the amount of time that heat can be provided by the geo-exchange system by just using sensible heat from the water is

$$\Delta t_S \cong 0.8042h$$

Similarly, the amount of time that heat can be provided by the geo-exchange system by just using latent heat from the water

$$\Delta t_L \cong 15.8974h$$

$$\Rightarrow Total\ Time = \Delta t_S + \Delta t_L\ \cong 16.7016h$$

Meaning, that if all the water in the tank could be frozen via heat transfer, it would be able to provide continuous heat for over 16 hours. However, this is most probably unrealistic.

B.5.4 Pipe Losses through Outdoor Coil

This calculation will need to be updated after the system has been run to get accurate pressure and temperature readings from the high-pressure and low-pressure sides of the heat pump, but, at the moment, the pressure loss through the outdoor coil is calculated to be

$$\Delta p_L \cong 56.182\ kPa$$

This was completed assuming a straight pipe, and this value will have to be updated to take into account any bends that are needed for the final design.

B.6 Incumbent Design

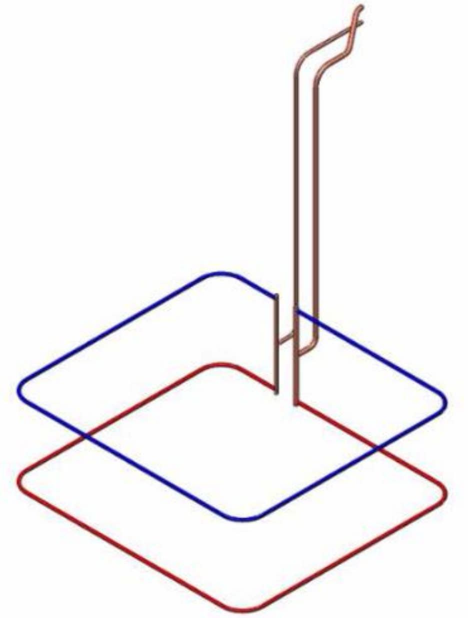

The incumbent design was selected by the previous design team for its scalability for future loops as well as its ease of manufacturing.

This design was able to form ice around the lower coil, having only one of the two coils use the latent heat of the water. This lowered the available heat energy that could be extracted, and with this coil design, the system was only able to achieve slightly over two hours of continuous operation.

B.7 Current Concepts

B.7.1 Helical Design

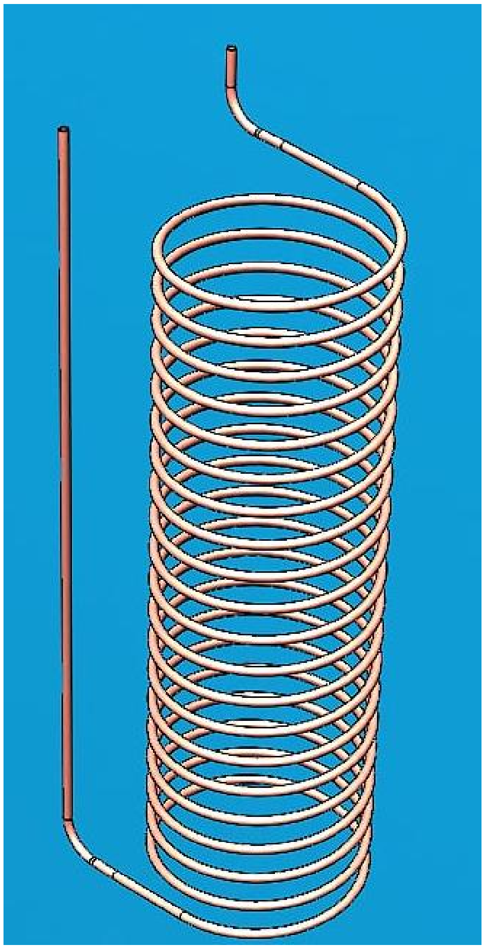

When doing research to determine ways to enhance the heat transfer, it was found that heat transfer could be increased via the introduction of turbulence to the system either through surface roughness, using insets inside the pipe, or a helical design. The helical design being easy resulted in further investigation into the increase of heat transfer due to the resulting centrifugal forces on the fluid being moved [11].

The Helical Design is used in many applications in industry because a secondary flow is induced by the centrifugal forces that consists of a pair of longitudinal vortices that result in highly non-uniform local heat transfer coefficients [11]. However, this results in an increase of not only the heat transfer rate, but also frictional losses. Therefore, the main issues that were found with this design were the space management due to the large height required to reach the needed 22 ft. of equivalent piping length, and pressure drop across it.

B.7.2 Fin Design – Coil and Fin

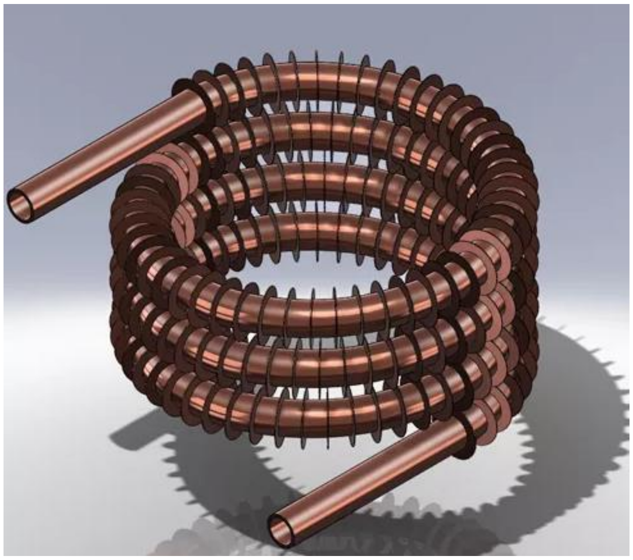

As shown in [15]

B.7.3 Fin Design – Serpentine Coil and Fin

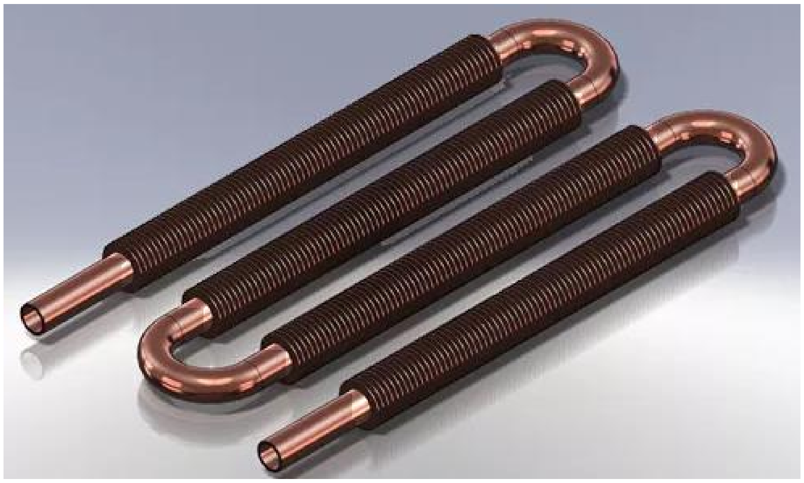

As shown in [15]

The use of fins is a design that would increase the heat transfer rate dramatically. However, the main issues in the use of this type of design is the increase in manufacturing complexity, most probably not manufactured in-house if anything but straight piping is sought and would still be expensive to buy off the shelf and assemble. For this reason, the team decided that this design would not be followed through.

B.7.4 Horizontal Flat Plate Design

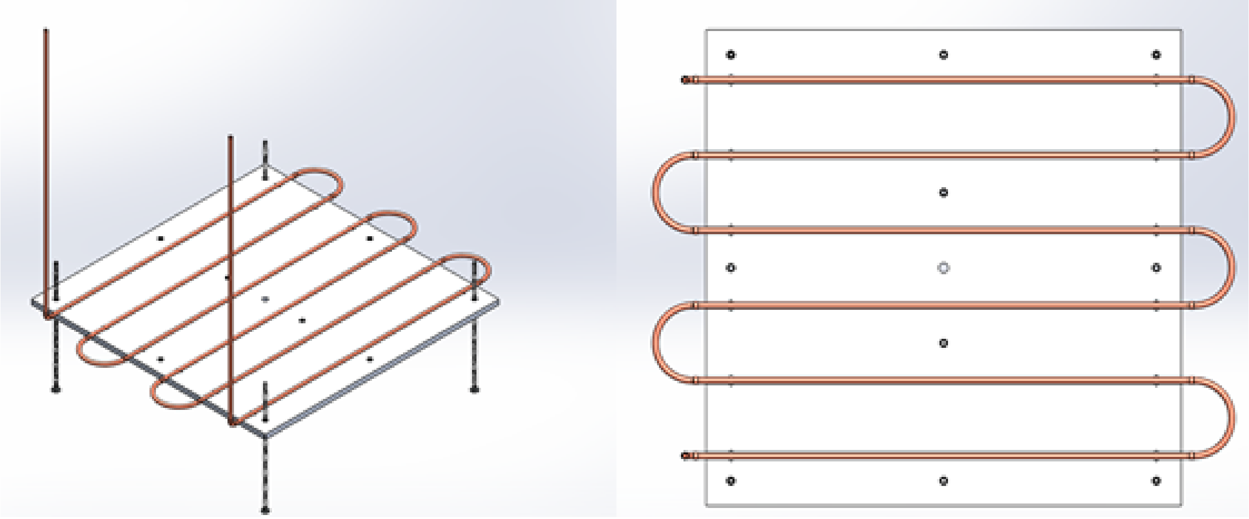

The horizontal flat plate design came about because of the push to decrease the complexity of manufacturing, as well as decreasing the need for expensive and custom parts. This design would use thin aluminum sheet metal that would be formed around the piping and use heat conductive paste to further increase the heat transfer.

B.8 Final Design - Vertical Flat Plate Design

For the final design, the team kept the formed sheet metal design for increasing the surface area, but the plate orientation was changed to vertical to increase the heat transfer. Placing the plates vertically allows the system to take greater advantage of the natural convection due to the changes in buoyancy in the water when temperature changes occur.

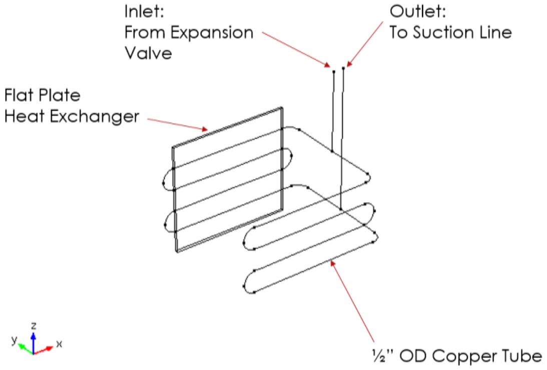
Inlet:
From Expansion
Valve
Outlet:
To Suction Line
Flat Plate
Heat Exchanger
½" OD Copper Tube
z
y
x

B.8.1 Support Designs

As these plates will be placed vertically, a more complex support system is need when compared with the horizontal plate design. Three support designs were considered, and the best one implemented during manufacturing.

B.8.1.1 Idea 1

This idea utilizes the sheet metal itself for support. The sheet metal would be formed around the pipe and then bent to create a triangular support that could be attached to the tank floor via weld nuts or pins.

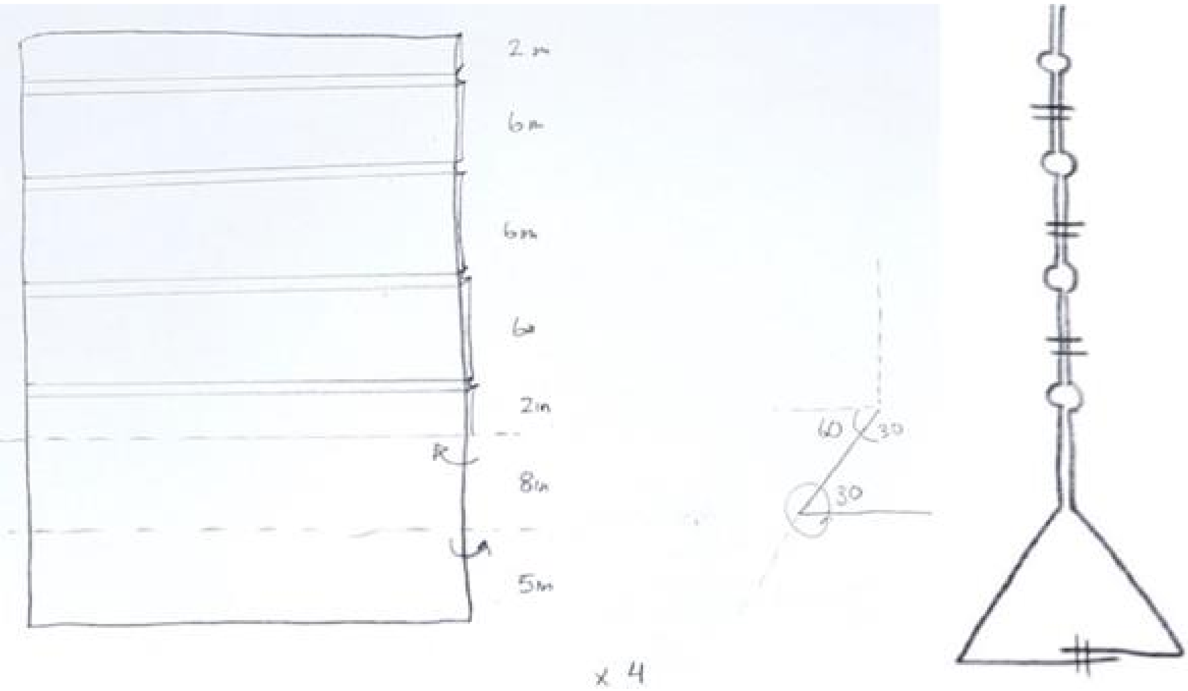

B.8.1.2 Idea 2

Zap straps or hangers would be used to hang the plates, but there would still be the issue of vibration damping.

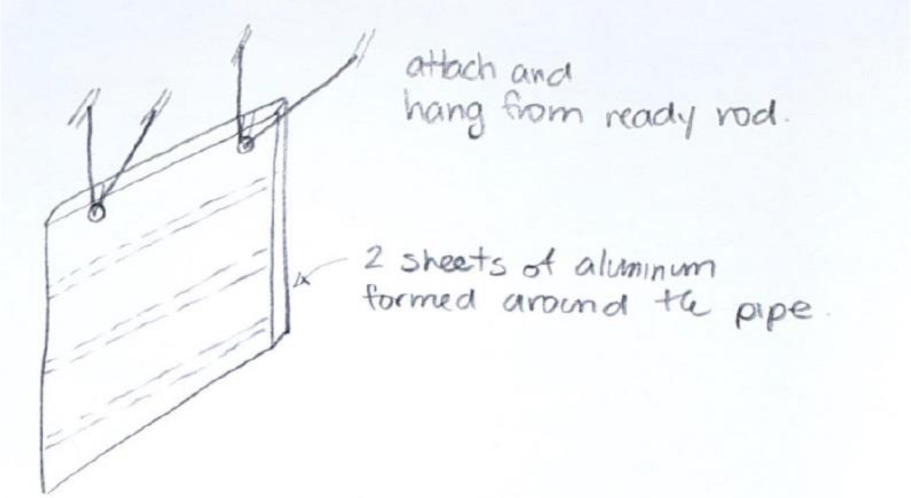
attach and
hang from ready rod.
2 sheets of aluminum
formed around the pipe.

B.8.1.3 Idea 3

This idea would use of threaded rod to attach the plates to each other as well as to the tank walls. The threaded rod would be connected to the tank walls via weld nuts.

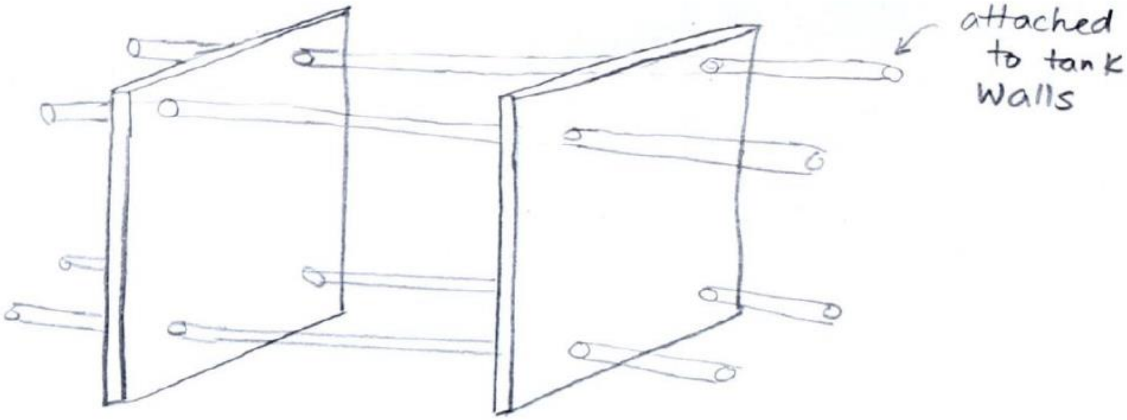
attached
to tank
Walls

B.9 Schedule Status

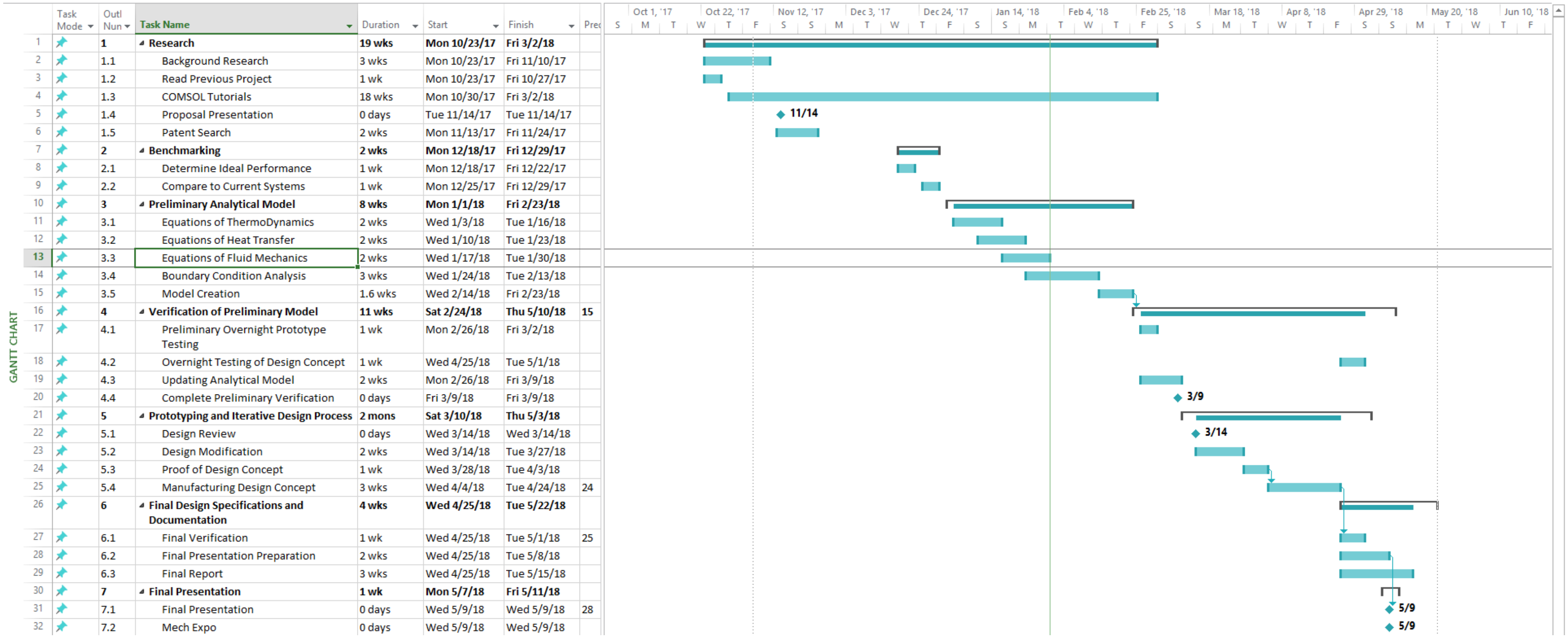

	Task Mode	Outl Nun	Task Name	Duration	Start	Finish	Prec
1	📌	1	**Research**	**19 wks**	**Mon 10/23/17**	**Fri 3/2/18**	
2	📌	1.1	Background Research	3 wks	Mon 10/23/17	Fri 11/10/17	
3	📌	1.2	Read Previous Project	1 wk	Mon 10/23/17	Fri 10/27/17	
4	📌	1.3	COMSOL Tutorials	18 wks	Mon 10/30/17	Fri 3/2/18	
5	📌	1.4	Proposal Presentation	0 days	Tue 11/14/17	Tue 11/14/17	
6	📌	1.5	Patent Search	2 wks	Mon 11/13/17	Fri 11/24/17	
7	📌	2	**Benchmarking**	**2 wks**	**Mon 12/18/17**	**Fri 12/29/17**	
8	📌	2.1	Determine Ideal Performance	1 wk	Mon 12/18/17	Fri 12/22/17	
9	📌	2.2	Compare to Current Systems	1 wk	Mon 12/25/17	Fri 12/29/17	
10	📌	3	**Preliminary Analytical Model**	**8 wks**	**Mon 1/1/18**	**Fri 2/23/18**	
11	📌	3.1	Equations of ThermoDynamics	2 wks	Wed 1/3/18	Tue 1/16/18	
12	📌	3.2	Equations of Heat Transfer	2 wks	Wed 1/10/18	Tue 1/23/18	
13	📌	3.3	Equations of Fluid Mechanics	2 wks	Wed 1/17/18	Tue 1/30/18	
14	📌	3.4	Boundary Condition Analysis	3 wks	Wed 1/24/18	Tue 2/13/18	
15	📌	3.5	Model Creation	1.6 wks	Wed 2/14/18	Fri 2/23/18	
16	📌	4	**Verification of Preliminary Model**	**11 wks**	**Sat 2/24/18**	**Thu 5/10/18**	15
17	📌	4.1	Preliminary Overnight Prototype Testing	1 wk	Mon 2/26/18	Fri 3/2/18	
18	📌	4.2	Overnight Testing of Design Concept	1 wk	Wed 4/25/18	Tue 5/1/18	
19	📌	4.3	Updating Analytical Model	2 wks	Mon 2/26/18	Fri 3/9/18	
20	📌	4.4	Complete Preliminary Verification	0 days	Fri 3/9/18	Fri 3/9/18	
21	📌	5	**Prototyping and Iterative Design Process**	**2 mons**	**Sat 3/10/18**	**Thu 5/3/18**	
22	📌	5.1	Design Review	0 days	Wed 3/14/18	Wed 3/14/18	
23	📌	5.2	Design Modification	2 wks	Wed 3/14/18	Tue 3/27/18	
24	📌	5.3	Proof of Design Concept	1 wk	Wed 3/28/18	Tue 4/3/18	
25	📌	5.4	Manufacturing Design Concept	3 wks	Wed 4/4/18	Tue 4/24/18	24
26	📌	6	**Final Design Specifications and Documentation**	**4 wks**	**Wed 4/25/18**	**Tue 5/22/18**	
27	📌	6.1	Final Verification	1 wk	Wed 4/25/18	Tue 5/1/18	25
28	📌	6.2	Final Presentation Preparation	2 wks	Wed 4/25/18	Tue 5/8/18	
29	📌	6.3	Final Report	3 wks	Wed 4/25/18	Tue 5/15/18	
30	📌	7	**Final Presentation**	**1 wk**	**Mon 5/7/18**	**Fri 5/11/18**	
31	📌	7.1	Final Presentation	0 days	Wed 5/9/18	Wed 5/9/18	28
32	📌	7.2	Mech Expo	0 days	Wed 5/9/18	Wed 5/9/18	

At the moment, the project is in the preliminary analytical model section of the schedule. The hand calculations are currently finishing up, which will be complete after running the current set up to get values for inlet and outlet temperature and pressure.

The boundary conditions that will need to be applied to the model have almost all been determined, and the project will be moving to start the creation of the model on schedule.

B.10 Areas of Concern

B.10.1 COMSOL

The teams understanding of the software is subpar. This is due to:

- Being unable to find effective resources to help advance learning
- The software has a complex user interface
- The software tutorials do not explain the building of the geometry or the gathering of the results
- Explanations over more complex simulations with multiple heat transfers and studies are hard to find

B.10.2 Manufacturing before Simulation

The team and the team's sponsors are looking to start the manufacturing of the plate design. The main area of concern for this is that the team has been unable to run accurate simulations on COMSOL to confirm the increase in efficiency that this design will provide. The calculations that have been completed provide confidence in this design, but the team does not want to move forward with manufacturing without the completion of the simulations.

Appendix C – Mathematical Derivations

C.1 Building Heat Loss

Indoor Design Temperature [°C (°F)]	21(72)
Outdoor Design Temperature [°C (°F)]	−8(17.6)
Heating Degree Day	
Effective R-Value [°F $\cdot h \cdot ft^2/BTU$]	
Basement Walls	13.697
1st and 2nd Floor Walls	22.876
Roof	38.725
Window (Double insulating glass w/ ½” air space)	2.04
Skylight (Double insulating glass w/ ½” air space)	2.04
Door (2-½” Solid Core – Flush)	3.70
Effective Perimeter R’-Value [°F $\cdot h \cdot ft/BTU$]	1.886
Air Change Per Hour	0.5

With these values, it was found that the total heat loss for a January 1% outdoor design temperature was $\dot{Q} \cong 35{,}654\ BTU/h$, or in metric units, $\dot{Q} \cong 10.45\ kW$. It should be emphasized, however, that since this is a custom new home—the amount of heat loss experienced by an average home in Vancouver could be significantly higher per square foot

The previous report stated a heat loss rate of $\dot{Q} = 25655.8\ BTUH$ with the difference due to choosing a poorly insulated building.

Room Description	Laundry/ Pantry	Kitchen/ Dining	Living Room	Den/ Guest	Powder Room	Mechanical Room	Master Bedroom	Bedroom 2	Bedroom 3	Bedroom 4	Ensuite Bathroom	Bathroom	Closet	Foyer	Loft
Room area: [ft.^{2}]	119.58	387.13	263.63	140.94	21.78	43.75	171.00	171.00	97.22	97.22	81.58	52.08	45.12	123.19	343.00
Height [ft.]	9.25	9.25	9.25	9.25	9.25	9.25	21.13	21.13	8.00	8.00	8.00	8.00	8.00	8.00	5.50
Length of perimeter wall [ft.]	22.42	41.42	32.75	13.75	9.42	8.75	26.25	26.25	9.33	9.33	11.00	5.00	6.08	24.50	77.00
North Wall:															
Width [ft.]	8.75	27.17	0.00	0.00	0.00	0.00	0.00	12.00	9.33	9.33	0.00	5.00	0.00	0.00	24.50
Height [ft.]	9.25	9.25	9.25	9.25	9.25	9.25	21.13	21.13	8.00	8.00	8.00	8.00	8.00	8.00	5.50
East Wall:															
Width [ft.]	0.00	14.25	14.25	0.00	0.00	0.00	14.25	14.25	0.00	0.00	0.00	0.00	0.00	0.00	14.00
Height [ft.]	9.25	9.25	9.25	9.25	9.25	9.25	21.13	21.13	8.00	8.00	8.00	8.00	8.00	8.00	10.71
South Wall:															
Width [ft.]	0.00	0.00	18.50	13.75	4.71	0.00	12.00	0.00	0.00	0.00	11.00	0.00	6.08	6.25	24.50
Height [ft.]	9.25	9.25	9.25	9.25	9.25	9.25	21.13	21.13	8.00	8.00	8.00	8.00	8.00	8.00	5.50
West Wall:															
Width [ft.]	13.67		0.00	0.00	4.71	8.75	0.00	0.00	0.00	10.42	0.00	0.00	0.00	18.25	14.00
Height [ft.]	9.25	9.25	9.25	9.25	9.25	9.25	21.13	21.13	8.00	8.00	8.00	8.00	8.00	8.00	10.71
Roof:															
Width [ft.]	0.00	0.00	0.00	0.00	0.00	0.00	14.25	14.25	9.33	9.33	11.00	5.00	6.08	6.75	24.50
length [ft.]	0.00	0.00	0.00	0.00	0.00	0.00	12.00	12.00	7.00	7.00	7.00	7.00	7.00	7.00	14.00
Window:															
Width [ft.]	0.00	6.21	6.21	0.00	0.00	0.00	4.50	13.63	3.17	3.17	0.00	0.00	0.00	4.50	0.00
Height [ft.]	0.00	8.00	8.00	0.00	0.00	0.00	5.17	7.75	4.50	4.50	0.00	0.00	0.00	5.17	0.00
Number of windows	0.00	2.00	2.00	0.00	0.00	0.00	2.00	1.00	1.00	1.00	0.00	0.00	0.00	1.00	0.00
Skylight:															
Width [ft.]	0.00	0.00	0.00	0.00	0.00	0.00	0.00	0.00	0.00	0.00	3.00	0.00	0.00	0.00	5.00
Height [ft.]	0.00	0.00	0.00	0.00	0.00	0.00	0.00	0.00	0.00	0.00	3.00	0.00	0.00	0.00	5.00
Number of skylight	0.00	0.00	0.00	0.00	0.00	0.00	0.00	0.00	0.00	0.00	1.00	0.00	0.00	0.00	2.00
Gross Wall Area	207.35	383.10	302.94	127.19	87.10	80.94	554.53	554.53	74.67	74.67	88.00	40.00	48.67	196.00	482.96
Gross window Area	0.00	99.33	133.08	0.00	0.00	0.00	152.09	105.59	14.25	14.25	0.00	0.00	0.00	46.00	0.00
Door area [ft^2]	0.00	0.00	0.00	0.00	0.00	0.00	0.00	0.00	0.00	0.00	0.00	0.00	0.00	24.50	0.00
Net Wall area	207.35	283.78	169.86	127.19	87.10	80.94	402.44	448.94	60.42	60.42	88.00	40.00	48.67	125.50	482.96
Gross roof area	0.00	0.00	0.00	0.00	0.00	0.00	213.75	213.75	65.33	65.33	77.00	35.00	42.58	47.25	428.75
Gross skylight area	0.00	0.00	0.00	0.00	0.00	0.00	0.00	0.00	0.00	0.00	9.00	0.00	0.00	0.00	50.00
Net roof area	0.00	0.00	0.00	0.00	0.00	0.00	213.75	213.75	65.33	65.33	68.00	35.00	42.58	47.25	378.75

Room Description	Laundry/ Pantry	Kitchen/ Dining	Living Room	Den/ Guest	Powder Room	Mechanical Room	Master Bedroom	Bedroom 2	Bedroom 3	Bedroom 4	Ensuite Bathroom	Bathroom	Closet	Foyer	Loft
Heat loss through walls [BTU/h]	493.10	674.83	403.93	302.46	207.14	192.47	957.01	1067.59	143.67	143.67	209.27	95.12	115.73	298.44	1,148.50
Heat loss through windows [BTU/h]	0.00	2,648.75	3,548.75	0.00	0.00	0.00	4,055.83	2,815.83	380.00	380.00	0.00	0.00	0.00	1,226.67	0.00
Heat loss through roof [BTU/h]	0.00	0.00	0.00	0.00	0.00	0.00	300.27	300.27	91.78	91.78	95.52	49.17	59.82	66.38	532.06
Heat loss through skylight [BTU/h]	0.00	0.00	0.00	0.00	0.00	0.00	0.00	0.00	0.00	0.00	240.00	0.00	0.00	0.00	1,333.33
Heat loss through door [BTU/h]	0.00	0.00	0.00	0.00	0.00	0.00	0.00	0.00	0.00	0.00	0.00	0.00	0.00	360.22	0.00
Heat loss through infiltration [BTU/h]	541.57	1,753.21	1,193.90	638.28	98.63	198.14	1,656.96	1,656.96	380.80	380.80	319.55	204.00	176.72	482.50	923.63
Perimeter Heat loss [BTU/h]	0.00	7.55	7.55	0.00	0.00	0.00	0.00	0.00	0.00	0.00	0.00	0.00	0.00	4.51	0.00
Room Heat Loss [BTU/h]	**1,034.67**	**5,084.34**	**5,154.14**	**940.73**	**305.76**	**390.61**	**6,970.08**	**5,840.66**	**996.25**	**996.25**	**864.34**	**348.29**	**352.27**	**2,438.71**	**3,937.52**
Total Square Footage [ft^2]	**2,158.22**														
Building Heat Loss [BTU/h]	**35,654.62**														
Building Heat Loss [kW]	**10.45**														

C.2 Heat Transfer through Outdoor Coil

Given:

The following values were acquired from the existing geo-exchange system, and from the previously shown simple building heat loss calculation.

HFC-410A Refrigerant

$$d = ID = 3/8\ in = (0.375in)\left(0.0254\frac{m}{in}\right) = 0.009525\ m$$

$$D = OD = 1/2\ in = (0.5in)\left(0.0254\frac{m}{in}\right) = 0.0127\ m$$

$$L = 22\ ft = (22ft)\left(12\frac{in}{ft}\right)\left(0.0254\frac{m}{in}\right) = 6.7056\ m$$

$$p_L = 95.2\ psig$$

$$\dot{Q}_{actual} = 10567\ W$$

Assumptions:

In order to carry forward with the calculations, tank fluid temperature assumptions were made considering an expected soil temperature of 4°C.

$$T_\infty = T_{H_2O} = 4°\mathrm{C}$$

$$T_w = T_{refrigerant}$$

At a pressure of P_L, the coinciding temperature is 30°F $\cong -1.1$°C. With a design for the geo-exchange system to bring the tank water temperature down to 0°C, a lower refrigerant temperature is required in order to allow for a greater amount of heat transfer, as the temperature difference between the fluid and pipe wall is one of the controlled variables that can be changed in the system. Therefore, assuming a refrigerant temperature of $T_W = -10°\mathrm{C}$, results in an outdoor coil design pressure of $p_L = 68.3\ psig$. With the given values, and assumed values, the total heat transfer rate through the outdoor coil can be found.

Solution:

$$T_f = \frac{T_\infty + T_w}{2}$$

$$= \frac{4℃ + (-10℃)}{2}$$

$$= -3℃ = 270.15K$$

$$\therefore \begin{cases} \beta = -32.74 \cdot 10^{-6} K^{-1} \\ C_{p,avg} = 4.211 \cdot 10^3 \dfrac{J}{kg \cdot ℃} \\ k = 574 \cdot 10^{-3} \dfrac{W}{m \cdot ℃} \\ \mu = 1652 \cdot 10^{-6} \dfrac{N \cdot s}{m^2} \\ Pr = 12.22 \\ \rho = 1000 \dfrac{kg}{m^3} \end{cases}$$

$$\Rightarrow \alpha = \frac{k}{\rho C_p} = \frac{574 \cdot 10^{-3} \dfrac{W}{m \cdot ℃}}{\left(1000 \dfrac{kg}{m^3}\right)\left(4.211 \cdot 10^3 \dfrac{J}{kg \cdot ℃}\right)} = 1.36 \cdot 10^{-7} \frac{m^2}{s}$$

$$\Rightarrow \nu = \frac{\mu}{\rho} = \frac{1652 \cdot 10^{-6} \ \dfrac{N \cdot s}{m^2}}{1000 \dfrac{kg}{m^3}} = 1.652 \cdot 10^{-6} \frac{m^2}{s}$$

$$Ra_D = \frac{g\beta(T_w - T_\infty)D^3}{\alpha\nu}$$

$$= \frac{\left(9.81 \dfrac{m}{s^2}\right)(-32.74 \cdot 10^{-6} K^{-1})(10℃ - 4℃)(0.0127m)^3}{\left(1.36 \cdot 10^{-7} \dfrac{m^2}{s}\right)\left(1.652 \cdot 10^{-6} \dfrac{m^2}{s}\right)}$$

$$\cong 40995.66$$

$$\overline{Nu_D} = \left\{0.60 + \frac{0.387Ra_D^{\frac{1}{6}}}{\left[1 + \left(\frac{0.559}{Pr}\right)^{\frac{9}{16}}\right]^{\frac{8}{27}}}\right\}^2$$

$$= \left\{0.60 + \frac{0.387(40995.66)^{1/6}}{\left[1 + \left(\frac{0.559}{12.22}\right)^{9/16}\right]^{8/27}}\right\}^2$$

$$\cong 7.649$$

$$\bar{h} = \frac{\overline{Nu_D}k}{D} = \frac{(7.649)\left(574 \cdot 10^{-3}\frac{W}{m \cdot ℃}\right)}{0.0127m} \cong 345.715\frac{W}{m^2 \cdot ℃}$$

$$\therefore \dot{Q} = \bar{h}A_s(T_\infty - T_w) = \bar{h}\pi DL(T_\infty - T_w)$$

$$\Rightarrow \dot{Q}' = \frac{\dot{Q}}{L} = \bar{h}\pi D(T_\infty - T_w)$$

$$= \left(345.715\ \frac{W}{m^2 \cdot ℃}\right)\pi(0.0127m)\big(4℃ - (-10℃)\big)$$

$$\cong 193.108\frac{W}{m}$$

Now, taking into account the existing length of tubing in the outdoor coil and multiplying it by the linear heat transfer rate results in the predicted heat transfer rate for the existing system.

$$\dot{Q} = \dot{Q}'L = \left(193.108\frac{W}{m}\right)(22ft)\left(12\frac{in}{ft}\right)\left(0.0254\frac{m}{in}\right) \cong 1294.91\ W$$

Compared with the heat loss rate of the building of $\dot{Q}_{actual} = 10567$ watts, the factor of difference between the two is

$$n = \frac{\dot{Q}_{actual}}{\dot{Q}} = \frac{10567\ W}{1294.91\ W} \cong 8.16$$

Since the temperature of the water in the tank can only be changed by changing location, it is not a controlled variable. Film temperature, however, can be changed by changing the refrigerant temperature, but is somewhat complicated as other factors of the heat pump need to be taken into account. Therefore, the easiest variable to change is the surface area of the outdoor coil by means of increasing the length of the copper tubing, adding fins, or adding a flat plate heat exchanger to increase the existing surface area from

$$A_s = \pi DL = \pi(0.0127m)(22ft)\left(12\frac{in}{ft}\right)\left(0.0254\frac{m}{in}\right) \cong 0.2675\ m^2$$

to

$$A_s' = nA_s = (8.16)(0.2675m^2) \cong 2.1831m^2$$

C.3 Energy & Power Capacity in Tank

In order to find the total amount of energy the tank can store while neglecting heat transfer through the tank walls from the ground (adiabatic conditions), a thermodynamic approach is taken, first only extracting the sensible heat from the tank fluid, and then extracting the latent heat of fusion, as follows:

$$Q_s - W = \Delta U + \Delta KE + \Delta PE, Q_s \coloneqq Sensible\ heat\ energy$$

$$\Rightarrow Q_s = \Delta U + W_b + W_{other}$$

$$Q_s = \Delta H + W_{other}$$

$$Q_s = \Delta H$$

$$Q_s \cong mC_{p,avg}\Delta T$$

$$Q_s \cong \rho V C_{p,avg}\Delta T$$

$$Q_s \cong \left(1000\frac{kg}{m^3}\right)(4\,ft)^3\left(12\frac{in}{ft}\right)^3\left(0.0254\frac{m}{in}\right)^3\left(4.22\cdot 10^3\frac{J}{kg\cdot {}^\circ\mathrm{C}}\right)(4^\circ\mathrm{C} - 0^\circ\mathrm{C})$$

$$Q_s \cong\ 30.591MJ$$

Using the heat loss rate calculated in the previous section, the total amount of time that the tank can provide heat energy to a building is

$$\dot{Q} \cong \frac{\Delta Q_s}{\Delta t}$$

$$\Rightarrow \Delta t \cong \frac{\Delta Q_s}{\dot{Q}}$$

$$\Delta t \cong \frac{30.591\cdot 10^6 J}{10567W}$$

$$\Delta t \cong (2894.98s)\left(\frac{1h}{3600s}\right)$$

$$\Delta t \cong 0.8042h$$

Now, extracting the latent heat of fusion from the fluid, the following amount of energy can be removed from the tank

$$Q_l = mh_{if}$$

$$= \rho V h_{if}$$

$$= \left(1000\frac{kg}{m^3}\right)(4\,ft)^3\left(12\frac{in}{ft}\right)^3\left(0.0254\frac{m}{in}\right)^3\left(333.7\cdot 10^3\frac{J}{kg}\right)$$

$$\cong 604.76MJ$$

Again, using the heat loss rate calculated in the previous section, the total amount of time that the tank can provide heat energy to a building when only considering the latent heat of fusion is

$$\dot{Q} \cong \frac{\Delta Q_{if}}{\Delta t}$$

$$\Rightarrow \Delta t \cong \frac{\Delta Q_{if}}{\dot{Q}}$$

$$\cong \frac{604.76\cdot 10^6 J}{10567W}$$

$$\cong (57230.74s)\left(\frac{1h}{3600s}\right)$$

$$\cong 15.8974h$$

Adding the calculated times that the tank can provide sensible heat and latent heat of fusion results in a total time of

$$t = \sum \Delta t$$

$$\cong 0.8042h + 15.8974h$$

$$\cong 16.7016h$$

This implies that if the specified building had a heat demand on the coldest day of the year for the specified location, it would be able to be heated continuously for approximately 16 hours if heat were to be extracted from the tank at a rate of approximately 10,567 watts.

Realistically, though, it would be difficult to freeze the entire geo-exchange tank without first locking out the heat pump due to liquid refrigerant being sent back to the compressor due to inadequate heat transfer. Therefore, although in an ideal scenario the tank could provide more than enough energy to heat a standard 2,000 square foot house in Vancouver for at least 10 hours of continuous run time, there are too many other factors that must be analyzed in order to have a system that works properly; some of these factors include, but are not limited to

- Heat transfer through the tank walls
- Heat transfer through the outdoor coil heat exchanger
- Frictional losses in the system
- Thermal resistance of ice, tank walls, and soil
- Convection heat transfer coefficient of liquid water or fluid used

C.4 Pipe Losses Through Outdoor Coil

Given:

The following values were acquired from the existing geo-exchange heat pump, heat pump specification sheets and from the displayed values on the heat pump when running.

Refrigerant used	HFC-410A Refrigerant
Inside diameter of copper tube	$d = 3/8\ in = (0.375 in)\left(0.0254\frac{m}{in}\right) = 0.009525\ m$
Outside diameter of copper tube	$D = OD = 1/2\ in = (0.5 in)\left(0.0254\frac{m}{in}\right) = 0.0127\ m$
Compressor voltage	$E = 240\ V$
Compressor current draw	$I = 6.0 A$
Total length of outdoor coil copper tube	$L = 22\ ft = (22 ft)\left(12\frac{in}{ft}\right)\left(0.0254\frac{m}{in}\right) = 6.7056\ m$
Pressure on high side of heat pump	$p_H = 324.7\ psig$
Pressure on low side of heat pump	$p_L = 95.2\ psig$
Heat pump capacity at 0°C	$\dot{Q} = 9900\ BTUH = (9900\ BTUH)\left(\frac{3.41214163\ W}{1\ BTUH}\right)$ $\cong 2.9014\ kW$

Assumptions:

As a starting point, it is assumed that the heat pump operates under the ideal vapor-compression refrigeration cycle, meaning that the refrigerant is never subcooled and only superheated due to compression, the throttling process is isenthalpic, and the compression process is reversible. This allows for finding values at specific locations of interest on the refrigeration cycle without a need to know the efficiencies of certain heat pump components. These locations will be numbered as shown on the figure on the following page.

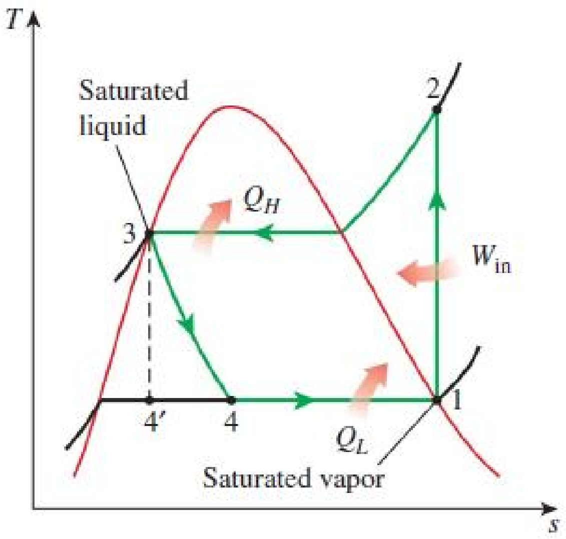

Next, the following values were found by interpolating thermodynamic and thermo-physical property charts and diagrams for refrigerant R410A. Although the refrigerant is a liquid-vapor mixture, property values were chosen as a saturated liquid to simplify equations, and results in a conservative solution.

Temperature on high pressure side of heat pump	$T_H \cong 49.2436\ ℃$
Temperature on low pressure side of heat pump	$T_L \cong -1.5513\ ℃$
Enthalpy at point 1	$h_1 = 422.1346\ kJ/kg$
Enthalpy at point 3	$h_3 = 285.3116\ kJ/kg$
Enthalpy of saturated liquid at point 4	$h_{4f} = 197.6179\ kJ/kg$
Enthalpy of vaporization at point 4	$h_{4fg} = 224.5167\ kJ/kg$
Specific volume of saturated liquid at point 4	$v_{4f} = 8.4487 \cdot 10^{-4}\ m^3/kg$
Specific volume of vaporization at point 4	$v_{4fg} = 0.9319\ m^3/kg$
Specific heat capacity of saturated liquid on low pressure side of heat pump	$C_p \cong 1.6\ kJ/kg \cdot ℃$
Thermal conductivity of saturated liquid on low pressure side of heat pump	$k \cong 0.1005\ W/m \cdot ℃$
Dynamic viscosity of saturated liquid on low pressure side of heat pump	$\mu = 164 \cdot 10^{-6}\ Pa \cdot s$

Due to the throttling process being assumed to be isenthalpic, the following equation is valid:

$$h_4 = h_3 = 285.3116\ kJ/kg$$

With the enthalpy at point four known, the quality of the refrigerant fluid can be found as shown:

$$x = \frac{y - y_f}{y_{fg}}$$

$$\Rightarrow x_4 = \frac{h_4 - h_{4f}}{h_{4fg}} = \frac{285.3116\ kJ/kg - 197.6179\ kJ/kg}{h_{4fg} = 224.5167\ kJ/kg} \cong 0.3906$$

Therefore, the specific volume of the refrigerant at point four is

$$v_4 = x_4 v_{4fg} + v_{4f} = (0.3906)(0.9319\, m^3/kg) + 8.4487 \cdot 10^{-4}\ m^3/kg$$
$$\cong 0.3648 \cdot 10^{-4}\ m^3/kg$$

With all the thermodynamic and thermo-physical values of interest found, solving for the losses through the outdoor coil can begin.

$$\dot{W}_c = EI = (240V)(6A) = 1440W$$

$$\therefore \dot{Q}_L = \dot{Q} - \dot{W}_c = 2901.4\, W - 1440\, W = 1461.4\, W$$

$$\dot{Q}_L = \dot{m}(h_1 - h_4)$$

$$\Rightarrow \dot{m} = \frac{\dot{Q}_L}{h_1 - h_4} = \frac{1461.4\, W}{422.1346\ kJ/kg - 285.3116\ kJ/kg} \cong 0.0107\ kg/s$$

$$\Rightarrow u_{m4} = \frac{\dot{m}}{\rho_4 A} = \frac{\dot{m}}{\frac{1}{v_4} \cdot \frac{\pi}{4} d^2} = \frac{0.0107\ kg/s}{\left(\frac{1}{0.3648 \cdot 10^{-4}\ m^3/kg}\right)\left(\frac{\pi}{4}\right)(0.009525\, m)^2} \cong 54.6865\ m/s$$

$$Re_d = \frac{4\dot{m}}{\pi d \mu} = \frac{4(0.0107\ kg/s)}{\pi(0.009525\, m)(164 \cdot 10^{-6}\, Pa \cdot s)} \cong 8705.9 > 2300 \therefore Turbulent$$

$$Pr = \frac{C_p \mu}{k} = \frac{(1.6\ kJ/kg \cdot ℃)(164 \cdot 10^{-6}\, Pa \cdot s)}{0.1005\ W/m \cdot ℃} \cong 2.6109$$

Since the refrigerant flow is turbulent in the outdoor coil, and its value is $3000 < Re_d < 5 \cdot 10^6$, the friction factor can be found via an equation developed by Petukhov:

$$f = (0.790 \ln(Re_d - 1.64))^{-2} = (0.790 \ln(8705.9 - 1.64))^{-2} \cong 0.0195$$

This results in the pressure drop across the outdoor coil being equal to

$$\Delta p_L = f \frac{\rho u_m^2}{2d}(x_2 - x_1) = f \frac{\frac{1}{v} u_m^2}{2d} L$$

$$\Delta p_L = (0.0195) \frac{\left(\frac{1}{0.3648 \cdot 10^{-4}\ m^3/kg}\right)(54.6865\ m/s)^2}{2(0.009525\ m)}(6.7056\ m) \cong 56181.77\ Pa$$

In imperial units this pressure drop is equivalent to

$$\Delta p_L = (56181.77\ Pa)\left(\frac{1\ lb}{4.448222\ N}\right)\left(\frac{0.0254\ m}{1\ in}\right)^2 \cong 8.15\ psig$$

C.5 Changing Heat Capacity and Freezing Point of Fluid

Comparing the specific heat capacity and freezing point of salt water to that of fresh water, its specific heat capacity drops from 4.217 $kJ/kg \cdot K$ to approximately 3.985 $kJ/kg \cdot K$ at a temperature of 0°C, while the freezing point drops from 0°C to -1.910°C. Now, using the same approach as used in the in previous section, the total amount of time the geo-exchange tank can be used to heat the building with respect to only the liquid fluid in the tank is as follows:

$$Q_s - W = \Delta U + \Delta KE + \Delta PE$$

$$\Rightarrow Q_s = \Delta U + W_b + W_{other}$$

$$Q_s = \Delta H + W_{other}$$

$$Q_s = \Delta H$$

$$Q_s \cong mC_{p,avg}\Delta T$$

$$Q_s \cong \rho V C_{p,avg}\Delta T$$

$$Q_s \cong \left(1000\frac{kg}{m^3}\right)(4\,ft)^3\left(12\frac{in}{ft}\right)^3\left(0.0254\frac{m}{in}\right)^3\left(3.985 \cdot 10^3\frac{J}{kg \cdot ^\circ\mathrm{C}}\right)\left(4^\circ\mathrm{C} - (-1.910^\circ\mathrm{C})\right)$$

$$Q_s \cong \ 42.68MJ$$

$$\dot{Q} \cong \frac{\Delta Q_s}{\Delta t}$$

$$\Rightarrow \Delta t \cong \frac{\Delta Q_s}{\dot{Q}}$$

$$\Delta t \cong \frac{42.68 \cdot 10^6 J}{10567W}$$

$$\Delta t \cong (4039s)\left(\frac{1h}{3600s}\right)$$

$$\Delta t \cong 1.12h$$

This can then be repeated with a water-glycol mix:

At five percent by mass ethylene glycol to water, the freezing temperature drops to $T = -2°\text{C}$ [13], and the specific heat capacity drops from $C_P = 4.202\ \ kJ/kg \cdot K$ to $C_P \cong 4.088\ \ kJ/kg \cdot K$ for a temperature of $T = 5°\text{C}$ [14].

$$Q_s \cong \rho V C_{p,avg} \Delta T$$

$$Q_s \cong \left(1000 \frac{kg}{m^3}\right)(4\ ft)^3 \left(12 \frac{in}{ft}\right)^3 \left(0.0254 \frac{m}{in}\right)^3 \left(4.088 \cdot 10^3 \frac{J}{kg \cdot °\text{C}}\right)\left(4°\text{C} - (-2)\right)$$

$$Q_s \cong\ 44.452\ MJ$$

$$\dot{Q} \cong \frac{\Delta Q_s}{\Delta t}$$

$$\Rightarrow \Delta t \cong \frac{\Delta Q_s}{\dot{Q}}$$

$$\Delta t \cong \frac{44.452 \cdot 10^6 J}{10567 W}$$

$$\Delta t \cong (4207 s)\left(\frac{1h}{3600 s}\right)$$

$$\Delta t \cong 1.169h$$

At ten percent by mass ethylene glycol to water, the freezing temperature drops to $T = -3°\text{C}$ [13], and the specific heat capacity drops to $C_P \cong 3.933\ \ kJ/kg \cdot K$ for a temperature of $T = 0°\text{C}$ and to $C_P \cong 3.942\ \ kJ/kg \cdot K$ for a temperature of $T = 5°\text{C}$ [14]. Using interpolation, $C_P \cong 3.9009\ \ kJ/kg \cdot K$ for a temperature of $T = 0.5°\text{C}$.

$$Q_s \cong \rho V C_{p,avg} \Delta T$$

$$Q_s \cong \left(1000 \frac{kg}{m^3}\right)(4\ ft)^3 \left(12 \frac{in}{ft}\right)^3 \left(0.0254 \frac{m}{in}\right)^3 \left(3.9009 \cdot 10^3 \frac{J}{kg \cdot °\text{C}}\right)\left(4°\text{C} - (-3)\right)$$

$$Q_s \cong\ 49.487\ MJ$$

$$\dot{Q} \cong \frac{\Delta Q_s}{\Delta t}$$

$$\Rightarrow \Delta t \cong \frac{\Delta Q_s}{\dot{Q}}$$

$$\Delta t \cong \frac{49.487 \cdot 10^6 J}{10567 W}$$

$$\Delta t \cong (4683s)\left(\frac{1h}{3600s}\right)$$

$$\Delta t \cong 1.301h$$

C.6 Heat Transfer Rate across a Straight Pipe

In order to validate COMSOL's heat transfer in pipes module, a constant surface temperature heat transfer scenario with the values in the table below will be compared to an analytical solution.

Parameter	**Value**
Pipe Length, L $[m]$	10.0
Inner Pipe Diameter, d $[in], [m]$	$0.5, 0.0127$
Outer Pipe Diameter, D $[in], [m]$	$0.625, 0.015875$
Thermal Conductivity of Copper, k $[W/m \cdot K]$	400
Inlet Temperature, T_{in} $[K]$	273.15
Surrounding Temperature, T_s $[K]$	500
Inlet Velocity, u $[m/s]$	0.0625
Inlet Pressure, p $[psi], [kPa]$	$50, 344.738$

$$Assume\ that\ T_{m,o} = 346.85K$$

$$\therefore \bar{T}_m = \frac{273.15K + 346.85K}{2} = 310K$$

Using 310 K for all material properties of water, results can be calculated as follows.

$C_p = 4178\ J/kg \cdot K$

$k_f = 0.628\ W/m \cdot K$

$Pr = 4.62$

$\rho = 993.048\ kg/m^3$

$\mu = 0.000695\ N \cdot s/m^2$

$$Re_D = \frac{\rho u_m D}{\mu} = \frac{(993.048\ kg/m^3)(0.125\ m/s)(0.0127\ m)}{0.000695\ N \cdot s/m^2} \cong 1134.1 < 2300 \therefore Laminar$$

$$Gz_D = \frac{D}{x} Re_D Pr = \frac{0.0127\ m}{1.0\ m}(2268.29)(4.62) \cong 6.6545$$

$$\overline{Nu}_D = 3.66 + \frac{0.0668 Gz_D}{1 + 0.04 Gz_D^{2/3}} = 3.66 + \frac{(0.0668)(133.09)}{1 + (0.04)(133.09)^{2/3}} \cong 4.0494$$

$$\bar{h} = \overline{Nu}_D \left(\frac{k_f}{D}\right) = (8.358)\left(\frac{0.628\ W/m \cdot K}{0.0127\ m}\right) \cong 200.2387 \frac{W}{m^2 \cdot K}$$

$$\dot{m} = \rho u_m A = \rho u_m \frac{\pi}{4} D^2 = (993.048\ kg/m^3)(0.125\ m/s)\frac{\pi}{4}(0.0127\ m)^2 \cong 0.0079\ kg/s$$

$$T_{m_o} = T_s - \exp\left(-\frac{\pi D L}{\dot{m} C_p}\bar{h}\right)\left(T_s - T_{m_i}\right)$$

$$T_{m_o} = 1000K - \exp\left[-\frac{\pi(0.0127\ m)(1.0\ m)}{(0.0079\ kg/s)(4178\ J/kg \cdot K)}\left(200.2387\ \frac{W}{m^2 \cdot K}\right)\right](500K - 273.16K)$$

$$T_{m_o} = 500K - \exp(-2.4321)(226.84)$$

$$T_{m_o} \cong 480.0721\ K > 346.85\ K$$

$$\therefore Assume\ T_{m_o} = 473.15\ K$$

$$\Rightarrow \bar{T}_m = \frac{273.15K + 473.15K}{2} = 373.15K$$

Using 373.15 K for all material properties of water, results can be calculated as follows.

$C_p = 4217\ J/kg \cdot K$

$k_f = 0.680\ W/m \cdot K$

$Pr = 1.76$

$\rho = 957.85\ kg/m^3$

$\mu = 0.000279\ N \cdot s/m^2$

$$Re_D = \frac{\rho u_m D}{\mu} = \frac{(973.71\ kg/m^3)(0.125\ m/s)(0.0127\,m)}{0.000365\ N \cdot s/m^2} \cong 2725.1 \sim > 2300$$

$$\therefore Laminar/Turbulent$$

$$Gz_D = \frac{D}{x} Re_D Pr = \frac{0.0127\,m}{1.0\,m}(2268.29)(1.76) \cong 6.0911$$

$$\overline{Nu}_D = 3.66 + \frac{0.0668 Gz_D}{1 + 0.04 Gz_D^{2/3}} = 3.66 + \frac{(0.0668)(133.09)}{1 + (0.04)(133.09)^{2/3}} \cong 4.019$$

$$\bar{h} = \overline{Nu}_D \left(\frac{k_f}{D}\right) = (8.358)\left(\frac{0.668\ W/m \cdot K}{0.0127\,m}\right) \cong 215.19 \frac{W}{m^2 \cdot K}$$

$$\dot{m} = \rho u_m A = \rho u_m \frac{\pi}{4} D^2 = (973.71\ kg/m^3)(0.125\ m/s)\frac{\pi}{4}(0.0127\,m)^2 \cong 0.0076\ kg/s$$

$$T_{m_o} = T_s - \exp\left(-\frac{\pi D L}{\dot{m} C_p}\bar{h}\right)\left(T_s - T_{m_i}\right)$$

$$T_{m_o} = 500K - \exp\left[-\frac{\pi(0.0127\,m)(1.0\,m)}{(0.0076\ kg/s)(4217\ J/kg \cdot K)}\left(215.19\ \frac{W}{m^2 \cdot K}\right)\right](500K - 273.16K)$$

$$T_{m_o} = 500K - \exp(-2.6847)(226.84)$$

$$T_{m_o} \cong 484.52\ K \cong 473.15K$$

Appendix D – Programming

D.1 Pipe Losses Through Outdoor Coil

```
%%%%%%%%%% Capstone Project - Pipe Losses through Outdoor Coil %%%%%%%%%%%

%%%%%%%%%%%%%%%%%%%%%% Variable Declarations %%%%%%%%%%%%%%%%%%%%%%%%%%%%%%
clear;                  % Clears workspace
clc;                    % Clears command window

COP = 3.2;              % Coefficient of Performance of heat pump at 0C
d = 0.375*0.0254;       % Inside diameter of copper tube [m]
D = 0.5*0.0254;         % Outside diameter of copper tube [m]
E = 240;                % Compressor voltage [V]
g = 9.81;               % Acceleration due to gravity [m/s^2]
I = 6;                  % Compressor current draw [A]
L = 22*12*0.0254;       % Length of copper tube [m]
p_H = 324.7;            % Pressure on high pressure side of heat pump [psig]
p_L = 95.2;             % Pressure on low pressure side of heat pump [psig]
Q = 9900/3.41214163;% Heat pump capacity at 0C [W]

%%%%%%%%%%%%%%%%%%%%%%%%%%%%%% Code %%%%%%%%%%%%%%%%%%%%%%%%%%%%%%%%%%%%%%%%
% Cross sectional area of outdoor coil tube [m^2]
A = (pi/4)*d^2;

% Refrigerant temperature on high pressure side of heat pump [C]
T_H = ((51.7-48.9)/(344-322))*(p_H-322)+48.9;

% Refrigerant temperature on low pressure side of heat pump [C]
T_L = ((-1.1-(-2.2))/(96.8-92.9))*(p_L-92.9)+(-2.2);

% Refrigerant enthalpy at point 1 (compressor inlet) on TS diagram [kJ/kg]
h1 = ((422.3-422)/(-1-(-2)))*(T_L-(-2))+422;

% Refrigerant enthalpy at point 3 (indoor coil outlet) on TS diagram
% [kJ/kg]
h3 = ((286.9-284.8)/(50-49))*(T_H-49)+284.8;

% Refrigerant enthalpy at point 4 (outdoor coil inlet) on TS diagram
% [kJ/kg] is equal to h3 because of isenthalpic throttling process
h4 = h3;

% Refrigerant enthalpy of saturated liquid at point 4 (outdoor coil inlet)
% [kJ/kg]
hf = ((198.5-196.9)/(-1-(-2)))*(T_L-(-2))+196.9;

% Refrigerant enthalpy of vaporaization at point 4 (outdoor coil inlet)
% [kJ/kg]
hfg = ((223.8-225.1)/(-1-(-2)))*(T_L-(-2))+225.1;

% Refrigerant specific volume of saturated liquid on low pressure side of
% heat pump [m^3/kg]
vf = ((0.0009-0.0008)/(-1-(-2)))*(T_L-(-2))+0.0008;
```

```
% Refrigerant specific volume of saturated vapor on low pressure side of
% heat pump [m^3/kg]
vg = ((0.0337-0.0348)/-1-(-2))*(T_L-(-2))+0.0348;

% Quality of refrigerant at point 4 (outdoor coil inlet) (0 < x < 1)
x = (h3-hf)/hfg;

% Refrigerant specific volume of vaporization on low pressure side of heat
% pump [m^3/kg]
vfg = vg - vf;

% Refrigerant specific volume at point 4 (outdoor coil inlet) [m^3/kg]
v4 = vf + x*vfg;

% Power input via compressor [W]
W = E*I;

% Heat transfer through outdoor coil [W]
Q_L = Q - W;

% Mass flow rate of refrigerant[kg/s]
mDot = Q_L/(h1*10^3-h4*10^3);

% Velocity of refrigerant at point 4 (outdoor coil inlet) [m/s]
u_m4 = mDot/((1/v4)*A);

% Refrigerant saturated liquid specific heat capacity - from Suva R410A
% Thermophysical Properties Chart (Pg 17) [J/kg*C]
Cp = 1.6e3;

% Refrigerant saturated liquid thermal conductivity - from Suva R410A
% Thermophysical Properties Chart (Pg 16) [W/m*C]
k = 100.5e-3;

% Refrigerant saturated liquid dynamic viscosity - from Suva R410A
% Thermophysical Properties Chart (Pg 14) [Pa*s]
mu = 164e-6;

% Reynolds number with respect to diameter at point 4 (outdoor coil inlet)
Re = 4*mDot/(pi*d*mu);

% Prandtl number of refrigerant at point 4 (outdoor coil inlet)
Pr = Cp*mu/k;

if(Re < 2300)
    f = 64/Re;
elseif(Re < 5e6)
    f = (0.790*log(Re-1.64))^-2;
else
    disp('Reynolds number is too large for current program algorithm');
    f = 0;
end
```

```
% Pressure drop across outdoor coil of the heat pump [Pa];
deltaP = f*(u_m4^2)/(2*d*v4)*L;

% Pressure drop across outdoor coil of the heat pump [psig];
deltaPImperial = deltaP*(0.0254^2)/4.448222;

fprintf(['The pressure drop across the outdoor coil of the Geo-Exchange'...
    'Heat Pump is approximately %.2f Pa\nor approximately %.2f psig \n']...
    ,deltaP,deltaPImperial);
```

D.2 Heat Transfer through Horizontal Outdoor Coil

```
%%%%% Capstone Project - Heat Transfer through Existing Outdoor Coil %%%%%%

%%%%%%%%%%%%%%%%%%%%%%%%% Variable Definitions %%%%%%%%%%%%%%%%%%%%%%%%%%%%
% alpha:=   Thermal difussivity of tank fluid [m^2/s]
% A:=       Surface area of outdoor coil
% A_prime:= Required Surface area of outdoor coil
% beta:=    Tank fluid compressibility factor [K^-1]
% Cp:=      Specific heat for tank fluid at film temperature [J/kg*K]
% deltaT:=  Temperature difference between wall and ambient temperature [C]
% h:=       Convection heat transfer coefficient for system [W/m^2*K]
% k:=       Thermal conductivity of tank fluid at film temperature [W/m*K]
% mu:=      Dynamic viscosity of tank fluid at film temperature [N*s/m^2]
% Nu:=      Nusselt number of system at film temperature
% n:=       Heat transfer rate difference factor
% nu:=      Kinematic viscosity of tank fluid at film temperature [m^2/s]
% Pr:=      Prandtl number of tank fluid at film temperature
% Q_dot:=   Heat transfer rate for existing outdoor coil
% Ra:=      Rayleigh number for system
% rho:=     Fluid density at film temperature
% T_f:=     Film temperature of tank fluid [K]

%%%%%%%%%%%%%%%%%%%%%% Variable Declarations %%%%%%%%%%%%%%%%%%%%%%%%%%%%%%
clear;                  % Clears workspace
clc;                    % Clears command window

g = 9.81;               % Acceleration due to gravity [m/s^2]
d = 0.375*0.0254;       % Inside diameter of copper tube [m]
D = 0.5*0.0254;         % Outside diameter of copper tube [m]
L = 22*12*0.0254;       % Length of copper tube [m]
Q_actual = 10537;       % Building heat loss rate [W]
T_infi = 4;             % Temperature of tank fluid [C]
T_w = -10;              % Temperature of refrigerant and copper tube wall [C]

%%%%%%%%%%%%%%%%%%%%%%%%%%%%%% Code %%%%%%%%%%%%%%%%%%%%%%%%%%%%%%%%%%%%%%%
A = pi*D*L;
deltaT = T_infi-T_w;
T_f = ((T_infi+T_w)/2)+273.15;
beta = -68.05e-6;
Cp = 4217;
k = 569e-3;
mu = 1750e-6;
Pr = 12.99;
```

```
rho = 1000;
alpha = k/(rho*Cp);
nu = mu/rho;

Ra = g*beta*(T_w-T_infi)*D^3/(alpha*nu);
Nu = (0.6+(0.387*(Ra^(1/6)))/((1+((0.559/Pr)^(9/16)))^(8/27)))^2;
h = Nu*k/D;
Q_dot = h*A*deltaT;
n = Q_actual/Q_dot;
A_prime = n*A;
s = ['The heat transfer rate through the outdoor coil of the Geo-Exchange
Heat Pump is ' ...
    'approximately\n%.2f W whereas the required heat transfer rate for the
spec home is ' ...
    '%.2f W. This means that the\nsurface area for the outdoor coil must be
increased by ' ...
    'approximately %.2f times for a total surface\narea of %.2f sq. m or %.2f
sq. in\n'];
fprintf(s, Q_dot, Q_actual, n, A_prime, A_prime/(0.0254^2));
```

D.3 Heat Transfer through Vertical Outdoor Coil

```
%%%%%%%%%% Capstone Project - Heat Transfer through Outdoor Coil %%%%%%%%%%

%%%%%%%%%%%%%%%%%%%%%%%%% Variable Definitions %%%%%%%%%%%%%%%%%%%%%%%%%%%
% alpha:=   Thermal difussivity of tank fluid [m^2/s]
% A:=       Surface area of outdoor coil
% A_prime:= Required Surface area of outdoor coil
% beta:=    Tank fluid compressibility factor [K^-1]
% Cp:=      Specific heat for tank fluid at film temperature [J/kg*K]
% deltaT:=  Temperature difference between wall and ambient temperature [C]
% h:=       Convection heat transfer coefficient for system [W/m^2*K]
% k:=       Thermal conductivity of tank fluid at film temperature [W/m*K]
% mu:=      Dynamic viscosity of tank fluid at film temperature [N*s/m^2]
% Nu:=      Nusselt number of system at film temperature
% n:=       Heat transfer rate difference factor
% nu:=      Kinematic viscosity of tank fluid at film temperature [m^2/s]
% Pr:=      Prandtl number of tank fluid at film temperature
% Q_dot:=   Heat transfer rate for existing outdoor coil
% Ra:=      Rayleigh number for system
% rho:=     Fluid density at film temperature
% T_f:=     Film temperature of tank fluid [K]

%%%%%%%%%%%%%%%%%%%%%% Variable Declarations %%%%%%%%%%%%%%%%%%%%%%%%%%%%%%
clear;                  % Clears workspace
%clc;                    % Clears command window

g = 9.81;               % Acceleration due to gravity [m/s^2]
d = 0.375*0.0254;       % Inside diameter of copper tube [m]
D = 0.5*0.0254;         % Outside diameter of copper tube [m]
L = 22*12*0.0254;       % Length of copper tube [m]
Q_actual = 10537;       % Building heat loss rate [W]
T_infi = 4;             % Temperature of tank fluid [C]
T_w = -10;              % Temperature of refrigerant and copper tube wall [C]
```

```
%%%%%%%%%%%%%%%%%%%%%%%%%%%%%% Code %%%%%%%%%%%%%%%%%%%%%%%%%%%%%%%%%%%%%%%
A = pi*D*L;
deltaT = T_infi-T_w;
T_f = ((T_infi+T_w)/2)+273.15;
beta = -68.05e-6;
Cp = 4217;
k = 569e-3;
mu = 1750e-6;
Pr = 12.99;
rho = 1000;
alpha = k/(rho*Cp);
nu = mu/rho;

Ra = g*beta*(T_w-T_infi)*D^3/(alpha*nu);
Nu = (0.825+(0.387*(Ra^(1/6)))/((1+((0.492/Pr)^(9/16)))^(8/27)))^2;
h = Nu*k/D;
Q_dot = h*A*deltaT;
n = Q_actual/Q_dot;
A_prime = n*A;
s = ['The heat transfer rate through the outdoor coil of the Geo-Exchange
Heat Pump is ' ...
    'approximately\n%.2f W whereas the required heat transfer rate for the
spec home is ' ...
    '%.2f W. This means that the\nsurface area for the outdoor coil must be
increased by ' ...
    'approximately %.2f times for a total surface\narea of %.2f sq. m or %.2f
sq. in\n'];
fprintf(s, Q_dot, Q_actual, n, A_prime, A_prime/(0.0254^2));
```

Appendix E – Product Specifications

Model: Climate Master model No. TCH012AGD40CLSS

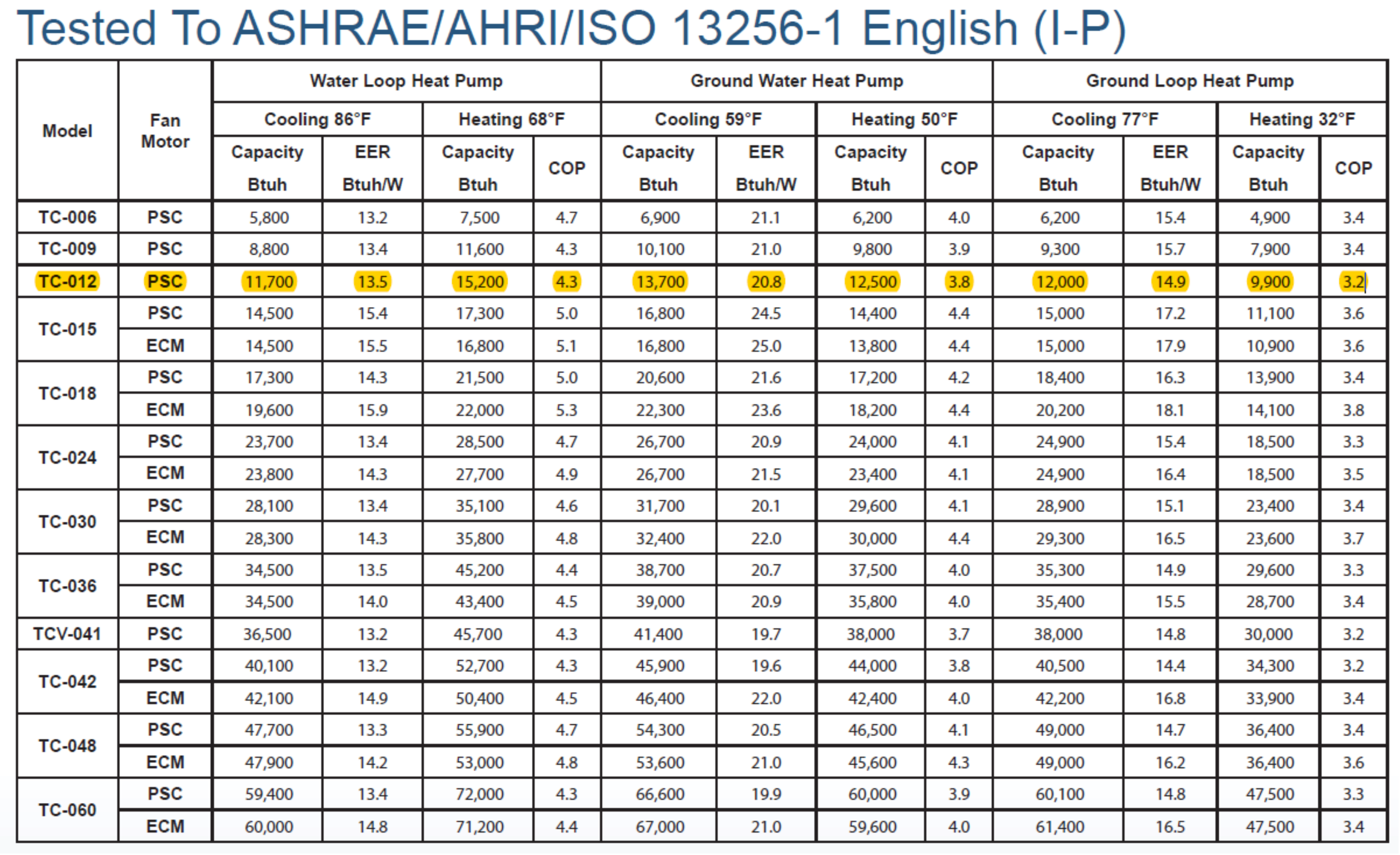

Tested To ASHRAE/AHRI/ISO 13256-1 English (I-P)

Model	Fan Motor	Water Loop Heat Pump				Ground Water Heat Pump				Ground Loop Heat Pump			
		Cooling 86°F		Heating 68°F		Cooling 59°F		Heating 50°F		Cooling 77°F		Heating 32°F	
		Capacity Btuh	EER Btuh/W	Capacity Btuh	COP	Capacity Btuh	EER Btuh/W	Capacity Btuh	COP	Capacity Btuh	EER Btuh/W	Capacity Btuh	COP
TC-006	PSC	5,800	13.2	7,500	4.7	6,900	21.1	6,200	4.0	6,200	15.4	4,900	3.4
TC-009	PSC	8,800	13.4	11,600	4.3	10,100	21.0	9,800	3.9	9,300	15.7	7,900	3.4
TC-012	PSC	11,700	13.5	15,200	4.3	13,700	20.8	12,500	3.8	12,000	14.9	9,900	3.2
TC-015	PSC	14,500	15.4	17,300	5.0	16,800	24.5	14,400	4.4	15,000	17.2	11,100	3.6
	ECM	14,500	15.5	16,800	5.1	16,800	25.0	13,800	4.4	15,000	17.9	10,900	3.6
TC-018	PSC	17,300	14.3	21,500	5.0	20,600	21.6	17,200	4.2	18,400	16.3	13,900	3.4
	ECM	19,600	15.9	22,000	5.3	22,300	23.6	18,200	4.4	20,200	18.1	14,100	3.8
TC-024	PSC	23,700	13.4	28,500	4.7	26,700	20.9	24,000	4.1	24,900	15.4	18,500	3.3
	ECM	23,800	14.3	27,700	4.9	26,700	21.5	23,400	4.1	24,900	16.4	18,500	3.5
TC-030	PSC	28,100	13.4	35,100	4.6	31,700	20.1	29,600	4.1	28,900	15.1	23,400	3.4
	ECM	28,300	14.3	35,800	4.8	32,400	22.0	30,000	4.4	29,300	16.5	23,600	3.7
TC-036	PSC	34,500	13.5	45,200	4.4	38,700	20.7	37,500	4.0	35,300	14.9	29,600	3.3
	ECM	34,500	14.0	43,400	4.5	39,000	20.9	35,800	4.0	35,400	15.5	28,700	3.4
TCV-041	PSC	36,500	13.2	45,700	4.3	41,400	19.7	38,000	3.7	38,000	14.8	30,000	3.2
TC-042	PSC	40,100	13.2	52,700	4.3	45,900	19.6	44,000	3.8	40,500	14.4	34,300	3.2
	ECM	42,100	14.9	50,400	4.5	46,400	22.0	42,400	4.0	42,200	16.8	33,900	3.4
TC-048	PSC	47,700	13.3	55,900	4.7	54,300	20.5	46,500	4.1	49,000	14.7	36,400	3.4
	ECM	47,900	14.2	53,000	4.8	53,600	21.0	45,600	4.3	49,000	16.2	36,400	3.6
TC-060	PSC	59,400	13.4	72,000	4.3	66,600	19.9	60,000	3.9	60,100	14.8	47,500	3.3
	ECM	60,000	14.8	71,200	4.4	67,000	21.0	59,600	4.0	61,400	16.5	47,500	3.4